UNIVERSITY OF CALIFORNIA, SAN DIEGO

Molecular and Cellular Mechanisms of Retinotopic Mapping in the Superior Colliculus

A dissertation submitted in partial satisfaction of the requirements for the degree
Doctor of Philosophy

in

Neurosciences

by

Nicholas James Bevins

Committee in charge:

Professor Greg Lemke, Chair
Professor Anirvan Ghosh, Co-Chair
Professor Hollis Cline
Professor Yishi Jin
Professor Nick Spitzer
Professor Yimin Zou

2011

The Dissertation of Nicholas James Bevins is approved, and it is acceptable in quality and form for publication on microfilm and electronically:

_____

_____

_____

_____

_____

_____

Co-Chair

_____

Chair

University of California, San Diego

2011

Dedication

To my father and my sister:

For instigating so many good things in my life.

Table of Contents

List of Figures

List of Tables

Acknowledgements

I am grateful to my mentor Dr. Greg Lemke for letting me join his lab and allowing me the freedom to pursue my interests.

I am grateful to Dr. Michael Reber for providing much of the impetus to the projects that constitute this dissertation.

I am indebted to all the members of the Lemke lab and the Molecular Neurobiology Laboratory at the Salk for helpful discussion and creating a productive atmosphere.

I am grateful to Dr. Mark Albers, Dr. Richard Axel, and Bill Campbell for providing a wonderful place to begin my scientific adventures.

The work presented in this thesis is one small brick in the great cathedral of science. I am indebted to the neuroscience community at UCSD for constantly reminding of the shared labor and shared enjoyment of neurosciences. The professors and students of the graduate program have been invaluable for the discussion of my work and the constant presentation of research as a joyful endeavor.

Research can be an emotionally demanding activity. I would like to thank my friends, who were always generous enough to share my happiness as well as my frustration, especially Saba Safiari, Rayna Brooks, Louis Nguyen, Ben Hulley, Danny Simpson, Adam Rusch, Jasmin Harris, Cosmo Buffalo, Jacquelyn Witt, Dorian Raymer, Michelle Munro, Pete Bluvas, Jim Campbell, Michael Quarshie, Phil Palmejar, and Liz Murphy.

I am constantly thankful for my family. In the good times, you share my joy. In the bad times, you bring me strength. Thank you: Mom, Dad, Bear, Randy, Amah, Steven, Truckee Papa, Airplane Papa, Uncle Al, Uncle Mike, Auntie Arrow, Auntie Staw, and Jessica.

The text of Chapter Two, in part, is a reprint of the material which has been submitted for publication. I was the primary researcher. Dr. Greg Lemke and Dr. Michael Reber directed and supervised the research which forms the basis for this chapter.

The text of Chapter Three, in part, is a reprint of the material which is being prepared for publication. I was the primary researcher. Dr. Greg Lemke directed and supervised the research which forms the basis for this chapter.

Vita

2004 B.A. Biochemistry, Columbia University in the city of New York

2004-2005 Research assistant: Howard Hughes Medical Institute and Columbia University Center for Neurobiology and Behavior, Richard Axel, P.I.

2005-2013 Medical Scientist Training Program, University of California, San Diego

2007-2011 Graduate Student Researcher, Department of Neurosciences, University of California, San Diego, Greg Lemke, P.I.

2010 M.S. Neurosciences, University of California, San Diego

2011 Ph.D. Neurosciences, University of California, San Diego

Publications:

Bevins, N., Lemke, G. and Reber, M. (2011) "Genetic dissection of EphA receptor signaling dynamics during retinotopic mapping." J. Neurosci. (In Press)

Teaching experience:

2009 Teaching Assistant. UCSD. Mammalian Physiology. George Fortes, Course Instructor.

2010 Teaching Assistant. UCSD School of Medicine. Basic Neurology. Mark Kritchevsky, Course Instructor.

2011 Teaching Assistant. UCSD School of Medicine. Mind, Brain, and Behavior. Mark Kritchevsky, Course Instructor.

Awards and Honors:
Varsity C award (football) – Columbia
Schlumberger scholarship – Columbia
Kriegler fellowship in molecular medicine – UCSD

ABSTRACT OF THE DISSERTATION

Molecular and Cellular Mechanisms of Retinotopic Mapping in the Superior Colliculus

by

Nicholas James Bevins

Doctor of Philosophy in Neurosciences

University of California, San Diego, 2011

Professor Greg Lemke, Chair

Professor Anirvan Ghosh, Co-Chair

Retinal ganglion cells (RGCs) project axons from their cell bodies in the eye to targets in the superior colliculus (SC) of the midbrain. The wiring of RGC axons to their synaptic targets creates an ordered representation, or ‘map’, of retinal space within the brain. The mechanisms of development of this map are the primary topic of this dissertation. The dissertation begins with an overview of the architecture and function of the murine visual system with a focus on RGCs. The paradigms of retinotopic map development have been divided into those involving guidance molecules and those involving correlated activity.

I describe a set of ratiometric ‘Relative Signaling’ (RS) rules that quantitatively predict how a composite gradient of EphA receptors expressed by RGCs is translated into topographic order in the SC. I describe the analysis of the retinotopic maps of novel compound mutant mice, which establish the general utility of the RS rules for predicting retinocollicular topography, including the equivalence of different EphA receptor gene products.

I describe how spontaneous, patterned activity in the retina during the time of retinocollicular mapping could be instructive to the development of retinotopy. I analyze the retinocollicular maps of novel compound mutant mice lacking the β2 subunit of the nicotinic acetylcholine receptor, which are thought to lack spontaneous, patterned activity in the retina. The analysis of retinocollicular maps in these compound mutant mice was ambiguous, but suggested that correlated activity does not play a role in retinocollicular mapping.

Finally, I speculate on how different dynamics of retinotopic mapping in amniotes and anamniotes may arise because of the differing degree of encephalization between the two groups. I also comment on how increased encephalization allows for a greater behavioral repertoire but comes at the costs of an inability to regenerate and a greater time to develop.

Chapter One – Description of the Murine Visual System

Abstract

This chapter provides an overview of the architecture and function of the murine visual system. The description focuses on retinal ganglion cells (RGCs), the output cells of the retina, as the development of RGC projections is the primary concern of the following chapters. Comparisons are made between the murine visual system and that of other model organisms used to study the development and function of the vertebrate visual system. Concluding the introduction is a short, phenomenological description of visual system development, with special reference to RGCs.

Introduction

Vision is a sensory process using light to build a spatial representation of the surrounding world. The process begins in the eye and is brought to fruition as a distributed computational process in the central nervous system (CNS). Thus, to understand the visual system one must explore it with the tools and techniques developed to study molecules, cells, circuits, and behavior. The experiments of this thesis begin with the mis-expression of one gene in a subset of cells in the retina. This distinct genetic perturbation leads to changes in several layers of complexity within the visual system.

This introductory chapter contains an outline of the architecture of the mouse visual system, a comparison between the mouse visual system and the visual system of other model organisms,and a brief overview of the development of the mouse visual system. This chapter is by no means a complete survey of the visual system. It is intended

to provide context to the experiments of later chapters, which are primarily concerned with the development of topography in the superior colliculus, a structure within the visual system (Chapters Two and Three) and the conceptual insights into neural development gained from these studies (Chapter Four).

Architecture of the Mouse Visual System

The eye and retina

Light enters the eye through the cornea and is subsequently refracted by the lens to project a focused image onto the photoreceptor cells, located in the posterior eye (Figure 1.1A)(Remtulla et al. 1985). Incident light activates rod and cone photoreceptors located on the outside of the retina. Rods are more sensitive to light than cones, and thus are more suited for vision under low light conditions (Toda et al. 1999; Fan et al. 2005). Mice have two kinds of cone photoreceptors, one that is mostly responsive to UV light (360 nm) and the other is responsive to medium wavelength light (508 nm) (Nikonov et al. 2006). The differential sensitivity of cones receptors allows the mouse to have limited color perception during well-lit conditions.

Activation of photoreceptors by incident light leads to activation of a circuit in the retina, which consists of photoreceptor cells, bipolar cells, horizontal cells, amacrine cells, and retinal ganglion cells (RGCs) (Figure 1.1B)(Protti et al. 2005). This internal circuit ultimately creates an overlapping mosaic of RGCs with distinct receptive field properties (Elstrott et al. 2008; Anishchenko et al. 2010). Thus, the output of an RGC already contains spatial information integrated from several photoreceptors.

A

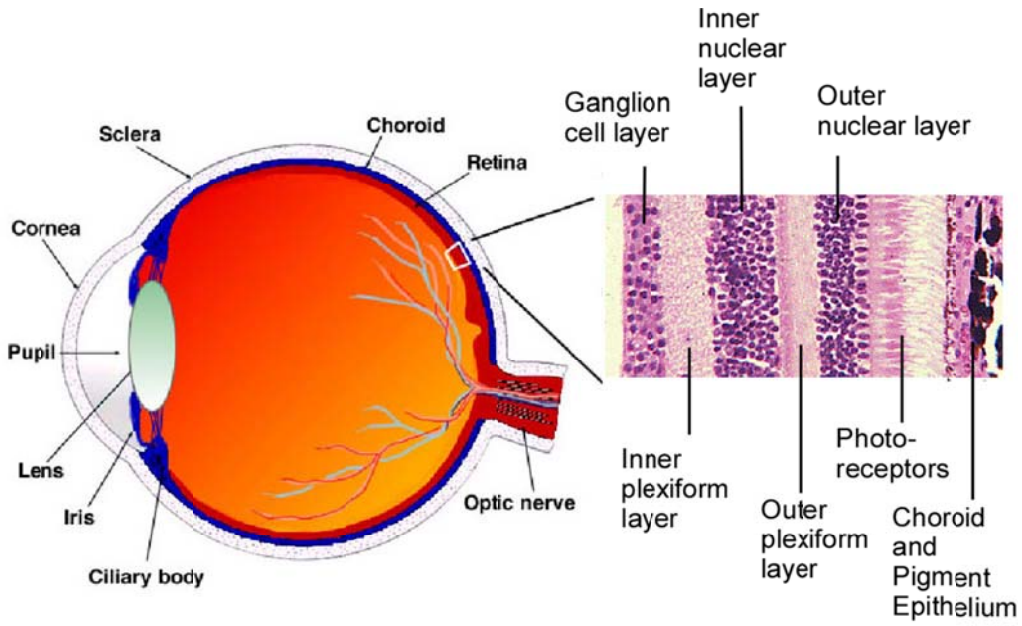
Sclera
Choroid
Retina
Cornea
Pupil
Lens
Iris
Ciliary body
Optic nerve
Ganglion cell layer
Inner nuclear layer
Outer nuclear layer
Inner plexiform layer
Outer plexiform layer
Photo-receptors
Choroid and Pigment Epithelium

B

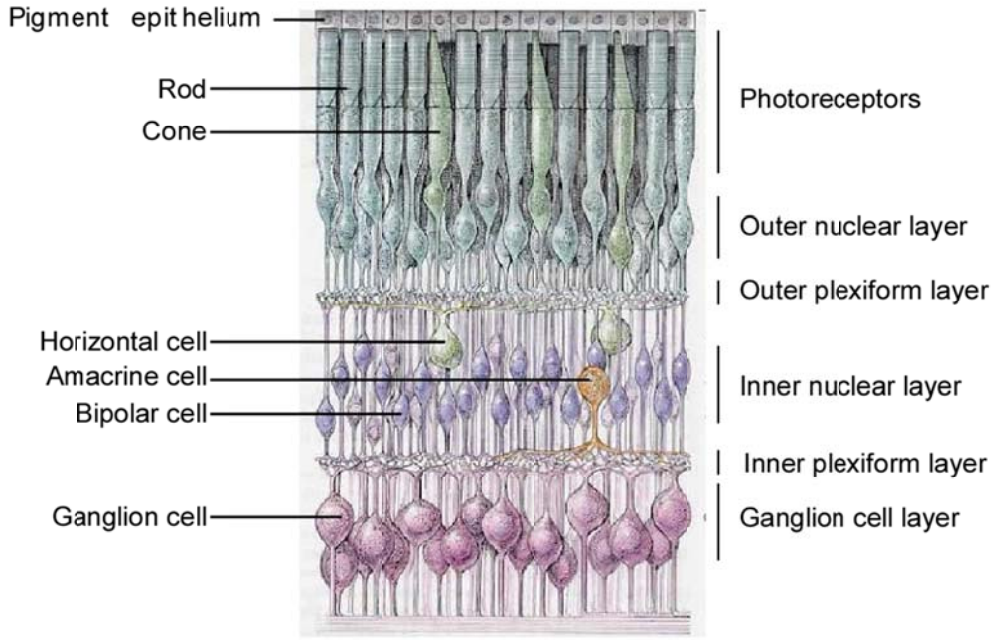
Pigment epithelium
Rod
Cone
Horizontal cell
Amacrine cell
Bipolar cell
Ganglion cell
Photoreceptors
Outer nuclear layer
Outer plexiform layer
Inner nuclear layer
Inner plexiform layer
Ganglion cell layer

Efferent RGC projections

RGC axons project from their somas to the optic disc, where they exit the eye and form the optic nerve (Silver et al. 1980; Silver et al. 1981). RGC axons in the optic nerve then project posteriorly and medially to the optic chiasm (Guillery et al. 1995). At the optic chiasm, 97% of RGC axons cross to the contralateral side of the brain, and the remaining 2-3% project ipsilaterally (Dräger 1974; Antonini et al. 1999). After leaving the chiasm, RGC axons directly project to the suprachiasmatic nucleus (SCN) of the hypothalamus, the dorsal lateral geniculate nucleus (dLGN) of the thalamus, the ventral lateral geniculate nucleus (vLGN) of the thalamus, the intermediate geniculate leaflet (IGL) of the thalamus, several small nuclei in the pretectal complex of the epithalamus, and the superior colliculus (SC) of the midbrain (Dräger 1974; Provencio et al. 1998). The various retinorecipient regions of the brain are responsible for distinct functions of the visual system. I will briefly review those functions in relation to their neuroanatomy.

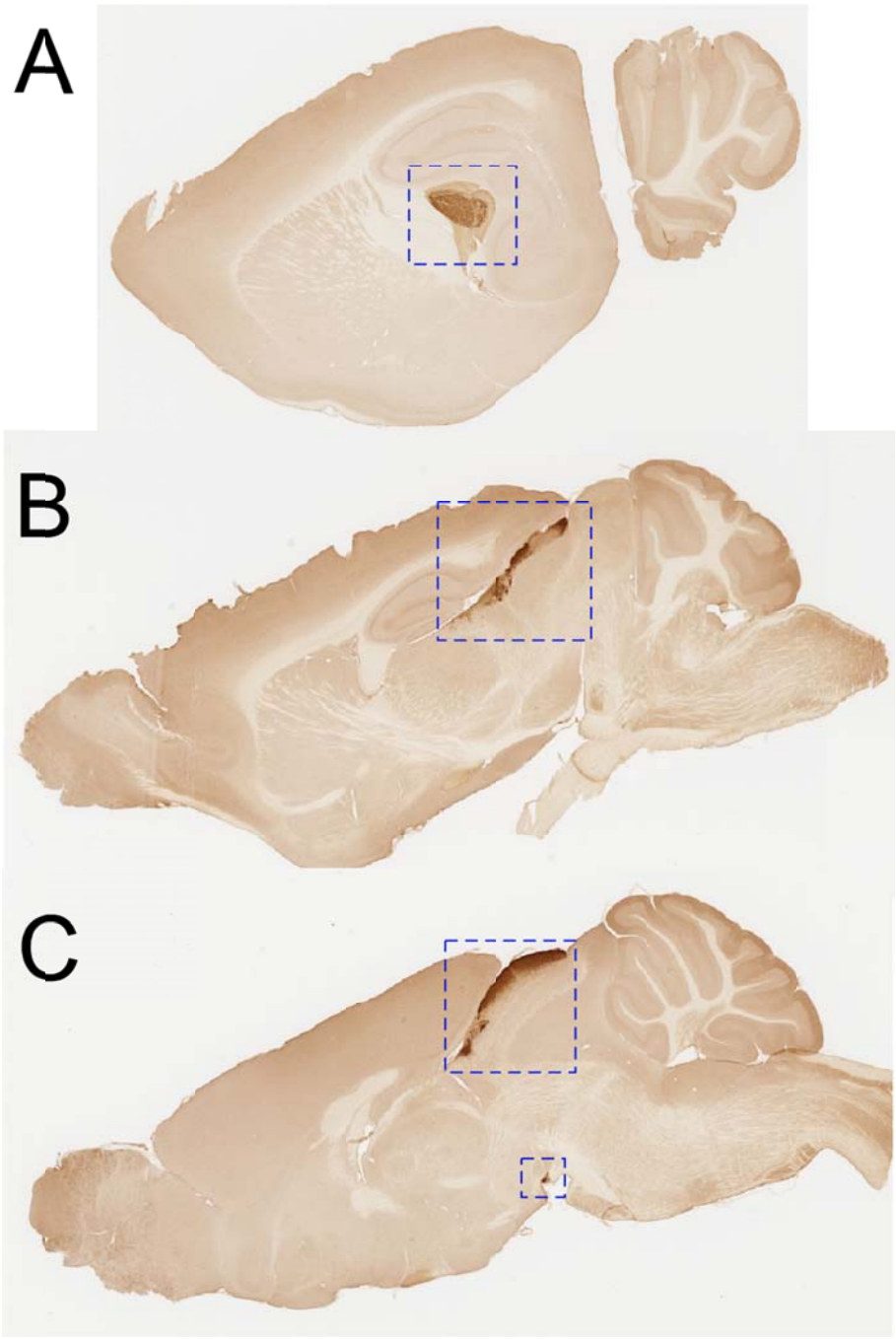

own

own

own

Circadian entrainment

Like most animals, mice show a cycle of activity that parallels the light-dark cycle of their environment (Panda et al. 2002a). The activity cycle can be adjusted to match a new light-dark cycle via projections from the eye (Harmer et al. 2001). RGC projections to the SCN, vLGN, and IGL are associated with entrainment of circadian rhythms to light (Cassone et al. 1988). A special class of RGCs, which express a photopigment making them directly responsive to light, is mostly responsible for photoentrainment to the circadian clock (Berson et al. 2002; Panda et al. 2002b; Panda et al. 2003). Additionally, RGCs with input from rods and cones also play a role in photoentrainment (Hattar et al. 2003).

Reflex eye movements

Mammals have a number of visual reflexes that allow a stable image to be projected on the retina during changes in luminance and movement of the animal. The pupillary light reflex adjusts pupil diameter in response to changes in incident light. RGCs expressing melanopsin, as well as RGCs with input from rods and cones that project to the olivary pre-tectal nucleus are required for this reflex (Hattar et al. 2003). The optokinetic reflex (OKR) and the vestibulo-ocular reflexe (VOR) together create a still image on the retina during head motion. RGC projections to several pre-tectal nuclei located anterior to the SC are required for functioning of the OKR and VOR (Cooper et al. 1986). The VOR and OKR are discussed in more detail in Chapter 4.

Multi-sensory integration in the superior colliculus

In mice, virtually all RGCs have projections into the superficial layers of the SC (Hofbauer et al. 1985). RGCs are organized into a retinotopic map in the SC such that the nasal-temporal axis of the retina is represented on the anterior-posterior axis of the SC, and the dorsal-ventral axis of the retina is represented on the lateral-medial axis of the SC (Dräger et al. 1975; Dräger et al. 1976). The experiments of Chapters Two and Three describe the development of this topography in the SC.

The superficial layers of the SC also receive retinotopic connections from the visual cortex, which align with the direct RGC connections (Mangini et al. 1980; Triplett et al. 2009). Additionally, cells in the deeper layers of the SC are responsive to contralateral auditory and somatosensory stimuli (Dräger et al. 1975; Dräger et al. 1976). The convergence of multisensory afferents onto a topographic map in the SC makes the SC an ideal location for integration of multisensory spatial information (Stein et al. 1990). Consistent with this idea, studies in primates have demonstrated that the SC plays a role in gating spatial attention (Carello et al. 2004; Krauzlis et al. 2004; Lovejoy et al. 2010).

Thalamic relay to the cortex

The dLGN is generally thought to act as a relay between the retina and the primary visual cortex (Dräger 1974). RGC projections to the dLGN are retinotopic (Wagner et al. 2000; Grubb et al. 2003). Retinorecipient cells in the dLGN show center-surround receptive field properties (Grubb et al. 2003) that are qualitatively similar to the RGCs that project onto them (Kuffler 1953). Neurons in the dLGN relay visual

information to the primary visual cortex (Caviness et al. 1980; Frost et al. 1980). Reciprocal connections between the primary visual cortex and the dLGN may play a role in computations (Simmons et al. 1982)

The primary visual cortex contains a representation of the contralateral visual hemi-field (Wagor et al. 1980; Kalatsky et al. 2003; Wang et al. 2007). Portions of the primary visual area, V1, are binocular in that they are activated by stimuli originating in either eye (Gordon et al. 1996a; Gordon et al. 1996b). Cells in V1 tend to respond best to moving lines of illumination (Dräger 1975). Adjacent to area V1 are other cortical regions with cells displaying sensitivities to discrete aspects of visual information such as edge orientation, global motion, or object motion (Kalatsky et al. 2003; Wang et al. 2007; Wang et al. 2011). These extrastriate areas are thought to be involved in transforming visual information into meaningful information about the external environment such as the recognition of features and objects (Wang et al. 2011).

Comparative Neuroanatomy of the Visual System

Comparison of mouse and primate visual systems

When considering the mouse visual system, it is nearly impossible to avoid thinking that mouse experiences the world just like a smaller, less sophisticated human. Such anthropomorphizing may be useful but is inaccurate. A number of key differences between the primate and rodent visual system undoubtedly make the visual experience of the rodent different from that of a human or non-human primate.

In the primate retina, a region near the center of the retina, the fovea, contains a much higher density of photoreceptors compared to the rest of the retina and is over-

represented in retinorecipient areas of the brain, providing greater visual acuity in the central area of the visual field (Provis et al. 1998). Mice have a more uniform density of photoreceptors; consequently, their central retinotopic maps are more uniform (Jeon et al. 1998). Additonally, primate eyes are located at the front of the head, whereas mouse eyes are located more laterally. As a consequence of eye placement, primates have a much larger area of the visual field that is represented in both retinae and in bilateral retinorecipient regions in the brain (Leamey et al. 2009).

As a consequence of these differences in visual system architecture, primates have an area of greater visual acuity within a smaller overall visual field than do mice. This may enable primates to better track prey. However, the increased visual field of mice allows them to detect predators approaching from lateral directions.

Comparison with non-mammalian vertebrate visual systems

Many experiments on the development and architecture of the visual system have been carried out in non-mammalian vertebrates. There are subtle differences between the visual system of mammals and non-mammalian vertebrates, and these are noted when relevant. Most importantly, the RGCs of non-mammalian vertebrates project to a midbrain structure called the tectum, which is the homolog of the mammalian SC. Retinotopy is present in the tectum in all vertebrates studied, and thus non-mammalian vertebrates are often used to study retinotopic mapping.

Many key experiments have made use of the differences in biology of non-mammalian vertebrates. Chick embryos are readily accessible through the shell and can be genetically manipulated during development by electroporation of nucleic acids

(Itasaki et al. 1999). The tectum of tadpoles and zebrafish is visible in an intact animal and can be directly visualized and manipulated (Gaze et al. 1974). Amphibians regenerate retino-tectal projections after dissection of the optic nerve. Notably, Roger Sperry cut the optic nerve and rotated the eyes of a salamander 180 degrees and allowed them to regenerate. After regeneration, when the salamander was presented with food it would extrude its tongue 180 degrees out of phase with the target food, indicating that the regenerated visual system was also rotated 180 degrees (Sperry 1943).

Development of the Visual System

Development of the visual system is a large field of study. Developmental processes begin with the decision of the ectoderm to bud out and form a primordial eye bud (Chow et al. 2001). The ectoderm in the eye bud then differentiates into various components of the eye, including the retina. The early retina consists of undifferentiated cells that undergo a series of divisions during which time the progeny of the stem cell population of the early retina differentiate into the cells of the neural retina (Cayouette et al. 2006).

The first RGCs are born near the central retina on embryonic day 11 (E11) in mouse and begin to extend primary axons toward the optic disc (Dräger 1985). At E12, the first axons exit the retina and grow posteriorally and medially to reach the optic chiasm near E13 (Colello et al. 1990). RGC axons then turn dorsally and grow over the diencephalon and begin to reach the anterior edge of the SC at E14 (Godement et al. 1984).

Development of retinotopy in the SC

Once RGC axons reach the posterior end of the SC, they extend short branches perpendicular to the main axon (Nakamura et al. 1989). These branches preferentially extend over the correct topographic position and are retracted at incorrect positions (Yates et al. 2001). Branch extension and retraction occurs as topography develops during the first postnatal week (Simon et al. 1992).

The cellular mechanisms of retinotopic mapping in the developing SC are the main area of inquiry of this thesis. Theoretical considerations of retinotopic mapping have generally taken two flavors: guidance cue-based mechanisms and activity-based mechanisms. Guidance cue mechanisms posit that interacting factors on RGCs and their target tissues act to guide the development of synapses in topographically appropriate locations. Activity-based mechanisms posit that spontaneous, patterned activity in the retina leads to correlated firing patterns in the SC, which are translated into topography.

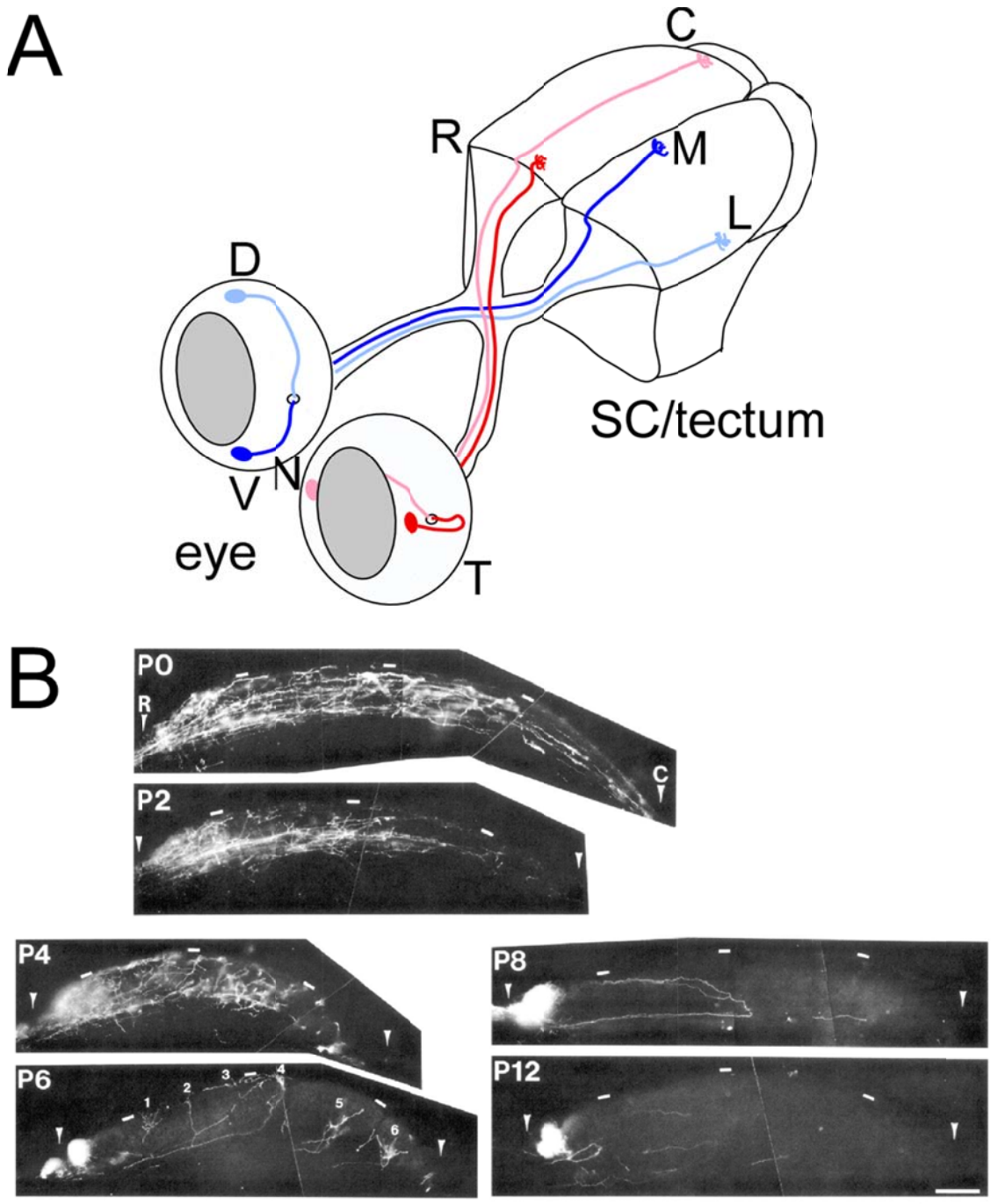

axis of
n

References

Anishchenko, A., M. Greschner, J. Elstrott, A. Sher, A. M. Litke, M. B. Feller and E. J. Chichilnisky (2010). "Receptive field mosaics of retinal ganglion cells are established without visual experience." Journal of Neurophysiology **103**(4): 1856-64.

Antonini, A., M. Fagiolini and M. P. Stryker (1999). "Anatomical correlates of functional plasticity in mouse visual cortex." J Neurosci **19**(11): 4388-406.

Berson, D. M., F. A. Dunn and M. Takao (2002). "Phototransduction by retinal ganglion cells that set the circadian clock." Science **295**(5557): 1070-3.

Carello, C. D. and R. J. Krauzlis (2004). "Manipulating intent: evidence for a causal role of the superior colliculus in target selection." Neuron **43**(4): 575-83.

Cassone, V. M., J. C. Speh, J. P. Card and R. Y. Moore (1988). "Comparative anatomy of the mammalian hypothalamic suprachiasmatic nucleus." J Biol Rhythms **3**(1): 71-91.

Caviness, V. S. and D. O. Frost (1980). "Tangential organization of thalamic projections to the neocortex in the mouse." J Comp Neurol **194**(2): 335-67.

Cayouette, M., L. Poggi and W. A. Harris (2006). "Lineage in the vertebrate retina." Trends Neurosci **29**(10): 563-70.

Chow, R. L. and R. A. Lang (2001). "Early eye development in vertebrates." Annu Rev Cell Dev Biol **17**: 255-96.

Colello, R. J. and R. W. Guillery (1990). "The early development of retinal ganglion cells with uncrossed axons in the mouse: retinal position and axonal course." Development **108**(3): 515-23.

Cooper, H. M. and M. Magnin (1986). "A common mammalian plan of accessory optic system organization revealed in all primates." Nature **324**(6096): 457-9.

Dräger, U. C. (1974). "Autoradiography of tritiated proline and fucose transported transneuronally from the eye to the visual cortex in pigmented and albino mice." Brain Res **82**(2): 284-92.

Dräger, U. C. (1975). "Receptive fields of single cells and topography in mouse visual cortex." J Comp Neurol **160**(3): 269-90.

Dräger, U. C. (1985). "Birth dates of retinal ganglion cells giving rise to the crossed and uncrossed optic projections in the mouse." Proc R Soc Lond, B, Biol Sci **224**(1234): 57-77.

Dräger, U. C. and D. H. Hubel (1975). "Responses to visual stimulation and relationship between visual, auditory, and somatosensory inputs in mouse superior colliculus." Journal of Neurophysiology **38**(3): 690-713.

Dräger, U. C. and D. H. Hubel (1976). "Topography of visual and somatosensory projections to mouse superior colliculus." Journal of Neurophysiology **39**(1): 91-101.

Elstrott, J., A. Anishchenko, M. Greschner, A. Sher, A. M. Litke, E. J. Chichilnisky and M. B. Feller (2008). "Direction selectivity in the retina is established independent of visual experience and cholinergic retinal waves." Neuron **58**(4): 499-506.

Fan, J., M. L. Woodruff, M. C. Cilluffo, R. K. Crouch and G. L. Fain (2005). "Opsin activation of transduction in the rods of dark-reared Rpe65 knockout mice." J Physiol (Lond) **568**(Pt 1): 83-95.

Frost, D. O. and V. S. Caviness (1980). "Radial organization of thalamic projections to the neocortex in the mouse." J Comp Neurol **194**(2): 369-93.

Gaze, R. M., M. J. Keating and S. H. Chung (1974). "The evolution of the retinotectal map during development in Xenopus." Proc R Soc Lond, B, Biol Sci **185**(80): 301-30.

Godement, P., J. Salaün and M. Imbert (1984). "Prenatal and postnatal development of retinogeniculate and retinocollicular projections in the mouse." J Comp Neurol **230**(4): 552-75.

Gordon, J. A., D. Cioffi, A. J. Silva and M. P. Stryker (1996a). "Deficient plasticity in the primary visual cortex of alpha-calcium/calmodulin-dependent protein kinase II mutant mice." Neuron **17**(3): 491-9.

Gordon, J. A. and M. P. Stryker (1996b). "Experience-dependent plasticity of binocular responses in the primary visual cortex of the mouse." J Neurosci **16**(10): 3274-86.

Grubb, M. S. and I. D. Thompson (2003). "Quantitative characterization of visual response properties in the mouse dorsal lateral geniculate nucleus." Journal of Neurophysiology **90**(6): 3594-607.

Guillery, R. W., C. A. Mason and J. S. Taylor (1995). "Developmental determinants at the mammalian optic chiasm." J Neurosci **15**(7 Pt 1): 4727-37.

Harmer, S. L., S. Panda and S. A. Kay (2001). "Molecular bases of circadian rhythms." Annu Rev Cell Dev Biol **17**: 215-53.

Hattar, S., R. J. Lucas, N. Mrosovsky, S. Thompson, R. H. Douglas, M. W. Hankins, J. Lem, M. Biel, F. Hofmann, R. G. Foster and K.-W. Yau (2003). "Melanopsin and rod-cone photoreceptive systems account for all major accessory visual functions in mice." Nature **424**(6944): 76-81.

Hofbauer, A. and U. C. Dräger (1985). "Depth segregation of retinal ganglion cells projecting to mouse superior colliculus." J Comp Neurol **234**(4): 465-74.

Itasaki, N., S. Bel-Vialar and R. Krumlauf (1999). "'Shocking' developments in chick embryology: electroporation and in ovo gene expression." Nat Cell Biol **1**(8): E203-7.

Jeon, C. J., E. Strettoi and R. H. Masland (1998). "The major cell populations of the mouse retina." J Neurosci **18**(21): 8936-46.

Kalatsky, V. A. and M. P. Stryker (2003). "New paradigm for optical imaging: temporally encoded maps of intrinsic signal." Neuron **38**(4): 529-45.

Krauzlis, R. J., D. Liston and C. D. Carello (2004). "Target selection and the superior colliculus: goals, choices and hypotheses." Vision Res **44**(12): 1445-51.

Kuffler, S. (1953). "Discharge patterns and functional organization of mammalian retina." Journal of Neurophysiology **16**(1): 37-68.

Leamey, C., A. Van Wart and M. Sur (2009). "Intrinsic patterning and experience-dependent mechanisms that generate eye-specific projections and binocular circuits in the visual pathway." Curr Opin Neurobiol.

Lemke, G. and M. Reber (2005). "Retinotectal mapping: new insights from molecular genetics." Annu Rev Cell Dev Biol **21**: 551-80.

Lovejoy, L. P. and R. J. Krauzlis (2010). "Inactivation of primate superior colliculus impairs covert selection of signals for perceptual judgments." Nat Neurosci **13**(2): 261-6.

Mangini, N. J. and A. L. Pearlman (1980). "Laminar distribution of receptive field properties in the primary visual cortex of the mouse." J Comp Neurol **193**(1): 203-22.

Nakamura, H. and D. D. O'Leary (1989). "Inaccuracies in initial growth and arborization of chick retinotectal axons followed by course corrections and axon remodeling to develop topographic order." J Neurosci **9**(11): 3776-95.

Nikonov, S. S., R. Kholodenko, J. Lem and E. N. Pugh (2006). "Physiological features of the S- and M-cone photoreceptors of wild-type mice from single-cell recordings." J Gen Physiol **127**(4): 359-74.

Panda, S., J. B. Hogenesch and S. A. Kay (2002a). "Circadian rhythms from flies to human." Nature **417**(6886): 329-35.

Panda, S., I. Provencio, D. C. Tu, S. S. Pires, M. D. Rollag, A. M. Castrucci, M. T. Pletcher, T. K. Sato, T. Wiltshire, M. Andahazy, S. A. Kay, R. N. Van Gelder and J. B. Hogenesch (2003). "Melanopsin is required for non-image-forming photic responses in blind mice." Science **301**(5632): 525-7.

Panda, S., T. K. Sato, A. M. Castrucci, M. D. Rollag, W. J. DeGrip, J. B. Hogenesch, I. Provencio and S. A. Kay (2002b). "Melanopsin (Opn4) requirement for normal light-induced circadian phase shifting." Science **298**(5601): 2213-6.

Protti, D. A., N. Flores-Herr, W. Li, S. C. Massey and H. Wässle (2005). "Light signaling in scotopic conditions in the rabbit, mouse and rat retina: a physiological and anatomical study." Journal of Neurophysiology **93**(6): 3479-88.

Provencio, I., H. M. Cooper and R. G. Foster (1998). "Retinal projections in mice with inherited retinal degeneration: implications for circadian photoentrainment." J Comp Neurol **395**(4): 417-39.

Provis, J. M., C. M. Diaz and B. Dreher (1998). "Ontogeny of the primate fovea: a central issue in retinal development." Progress in Neurobiology **54**(5): 549-80.

Remtulla, S. and P. E. Hallett (1985). "A schematic eye for the mouse, and comparisons with the rat." Vision Res **25**(1): 21-31.

Silver, J. and J. Sapiro (1981). "Axonal guidance during development of the optic nerve: the role of pigmented epithelia and other extrinsic factors." J Comp Neurol **202**(4): 521-38.

Silver, J. and R. L. Sidman (1980). "A mechanism for the guidance and topographic patterning of retinal ganglion cell axons." J Comp Neurol **189**(1): 101-11.

Simmons, P. A., V. Lemmon and A. L. Pearlman (1982). "Afferent and efferent connections of the striate and extrastriate visual cortex of the normal and reeler mouse." J Comp Neurol **211**(3): 295-308.

Simon, D. K. and D. D. O'Leary (1992). "Development of topographic order in the mammalian retinocollicular projection." J Neurosci **12**(4): 1212-32.

Sperry, R. (1943). "Effect of 180 degree rotation of the retinal field on visuomotor coordination." Journal of Experimental Zoology.

Stein, B. E. and M. A. Meredith (1990). "Multisensory integration. Neural and behavioral solutions for dealing with stimuli from different sensory modalities." Ann N Y Acad Sci **608**: 51-65; discussion 65-70.

Toda, K., R. A. Bush, P. Humphries and P. A. Sieving (1999). "The electroretinogram of the rhodopsin knockout mouse." Vis Neurosci **16**(2): 391-8.

Triplett, J. W., M. T. Owens, J. Yamada, G. Lemke, J. Cang, M. P. Stryker and D. A. Feldheim (2009). "Retinal input instructs alignment of visual topographic maps." Cell **139**(1): 175-85.

Wagner, E., P. McCaffery and U. C. Dräger (2000). "Retinoic acid in the formation of the dorsoventral retina and its central projections." Dev Biol **222**(2): 460-70.

Wagor, E., N. J. Mangini and A. L. Pearlman (1980). "Retinotopic organization of striate and extrastriate visual cortex in the mouse." J Comp Neurol **193**(1): 187-202.

Wang, Q. and A. Burkhalter (2007). "Area map of mouse visual cortex." J Comp Neurol **502**(3): 339-57.

Wang, Q., E. Gao and A. Burkhalter (2011). "Gateways of ventral and dorsal streams in mouse visual cortex." J Neurosci **31**(5): 1905-18.

Yates, P. A., A. L. Roskies, T. Mclaughlin and D. D. O'Leary (2001). "Topographic-specific axon branching controlled by ephrin-As is the critical event in retinotectal map development." J Neurosci **21**(21): 8548-63.

Chapter Two – Summed EphA Receptor Activity is a Determinant of Retinal Ganglion Cell Topography in the Superior Colliculus.

Abstract

Retinal ganglion cells (RGCs) project axons from their cell bodies in the eye to targets in the superior colliculus (SC) of the midbrain. The wiring of these axons to their synaptic targets creates an ordered representation, or 'map,' of retinal space within the brain. Many lines of investigation have demonstrated that the development of this map requires complementary gradients of EphA receptor tyrosine kinases and their ephrin-A ligands, yet basic features of EphA signaling during map formation remain to be resolved. These include the individual roles played by the multiple EphA receptors that make up the retinal EphA gradient. We have developed a set of ratiometric 'Relative Signaling' (RS) rules that quantitatively predict how the composite low-nasal-to-high-temporal EphA gradient is translated into topographic order among RGCs. A key feature of these rules is that the component receptors of the gradient – in the mouse, EphA4, EphA5, and EphA6 – must be functionally equivalent and interchangeable. To test this aspect of the model, we generated compound mutant mice in which the periodicity, slope, and receptor composition of the gradient is systematically altered with respect to the levels of EphA4, EphA5, and a closely related receptor EphA3 that we ectopically express. Analysis of the retinotopic maps of these new mouse mutants establishes the general utility of the RS rules for predicting retinocollicular topography and demonstrates

that individual EphA gene products are approximately equivalent with respect to axon guidance and target selection.

Introduction

Nervous systems frequently organize representations of the external world into 'topographic maps' – systems of synaptic connections in which the positional coordinates of a set of input neurons are maintained in their wiring to synaptic targets (Kaas 1997; Luo et al. 2007). The best known and most intensively studied of such maps is the projection of RGCs from the vertebrate eye to their synaptic targets in the SC (or tectum) of the midbrain (Sperry 1963; O'Leary et al. 1999a). This retinocollicular map is Cartesian, in that the orthogonal nasal-temporal (N-T) and dorsal-ventral (D-V) axes of the retina are mapped onto the orthogonal caudal-rostral (C-R) and lateral-medial (L-M) axes, respectively, of the SC (Figure 2.1A) (Dräger et al. 1976; Law et al. 1980; Lemke et al. 2005).

Roger Sperry hypothesized that molecular cues expressed as orthogonal gradients in the retina and the SC provide spatial information that is critical for the development of retinotopic maps (Sperry 1963). The techniques of molecular biology have since allowed for the identification of some of the hypothesized molecular cues, lending credence to Sperry's theory (O'Leary et al. 1999b; Lemke et al. 2005; Feldheim et al. 2010). Using techniques to visualize the expression patterns of many genes simultaneously, it is now clear that many molecules are expressed in a graded manner in the developing retina (Díaz et al. 2003; Shintani et al. 2004). The function of many of these molecues in the

retina has yet to be determined. However, a molecular description of the establishment and function of a gradient of guidance molecules in the retina is beginning to take shape.

The first step in creating a guidance molecule gradient is the initial patterning of the retina. It is generally believed that gradients of diffusible molecules establish the initial N-T and D-V axes of the retina, similar to the initial axial patterning of the embryo (Chow et al. 2001). Gradients of diffusible molecules are then translated into a graded expression pattern of transcription factors in RGCs (Díaz et al. 2003). The transcription factors Tbx5 (Koshiba-Takeuchi et al. 2000), Pax2 (Dressler et al. 1990; Sanyanusin et al. 1995), and Vax2 (Schulte et al. 1999; Mui et al. 2002) have been observed to be expressed in a gradient along the D-V axis in vertebrates. The transcription factors Vax2 (Mui et al. 2002), FoxD1 (Takahashi et al. 2009), and FoxG1 (Takahashi et al. 2003) are expressed in a gradient on the N-T axis. Some of these transcription factors have been shown to directly instruct the gradient of guidance molecules, e.g. Vax2 instructs the gradient of EphA5 (Mui et al. 2002), but a complete description of the transcriptional control of gradient expression has not been accomplished. Presumably, the combinatorial action of several transcription factors, some graded and some not, patterns the gradient of guidance molecules.

Guidance molecule identification

Friedrich Bonhoeffer and colleagues were able to establish the preference of an RGC for its topographically appropriate region of the tectum using an *in vitro* system in which they cultured chick RGCs from the nasal retina and saw they were repelled by a protein on the posterior tectal membrane (Walter et al. 1987a; Walter et al. 1987b). This

result indicated that one of the guidance molecule interactions of the retinal N-T axis of chemorepulsive; the molecule was later identified as ephrinA2, a ligand for the EphA family of receptors (Cheng et al. 1994). It has since been shown that the EphA receptors and their ligands play a crucial role in guidance of the retinal N-T axis and will be discussed in further detail.

Subsequent studies identified other molecules that act as guidance cues in development of the D-V axis. The EphB receptor tyrosine kinases are expressed in a high ventral to low dorsal gradient in the retina, and their ligands are expressed in a high lateral to low medial gradient in the SC (Hindges et al. 2002). The EphB-ephrinB interaction acts as both an attractant and repellant to pattern mapping of the D-V to M-L axis (McLaughlin et al. 2003a). The receptor tyrosine kinase Ryk is expressed in a high ventral to low dorsal gradient, and its ligand Wnt3 is expressed in a high medial to low lateral gradient in the SC (Schmitt et al. 2006). The Wnt-Ryk interaction is thought to act as a counter-gradient to balance the EphB-ephrinB mediated mapping (Schmitt et al. 2006).

EphA[1] gradients

The initial observation that a protein is involved in the repulsion of temporal RGC axons from the posterior tectum led to the identification of ephrinA2 (Cheng et al. 1994) and ephrinA5 (Drescher et al. 1995), which are both expressed in a low-rostral-to-high-

[1] As members of the Eph family of receptors and their ephrinA ligands were repeatedly discovered in different systems they were each given unique names, which led to profusion of the nomenclature designating each member. A coherent nomenclature for this family was announced and is used in this document without reference to the former names of individual genes. Lemke, G. (1997). "A coherent nomenclature for Eph receptors and their ligands." Mol Cell Neurosci **9**(5-6): 331-2.

caudal gradient in the SC (Cheng et al. 1995). Consistent with these ephrinAs acting as guidance molecules, the mouse knockout of EphrinA2 and EphrinA5 exhibits errors in topography along the R-C axis of the SC (Frisén et al. 1998; Feldheim et al. 2000).

EphrinAs are ligands for the EphA family of receptor protein tyrosine kinases (Gale et al. 1996). RGCs express EphA4, EphA5, and EphA6 (Díaz et al. 2003). Consistent with EphAs acting as guidance molecules, mouse knockouts of EphA4 (Walkenhorst et al. 2000) and EphA5 KO (Feldheim et al. 2004) show targeting errors in the SC. Mouse knockouts of EphA6 are not viable (George Yancopoulos, unpublished communication).

In the mouse, as in the chick, binding of ephrin-As to EphA-receptor-expressing axons is 'chemorepulsive,' in that it induces actin bundling, and axon (and axon branch) retraction (Feldheim et al. 2004). EphAs binding to ephrinAs leads to clustering of receptor-ligand complexes at the cell membrane, and it is the clustering that leads to autophosphorylation and activation of the receptors (Davis et al. 1994). Once activated, EphAs begin an intracellular signaling pathway that culminates in the destabilization of the cytoskeleton (Wahl et al. 2000; Jurney et al. 2002; Wong et al. 2004).

In the retina, RGCs express EphA receptors in a low-nasal-to-high-temporal gradient, and in the SC, ephrin-As are expressed in a low-rostral-to-high-caudal gradient (Reber et al. 2004; McLaughlin et al. 2005). Thus, RGCs expressing the highest level of EphA receptors project to the region of the SC with the lowest levels of ephrin-A, and vice versa (Figure 2.1B). All of these observations are consistent with a role for the chemorepulsive interaction of EphA receptors and ephrinA ligands in the development of retinotopy. In order to demonstrate an instructive role for the *gradient* of EphA receptors

and to understand the mode of gradient action, it is necessary to systematically alter the configuration – the slope, orientation, or periodicity – of the gradient without ablating it, and to then systematically measure changes in the configuration of the resulting retinocollicular map.

We have done so, using a line of *EphA3* knock-in mice and a set of mapping rules that we refer to as the 'Relative Signaling' (RS) model (Reber et al. 2004). Together with a precise measurement of the retinal EphA gradient, the RS model quantitatively predicts how the gradient instructs retinotopic map development. We have now generated a set of combined *EphA3* knock-in*/EphA5* knock-out mouse mutants in which the EphA receptor gradient in the retina is altered, but not ablated, and measured the retinocollicular maps of these new mutants. Analysis of these maps confirms the general utility of the RS model as a method for translating EphA gradients into topographic maps. The accuracy with which the model predicts topography indicates that EphA3, EphA4, EphA5, and EphA6 are largely interchangeable with respect to their activity during mapping, and demonstrates that the shape and relative magnitude of EphA gradients are essentially informative for the development of retinotopy.

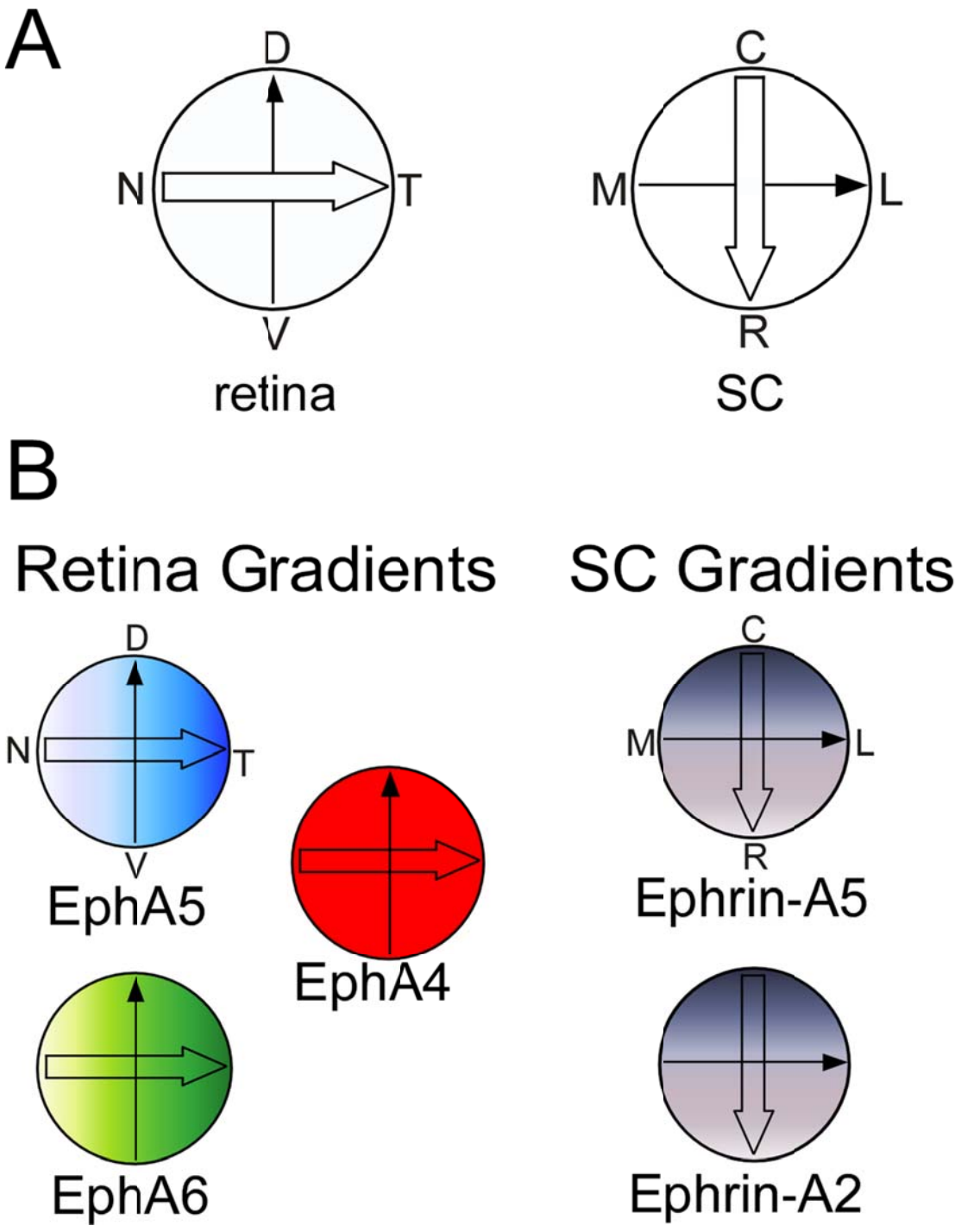
A
D
N
T
V
retina
C
M
L
R
SC
B
Retina Gradients
SC Gradients
D
N
T
V
EphA5
EphA4
EphA6
C
M
L
R
Ephrin-A5
Ephrin-A2

is of

ina,

Results

The Relative Signaling (RS) model

The RS model of topographic mapping is derived from observations originally made in the *Isl2-EphA3* knock-in mouse (Brown et al. 2000). A subset of mouse RGCs (~40%), distributed evenly throughout the retina (i.e., in approximately every other cell), express the transcription factor Islet2 (Isl2) (Pak et al. 2004). In the *Isl2-EphA3* knock-ins, EphA3 is produced ectopically and specifically only in these $Isl2^+$ RGCs (Brown et al. 2000). There are therefore two populations of RGCs that are distinguished by their EphA expression levels: one whose cells express an endogenous level of EphA, and a second whose cells express this endogenous level of EphA plus additional EphA3 (Figure 2. 2A) (Brown et al. 2000). (Target cells of the SC express neither Isl2 nor EphA3.) The added level of EphA3 is the same in all $Isl2^+$ RGCs, and mice that are homozygous for the *Isl2-EphA3* allele express twice as much EphA3 as do *Isl2-EphA3* heterozygotes (Reber et al. 2004).

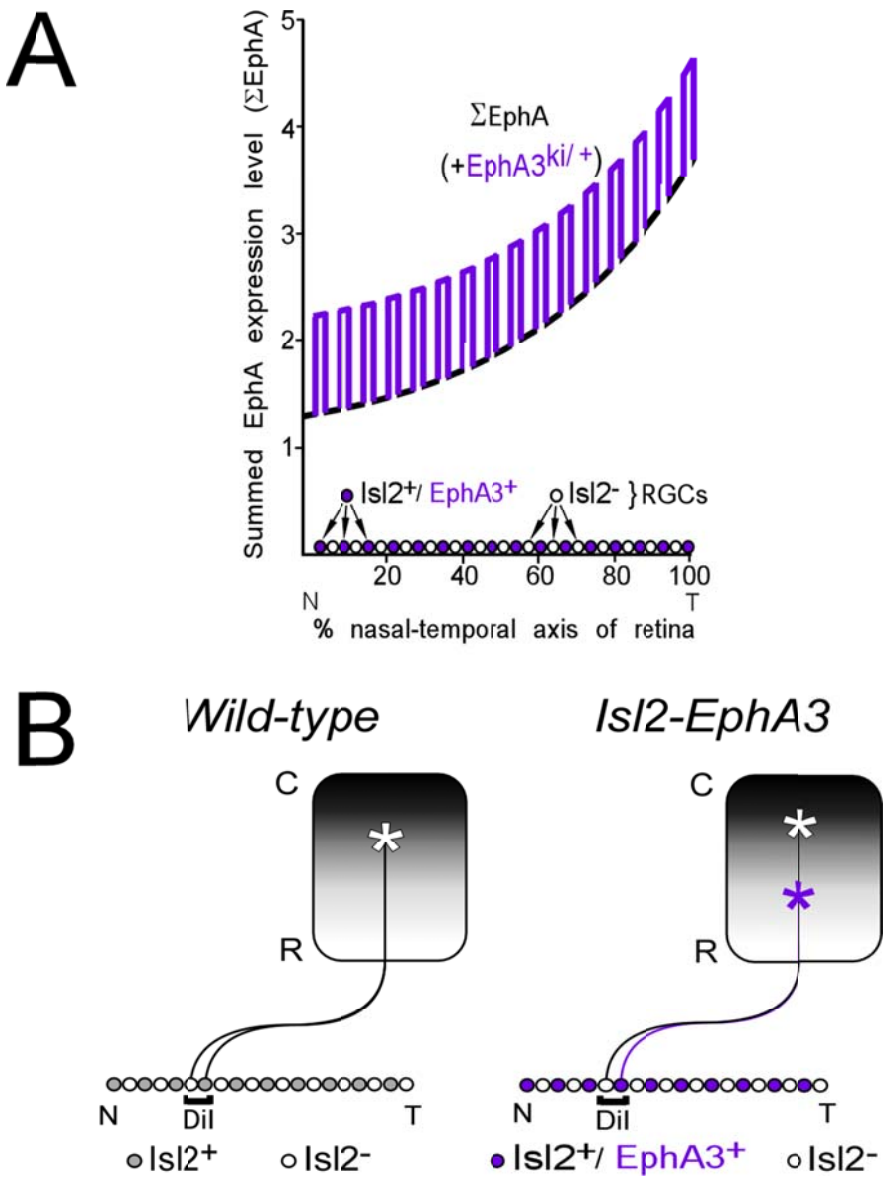
A
Summed EphA expression level (ΣEphA)
5
4
3
2
1
ΣEphA
(+EphA3ki/ +)
Isl2+/ EphA3+
Isl2- } RGCs
20
40
60
80
100
N
T
% nasal-temporal axis of retina
B
Wild-type
Isl2-EphA3
C
R
N
DiI
T
Isl2+
Isl2-
C
R
N
DiI
T
Isl2+/ EphA3+
Isl2-

The retinocollicular map of wild-type mice, as visualized using DiI tracing at postnatal day 7 (P7), is a direct linear transfer of the NT axis of the retina onto the CR axis of the SC (Brown et al. 2000). In marked contrast, *Isl2-EphA3* homozygotes (*Isl2-EphA3*$^{ki/ki}$) display a retinocollicular map that is duplicated across the full NT axis of the retina, in the sense that each point in visual space is represented by two separate points in the SC (Brown et al. 2000; Triplett et al. 2009). A single DiI injection in the retina labels a population of RGCs in the retina consisting of both Isl2^{-} and adjacent Isl2^{+}/EphA3^{+} RGCs. The Isl2^{+}/EphA3^{+} RGCs of a given, labeled population project to a more rostral collicular site than adjacent, labeled Isl2^{-} RGCs due to their increased aggregate EphA expression levels and subsequent increased sensitivity to the chemorepulsive CR gradient of ephrin-A in the SC (Figure 2.2B). The preferential occupation of the rostral SC by axon terminals of EphA3^{+} RGCs displaces the axon terminals of their wild-type counterparts from these sites and thereby shifts the entire wildtype map caudally (Brown et al. 2000).

The retinocollicular map of the heterozygous *Isl2-EphA3* (*Isl2-EphA3*$^{ki/+}$) mouse exhibits a unique property that is not seen in the *Isl2-EphA3*$^{ki/ki}$ mouse – namely, mapping 'collapse' – which has driven both the derivation and analysis of RS mapping rules (Brown et al. 2000; Reber et al. 2004). Like the *Isl2-EphA3*$^{ki/ki}$ mouse, the retinocollicular map of the *Isl2-EphA3*$^{ki/+}$ mouse is duplicated for the nasal-most 76% of the NT axis (nasal = 0, temporal = 100), in that a focal DiI injection in the retina labels two termination zones (TZs) in the SC. In contrast to the *Isl2-EphA3*$^{ki/ki}$ mouse, however, focal DiI injections in the retina of a *Isl2-EphA3*$^{ki/+}$ mouse made at positions more temporal than 76% label only a single TZ in the SC, rather than two (Brown et al. 2000).

We refer to this phenomenon as mapping 'collapse' because it occurs suddenly, without a gradual narrowing of the distance between duplicate TZs. We designate the NT position at which collapse occurs as the 'collapse point' (Reber et al. 2004); for the *Isl2-EphA3*$^{ki/+}$ mice, this point is reached at 76% of the N-T axis of the retina. The RS model provides a causal explanation for why collapse occurs, and why it occurs in the temporal retina.

The RS model makes use of a precise measurement of the gradient of endogenously expressed EphA receptors in the retina. The EphA family of receptor tyrosine kinases consists of eight proteins (EphA 1-8), which all bind to, and are activated by, any of five ephrin-A ligands (Pasquale 2005). The endogenous RGC EphA gradient in wild-type mice is composed of an aggregate of the distributions of the three EphA receptors – EphA4, EphA5, and EphA6 (Marcus et al. 2000; Reber et al. 2004). Together with EphA3, these three receptors occupy the same clade within the EphA family. As single receptors, they bind the principal collicular ligands, ephrin-A2 and -A5, with similar, albeit non-identical affinities (Gale et al. 1996; Monschau et al. 1997). EphA4 is expressed at a constant level across the NT axis of the retina (red curve in Figure 2.3A and equation term in Figure 2.3C), whereas the levels of EphA5 and EphA6 (blue and green curves, respectively, in Figure 2.3A and equation terms in Figure 2.3C) increase smoothly and exponentially from the nasal to the temporal pole (Reber et al. 2004). We have measured these gradients, relative to each other, as mRNA distributions in RGCs across the retina, and have shown that the EphA5 and EphA6 gradients are indeed well fit by exponentials (Reber et al. 2004). The linear summation of EphA4, EphA5, and EphA6 describes the EphA gradient in the retina, and is represented by the term ΣEphA.

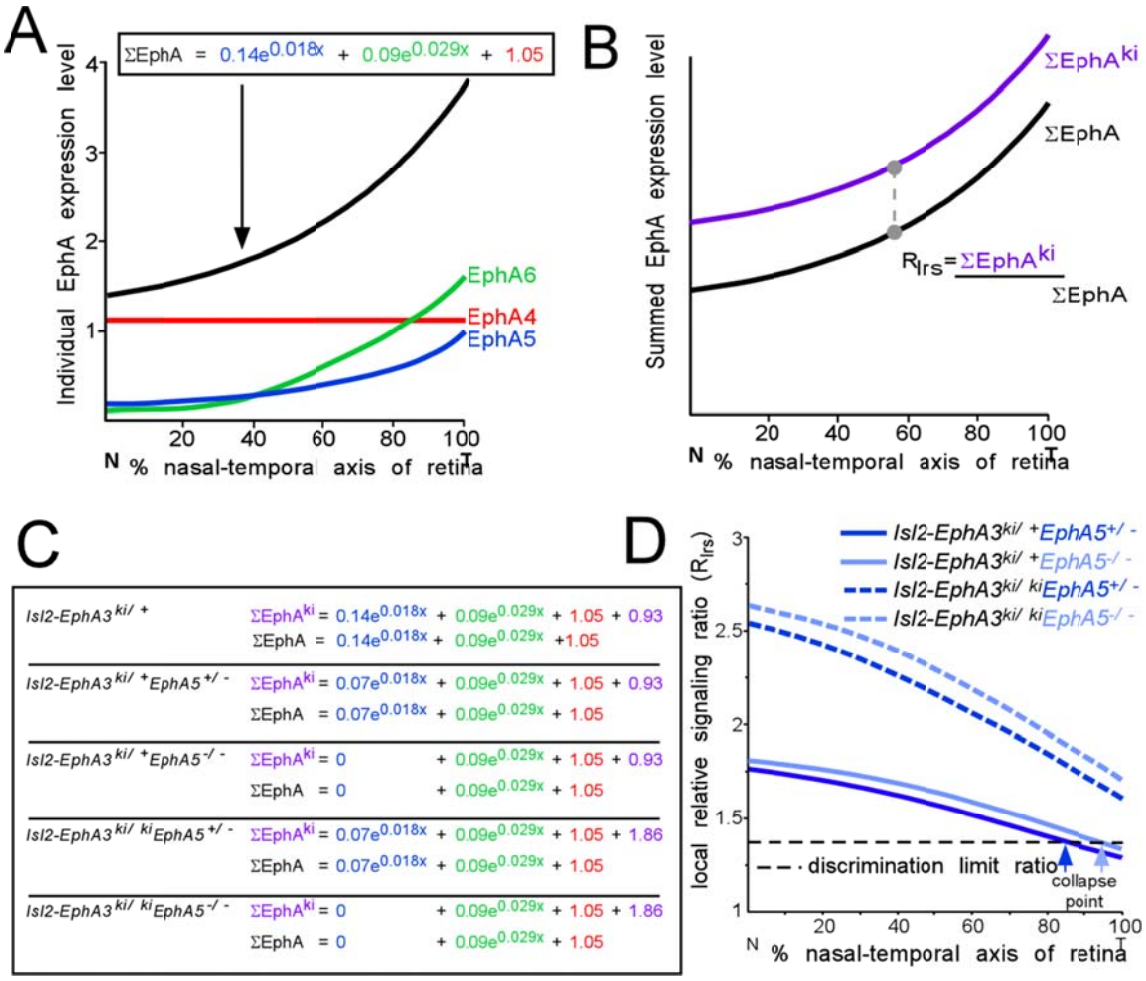

Figure 2.3 Calculation and predictions of the local relative signaling ratio (R_{lrs})

A The EphA gradient of a wild-type mouse is composed of EphA4 (red), EphA5 (blue), and EphA6 (green). Each EphA mRNA is plotted as a function of position on the N-T axis of the retina (x), based on curve fitting of the measured expression levels of each mRNA in Reber et al. 2004. ΣEphA is the total amount of EphA expressed by an RGC at position x on the N-T axis of the retina and is plotted as a linear summation of the functions for each of the endogenously expressed EphAs.

B In *Isl2-EphA3* knock-in mice, $Isl2^+$ RGCs express a constant amount of ectopic EphA3 regardless of their position in the retina; thus, the ΣEphA function for $Isl2^+$ RGCs ($\Sigma EphA^{ki}$) is simply the addition of a constant, corresponding to the measured EphA3 expression level, to the endogenous ΣEphA function. The R_{lrs} function is calculated by dividing $\Sigma EphA^{ki}$ at position x by ΣEphA for the same position x.

C The $\Sigma EphA^{ki}$ and ΣEphA functions for all possible compound *Isl2-EphA3* knock-in/*EphA5* knock-out mutants are shown.

D The R_{lrs} functions of all possible *Isl2-EphA3* knock-in/*EphA5* knock-out mutants are shown. Those genotypes for which the R_{lrs} function falls below the discrimination limit ratio (dashed horizontal line) are predicted to display collapsed maps, with collapse occurring at the location where the R_{lrs} function crosses the discrimination limit ratio (arrows). The *Isl2-EphA3*$^{ki/+}$/*EphA5*$^{+/-}$ and *Isl2-EphA3*$^{ki/+}$/*EphA5*$^{-/-}$ maps are predicted to collapse at 85% and 95%, respectively. The *Isl2-EphA3*$^{ki/ki}$/*EphA5*$^{+/-}$ and *Isl2-EphA3*$^{ki/ki}$/*EphA5*$^{-/-}$ maps are predicted to be fully duplicated.

The two populations of RGCs ($Isl2^+$ and $Isl2^-$) in a knock-in mouse produce two NT gradients of ΣEphA: a normal endogenous gradient (black curve in Figure 2.3A) and a second knock-in gradient that includes ectopic EphA3 (purple curve in Figure 2.3B). In the RS model, collapse occurs when the *ratiometric* difference in EphA signaling between immediately adjacent $Isl2^+/EphA3^+$ and $Isl2^-/EphA3^-$ RGCs is too small for the mapping system to distinguish. In this event, an as-yet-unidentified mapping force causes the adjacent RGCs to map together in the SC, as they would do normally (see Discussion). All $Isl2^+$ RGCs express the same amount of ectopic EphA3, thus, the *absolute* difference in EphA activity between adjacent $Isl2^+$ and $Isl2^-$ RGCs is the same for adjacent RGCs anywhere in the retina. However, the *ratiometric* difference in EphA activity between adjacent $Isl2^+$ and $Isl2^-$ RGCs does change: it decreases from nasal to temporal.

In the RS formalism, the ratiometric difference in EphA signaling between adjacent $Isl2^+/EphA3^+$ and $Isl2^-/EphA3^-$ RGCs is designated the local relative signaling ratio (R_{lrs}) (Reber et al. 2004). The equation for R_{lrs} as a function of NT position is given by dividing the ΣEphA equation for the knock-in distribution by that for the wild-type distribution (Figure 2.3B) (Reber et al. 2004). The value of R_{lrs} below which the system cannot discriminate is the 'discrimination limit ratio' and can be directly derived from the R_{lrs} function and the location of map collapse in *Isl2-EphA3*$^{ki/+}$ mice: this occurs at 76% of the NT axis of the retina, where the value of R_{lrs} is 1.36 (Reber et al. 2004). Thus, the discrimination limit ratio is 1.36, and when the R_{lrs} function falls below this value – *in any mouse genotype* - the retinocollicular map is predicted to collapse.

The R_{lrs} function can be changed by altering either the slope or magnitude of the underlying ΣEphA equation, which can be done experimentally either by increasing the dosage of the knock-in allele, as in the *Isl2-EphA3*$^{ki/ki}$ mice, or by crossing this knock-in mouse with knock-out mice for one or more of the *EphA* genes that contribute to the endogenous, wild-type gradient. The latter manipulation is particularly powerful since R_{lrs} can be systematically changed in the absence of any change to the absolute level of EphA3 expression. We have performed this manipulation previously by crossing the *Isl2-EphA3* knock-in mice with an *EphA4* knock-out (Reber et al. 2004). These crosses produce four genotypes of mice, which are either *Isl2-EphA3*$^{ki/ki}$ or *Isl2-EphA3*$^{ki/+}$ and at the same time express either half as much (*EphA4*$^{+/-}$), or do not express (*EphA4*$^{-/-}$), EphA4. Each of these genotypes has its own R_{lrs} function that predicts if mapping collapse either does or does not occur, and if it does, at what position along the NT axis of the retina collapse is observed (Reber et al. 2004).

EphA5 tests of the RS model

These results notwithstanding, several salient features and underlying assumptions of the RS model remain to be assessed. Among the most critical of these is the assumption that all of the EphA receptor genes expressed by RGCs – EphA4, EphA5, EphA6, and in the knock-ins, EphA3 - are functionally interchangeable and equivalent. This very stringent assumption is implicit in the expectation that ΣEphA, the summed value of EphA4, EphA5, and EphA6 at each point along the NT axis of the retina, accurately describes the functional properties of the aggregate EphA gradient, and translates directly into differences in aggregate EphA *activity* during mapping. Indeed,

ΣEphA has no functional meaning unless EphA3-6 are interchangeable. To alter ΣEphA we have made use of an *EphA5* knock-out mouse that carries an in-frame insertion of beta-galactosidase, which preserves the extracellular, transmembrane, and juxtamembrane domains of the EphA5 protein but ablates its tyrosine kinase activity (Feldheim et al., 2004; Cooper et al. 2009). We have tested the predictions of the RS model by generating compound mutants of the *Isl2-EphA3* knock-in allele and the *EphA5* knock-out allele and measuring their retinocollicular maps.

The predictions of the RS rules with regard to EphA5 loss-of-function are made by modifying the previously described RS equations to reflect the contribution of EphA5 to the endogenous ΣEphA gradient. The R_{lrs} functions for all possible *Isl2-EphA3* knock-in/*EphA5* knock-out compound mutant mice, based on the measured exponential distribution of EphA5 in the retina (Reber et al. 2004), are displayed in Figure 2.3D. These functions are generated by dividing the equations that describe the aggregate heterozygous knock-in EphA level ($\Sigma EphA^{ki}$) as a function of NT retinal position in the relevant genotype by the equation that describes aggregate wild-type EphA level (ΣEphA) as a function of NT retinal position in the same genotype (Figure 2.3C). These R_{lrs} functions predict collapse points at 85% and 95% for the $Isl2\text{-}EphA3^{ki/+}/EphA5^{+/-}$ and $Isl2\text{-}EphA3^{ki/+}/EphA5^{-/-}$ mice, respectively, based on where the R_{lrs} function crosses the discrimination limit ratio (Figure 2.3D). The R_{lrs} functions for the $Isl2\text{-}EphA3^{ki/k/i}/EphA5^{+/-}$ and $Isl2\text{-}EphA3^{ki/ki}/EphA5^{-/-}$ mice predict non-collapsing maps since these R_{lrs} curves do not cross the discrimination limit ratio (Figure 2.3D).

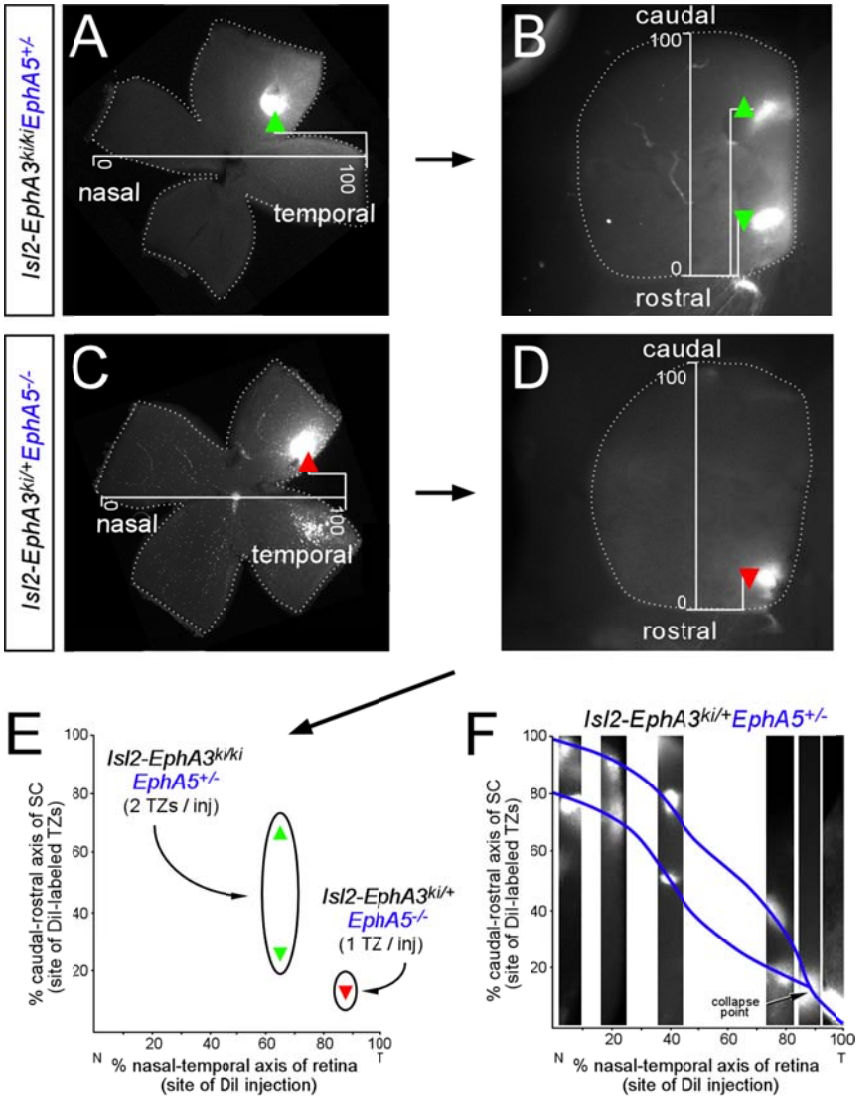

Figure 2.4 Visualization and measurement of the retinocollicular maps *of Isl2-EphA3* knock-in/ *EphA5* knock-out compound mutant mice

A An example of the injection site in the retina visualized in a whole mount preparation. The location of the injection site is mapped as percentage of the nasal-temporal axis of the retina. The SC corresponding to this retina is shown in panel B.

B An example of the termination zone of labeled RGC axons in the SC visualized in a whole mount preparation. The location of the termination zone(s) is mapped as percentage of the rostral-caudal axis of the SC. This SC displays two distinct termination zones.

C The injection site and retina corresponding to the SC in panel D.

D The termination zone of the retina seen in panel C. A single, well defined TZ is visible.

E Data points are plotted on a Cartesian graph. Each map point (black box) is at the intersection of the location of the injection site in the retina, plotted on the x axis, and the location of the TZ(s) in the SC, plotted on the y axis. The points shown correspond to the retina and SC of panels A and B (green) and panels C and D (red).

F A map for any genotype is made by plotting multiple map points from animals of the same genotype. Sections of the SC of multiple animals are shown at the position of the x axis corresponding to the location of their respective injections in the retina (not shown). The blue line represents the continuity of the map *in vivo*. The points shown here correspond to the *Isl2-EphA3* $^{ki/+}$*/EphA5* $^{+/-}$ genotype.

We measured the retinocollicular maps of these mice anatomically, using focal retinal injections of DiI (Brown et al., 2000; Reber et al., 2004). DiI injected into the retina (Figures 2.4A and 2.4C) diffuses down the axons of RGCs into the SC and becomes concentrated at synaptic TZs, where it is readily visualized in collicular whole mounts 24 hours after injection (Figures 2.4B and 2.4D). An example of a single TZ is shown in Figure 2.4B and an example of a duplicated TZ is shown in Figure 2.4D. To visualize the entire retino-collicular map of any given genotype, we plot multiple data points on a Cartesian graph where the x axis is the N-T axis of the retina and the y axis is the R-C axis of the SC. The location site of the injection and the corresponding TZ(s) are then plotted as points on this graph (Figure 2.4C). Systematic injections across the full NT extent of the retina, together with careful measurement of the nasal-temporal position of the injection site and the rostral-caudal axial position of the collicular TZ(s) labeled by these injections, allows for a delineation of the entire retinocollicular map for a given genotype (Figure 2.4F).

The RS model makes two precise predictions about compound Isl2-EphA3 knock-in, EphA5 knock-out compound mutants: whether or not the map will be fully duplicated, and if the map is not fully duplicated, at what point along the N-T axis of the retina the map will collapse from duplicated to single. The first prediction is binary, with collapse either occurring or not, and testing this prediction is a straightforward matter of observing if the map is fully duplicated or not. The second prediction is analog – collapse could occur anywhere along the retinal N-T axis. Testing the second prediction requires a precise measurement of the location on the retinal N-T axis where collapse is seen. We

have used the locations of the lateral and medial rectus muscles, on the exterior of the globe, to determine the nasal and temporal poles of the retina, respectively. Mice do not have an appreciable fovea (Jeon et al. 1998) or any other landmark within the retina to determine the orientation of the location of the nasal and temporal poles after dissection. Thus, we must rely on the accuracy of our dissections to determine the location of the injection site within the retina with the acknowledgment that there is some error in this measurement but any attempt to precisely quantify that error would be speculation.

The *Isl2-EphA3*$^{ki/+}$*/EphA5*$^{+/-}$ and *Isl2-EphA3*$^{ki/+}$*/EphA5*$^{-/-}$ maps that we measured using these methods are shown in Figures 2.5A and 2.5B, respectively. As predicted, both of these maps display the phenomenon of mapping collapse in the temporal retina. In addition, their collapse points are situated at approximate positions along the NT axis – 85% and 95%, respectively – that are predicted by the location at which the R_{lrs} functions of Figure 2.3 cross the discrimination limit ratio.

The RS rules predict that all compound mutants of *Isl2-EphA3*$^{ki/ki}$ homozygous knock-ins and any combination of *EphA4*, *EphA5*, or *EphA6* knock-outs, either heterozygous or homozygous, should all exhibit fully duplicated, non-collapsing retinocollicular maps that are largely indistinguishable from each other. This is due to the fact that the *Isl2-EphA3*$^{ki/ki}$ homozygous knock-ins already display a fully duplicated map (Triplett et al. 2009), and all reductions in endogenous EphA levels that are generated by crossing the knock-ins with any *EphA* knock-outs result in increases in R_{lrs}. The *Isl2-EphA3*$^{ki/ki}$*/EphA5*$^{+/-}$ and *Isl2-EphA3*$^{ki/ki}$*/EphA5*$^{-/-}$ maps are shown in Figures 2.5C and 2.5D, respectively. As predicted, both genotypes show fully duplicated, non-collapsing maps.

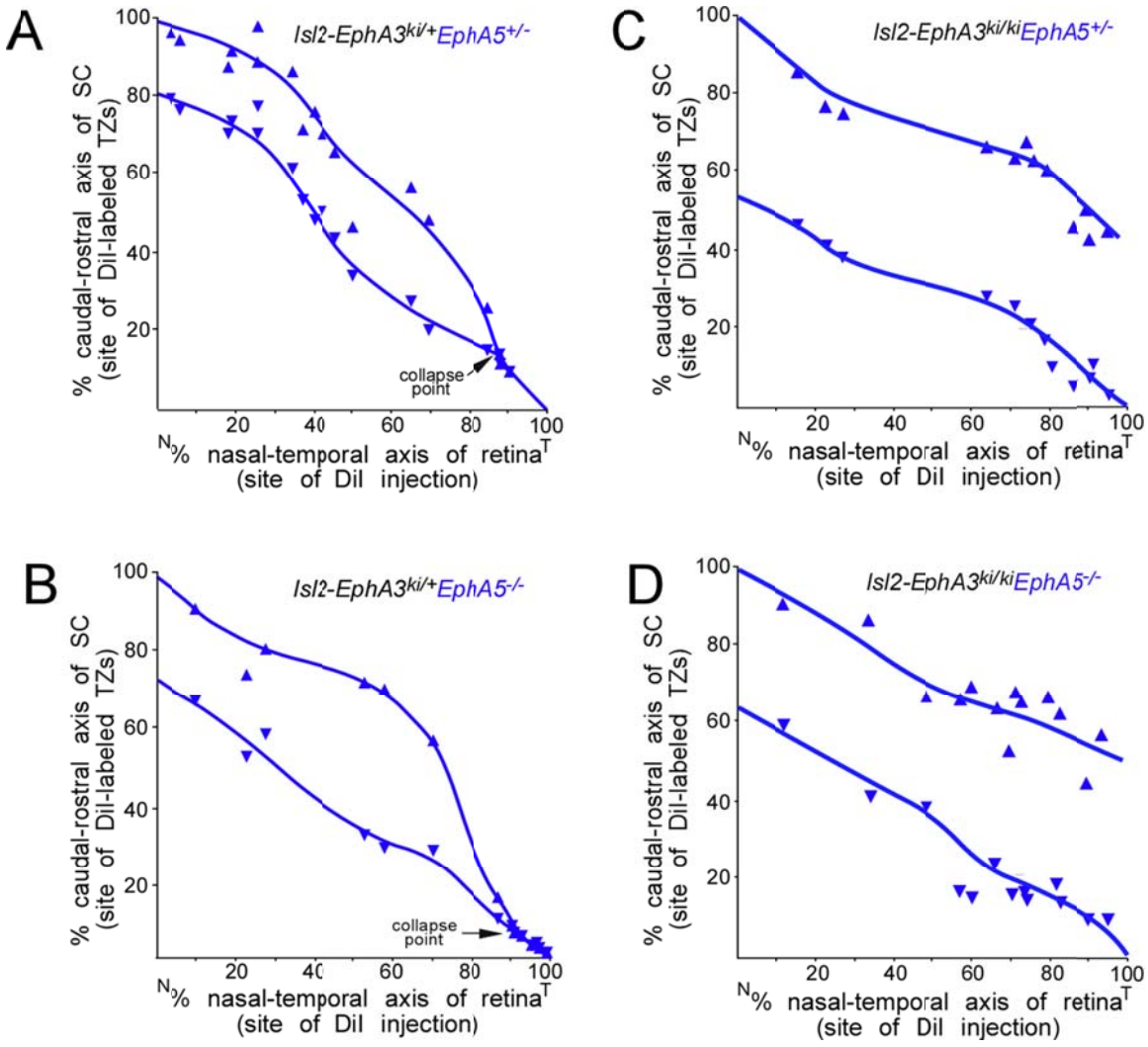

Figure 2.5 Anterograde labeling of Isl2-EphA3 knockin, EphA5 knockout compound mutant retinocollicular maps.

A Retinocollicular map of *Isl2-EphA3$^{ki/+}$/EphA5$^{+/-}$* compound mutant. The position of the injection site in the retina is graphed on the x axis. The position of TZ(s) in the SC is graphed on the y axis. Each pair of points corresponds to a single retinal injection in a single mouse. The upward pointing triangles correspond to the caudal TZ in an animal with two TZs. The downward pointing triangles correspond to the rostral TZ in an animal with two TZs. The hourglass shapes correspond to a collapsed TZ in an animal showing a single TZ. The collapse point is located at about 85% of the NT axis, which is at the predicted position.

B Retinocollicular map of *Isl2-EphA3$^{ki/+}$/EphA5$^{-/-}$* compound mutant. As predicted, the map collapses. The collapse point is located at about 90% of the NT axis, which is very close to the predicted position.

C Retinocollicular map of *Isl2-EphA3$^{ki/ki}$/EphA5$^{+/-}$* compound mutant. As predicted, the map is fully duplicated.

D Retinocollicular map of *Isl2-EphA3$^{ki/ki}$/EphA5$^{-/-}$* compound mutant. As predicted, the map is fully duplicated.

Relative signaling also predicts mapping density

The *Isl2-EphA3*$^{ki/+}$*/EphA5*$^{+/-}$, */EphA5*$^{-/-}$, */EphA4*$^{+/-}$, and */EphA4*$^{-/-}$ compound mutant mice all display retinocollicular maps that collapse, with collapse points that closely match those predicted by the RS rules. However, there is a striking difference in the extent of rostral-caudal separation of duplicated collicular TZs between the *EphA4* and *EphA5* loss-of-function compound mutants. TZ separation in the *Isl2-EphA3*$^{ki/+}$*/EphA5*$^{+/-}$ compound mutants is ~20% of the collicular CR axis (Figure 2.5A) – an axial separation that is very similar to that seen in the *Isl2-EphA3*$^{ki/+}$ knock-ins alone (Brown et al. 2000). The average TZ separation in the *Isl2-EphA3*$^{ki/+}$*/EphA5*$^{-/-}$ mice (~30%; Figure 2.5B) is only slightly greater than that of the *Isl2-EphA3*$^{ki/+}$*/EphA5*$^{+/-}$ mice. In marked contrast, TZ separation in the *Isl2-EphA3*$^{ki/+}$*/EphA4*$^{+/-}$ and */EphA4*$^{-/-}$ mice is much larger – greater than 50% of the CR SC axis (Reber et al., 2004).

In all of the ten different genotypes of knock-in mice that we have analyzed, the number of Isl2^{+} RGCs is constant, and these Isl2^{+} RGCs always map to the rostral portion of the SC. The rostral-caudal separation of TZs is therefore a direct measurement of the density of Isl2^{+} RGCs in the rostral portion of the SC (Figure 2.6A). Under the ratiometric RS formalism, the mapping density, that is, the number of RGCs mapping within a given SC area, of Isl2^{+} RGCs should be determined by the total amount of EphA expressed by Isl2^{+} RGCs relative to the total amount of EphA expressed by Isl2^{-} RGCs. This ratio, which we refer to as the Population Relative Signaling Ratio (R_{prs}), is analogous to the R_{lrs} described previously but is a function of the total amount of EphA expressed by all RGCs of a given type, Isl2^{+} or Isl2^{-}. Given our measurement of the EphA receptor expression levels in RGCs, R_{prs} can be calculated precisely for any

compound mutant mouse using the steps described below. The total amount of EphA expressed by a given population of RGCs ($Isl2^+$ or $Isl2^-$) is calculated by integrating the ΣEphA function for that RGC population across the entire NT axis of the retina (Figure 2.6B). The R_{prs} is then calculated by dividing the integral of the ΣEphA for $Isl2^+$ RGCs by the integral of the ΣEphA function for $Isl2^-$ RGCs (Figure 2.6C). The R_{prs} values for all *Isl2-EphA3* knock-in and *EphA4* or *EphA5* knock-out compound mutant geneotypes, are plotted on the x axis of Figure 2.6D, with the area of the SC occupied by $Isl2^+$ RGCs plotted on the y axis. The area of the SC occupied by $Isl2^+$ RGCs is inversely proportional to the R_{prs} value, which is consistent with the chemo-repulsive action of EphA-ephrin-A forward signaling.

In all maps that collapse, $Isl2^-$ RGCs from the temporal retina are 'pulled' into the rostral SC, causing them to map onto the entire rostral-caudal extent of the SC. The density of $Isl2^-$ RGCs is therefore the same for all genotypes in collapsed maps. The $Isl2^-$ RGCs that move into the rostral SC open up space in more caudal areas, where $Isl2^+$ RGCs can then map. Mapping collapse causes the density of RGCs in the SC to become heterogeneous, and the extent to which $Isl2^+$ RGCs move into the caudal colliculus is proportional to the value of R_{prs}. Without mapping collapse, the density of RGC mapping will be homogenous throughout the SC. The density of $Isl2^+$ and $Isl2^-$ RGCs is therefore always the same in maps that are fully duplicated, despite dramatic differences in R_{prs} values between genotypes. In wild-type maps, the mapping density is homogenous because the R_{prs} value is one.

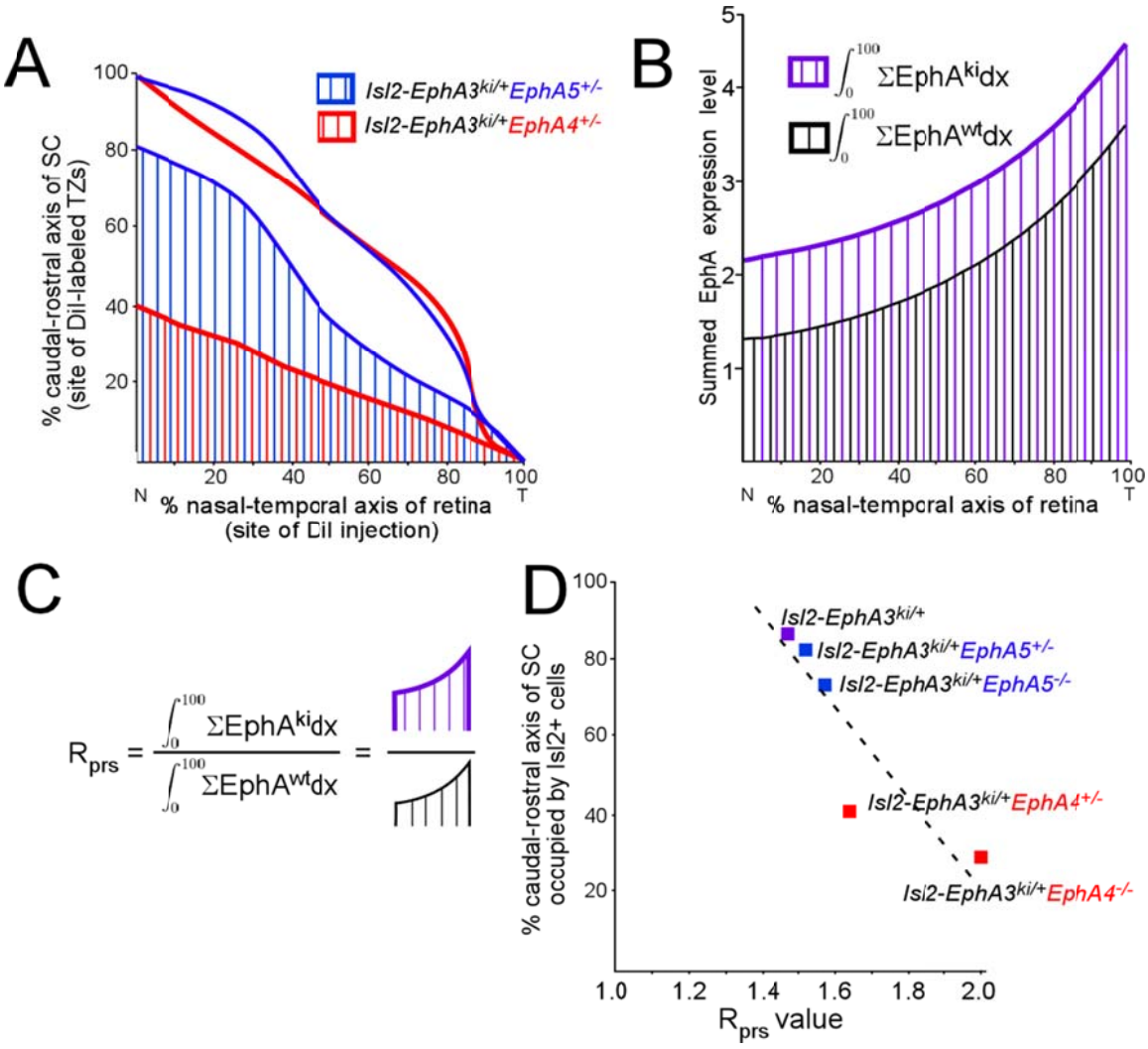

Figure 2.6 Population relative signaling ratio and mapping density

A The retinocollicular maps for mice of the *Isl2-EphA3$^{ki/+}$/EphA5$^{+/-}$* genotype (blue lines) and *Isl2-EphA3$^{ki/+}$/EphA4$^{+/-}$* genotype (red lines) (Reber et al. 2004) are shown. The lower line of each map corresponds to the location of Isl2^{+} RGCs. The area covered with vertical lines shows the area of the SC where Isl2^{+} RGCs map in *Isl2-EphA3$^{ki/+}$/EphA5$^{+/-}$* mice (blue lines) and *Isl2-EphA3$^{ki/+}$/EphA4$^{+/-}$* mice (red lines).

B The total amount of EphA expressed by a population of RGCs can be calculated by integrating the function for ΣEphA for that population of RGCs for x=0 to x=100, which corresponds to the entire NT axis of the retina. The integral for ΣEphA^{ki} (purple) will always be larger than that for ΣEphA (black) in a knock-in mouse.

C The population relative signaling ratio R_{prs} is calculated for any given genotype by dividing the integral of the ΣEphA^{ki} function by the integral of the ΣEphA relevant for that genotype.

D The R_{prs} values for *Isl2-EphA3$^{ki/+}$* compound mutants (x axis) and the percentage of the SC occupied by Isl2^{+} RGCs (y axis) are shown.

The EphA5$^{-/-}$ retinocollicular map

The RS rules predict that the retinocollicular maps of straight *EphA4*, *EphA5* or *EphA6* knock-out mice should be very similar to the map of wild-type mice (Reber et al., 2004); that is, there should be no appreciable effect on the configuration of the map by removing these individual receptors. This prediction, which has not been tested rigorously, arises from the application of 'general relative signaling' rules, which are a straightforward extension of the local relative signaling rules (Reber et al., 2004). We have previously demonstrated that the application of general relative signaling yields the wild-type retinocollicular map in the mouse (Reber et al., 2004). In the general RS formalism, the configuration of the wild-type mouse retinocollicular map is predicted, with remarkable accuracy by simply dividing the measured ΣEphA value at the extreme temporal pole of the retina ($\Sigma EphA_t$) by the equation that specifies ΣEphA as a function of position across the NT axis of the retina (Reber et al., 2004). This operation yields the ΣEphA ratio between the temporal pole RGC and all other RGCs across this axis, which is designated the general RS ratio (R_{grs}). [Note that the *local* relative signaling ratio for immediately adjacent RGCs (R_{lrs}) is derived by simply dividing their respective R_{grs} values (Reber et al., 2004).] We asked whether a general RS rule would predict the NT-to-CR retinocollicular map in *EphA5* mouse knock-outs, which retain expression of the EphA4 and EphA6 components of the endogenous ΣEphA gradient.

The general RS ratio (R_{grs}) equation for *EphA5*$^{-/-}$ mice, which lack the graded EphA5 component of the composite ΣEphA gradient, is indicated and plotted in Figure

2.7A. This plot is very similar to both the predicted and measured wild-type retinocollicular map (Reber et al., 2004). The *EphA5*$^{-/-}$ retinocollicular map that we determined by repeated DiI injections is illustrated in Figure 2.7B. With the exception of the nasal third of the retina, where there is a slight rostral deviation from prediction, this measured *EphA5*$^{-/-}$ map is in very close agreement with the *EphA5*$^{-/-}$ map predicted by general relative signaling.

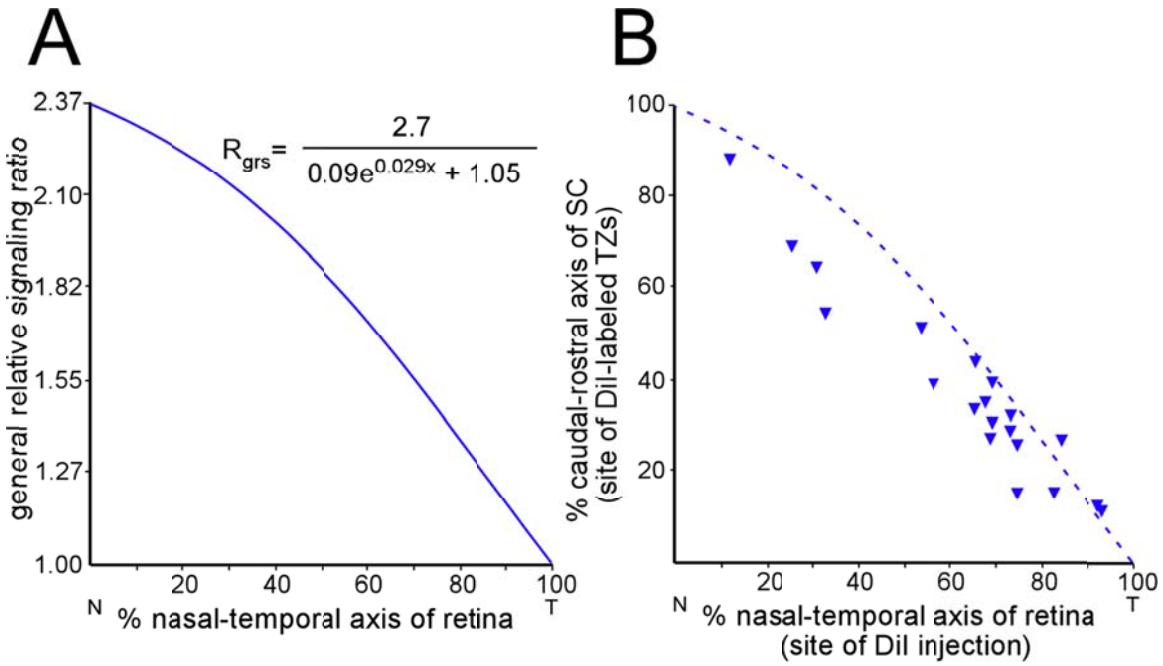

Figure 2.7 General relative signaling prediction of the *EphA5*$^{-/-}$ map

A The general relative signaling ratio (R_{grs}) function is calculated by dividing the ΣEphA value at the temporal pole of the retina by the ΣEphA value at position x. The R_{grs} function of *EphA5*$^{-/-}$ mice is shown. The value of the R_{grs} is plotted on the y-axis for each position along the N-T (x) axis of the retina.

B The *EphA5*$^{-/-}$ retinocollicular map, as determined by repeated DiI injections across the NT axis of the retina, is shown (blue triangles) superimposed on the R_{grs} function (dashed blue line).

Discussion

Requirement of a specific EphA gradient for the development of retinotopy

Sperry's chemoaffinity hypothesis has been a guiding principle of the study of neural development since its inception (Sperry, 1963). Genetic and molecular experiments have clearly demonstrated that for mapping of the NT axis of the retina onto the CR axis of the SC the EphA receptors and collicular ephrin-A ligands act as the molecular cues of Sperry's hypothesis (Flanagan and Vanderhaeghen, 1998). However, to specify position using a limited number of molecular cues the developing nervous system must use the information contained within the gradient of gene expression *levels* (Gierer 1988). A formal test of this hypothesis requires a quantitative model of the role that gradients play in topographic mapping, followed by tests of the model's predictions. Relative Signaling (Reber et al., 2004) is one such a model and we here report its ability to predict topography across multiple novel genotypes.

The rules of the RS model are based on the principle that topographic order is established through ratiometric differences in EphA receptor expression and signaling activity among RGCs. These ratiometric differences may be manipulated experimentally. As detailed above, by removing half or all of the graded EphA5 receptor in the *Isl2-EphA3/EphA5* compound mutants, we have altered both the periodicity and the *slope* of the ΣEphA gradient. In contrast, our earlier tests of the RS model altered the periodicity and the *magnitude* of the EphA receptor gradient, by removing half or all of ungraded EphA4 in the *Isl2 EphA3/EphA4* compounds mutants (Reber et al., 2004). These different

manipulations lead to distinct sets of RS ratios, yet in all settings, it is these ratios that set the configuration of the retinocollicular map.

EphA forward signaling during development

The robustness of the RS rules across multiple EphA3, EphA4, and EphA5 mutant mouse genotypes supports the implicit assumption that the activities of these proteins are equivalent with respect to the events of retinocollicular mapping. As noted above, this assumption is reflected in the summation of EphA receptor activity to yield ΣEphA and in the predictions made by ratiometric RS difference comparisons in ΣEphA (rather than individual EphA receptors). Although the measured binding affinities of EphA3, EphA4, EphA5, and EphA6 for ephrin-A2 and ephrin-A5 are not identical (Gale et al., 1996; Monschau et al., 1997), these measurements were generally carried out in settings in which the binding of artificially-clustered single ephrin-As were monitored against a single EphA receptor. This is not the case *in vivo*, where multiple EphAs typically signal as exceptionally large, multimeric complexes that often interact with multiple ephrin-As (Palmer et al. 2003). It is therefore possible that the observed equivalence of EphAs in retinocollicular mapping might reflect signaling complex averaging of differences in individual EphA-ephrin-A affinities. It should be noted that the interchangeability of EphAs with respect to retinocollicular mapping is dramatically evident in evolution. The principal graded EphA receptor that contributes to the RGC gradient in the chick, where the EphA gradient was first discovered, is EphA3 (Cheng et al. 1995). This receptor is not even expressed by mouse RGCs (Brown et al., 2000), which instead substitute EphA5

and EphA6. The phenomenon of EphA equivalence in retinocollicular mapping may have general relevance since EphA receptors guide cytoskeletal rearrangements in many additional biological contexts outside of the nervous system (Pasquale, 2005).

Previous tests of the RS model relied on the addition or removal of a complete EphA gene or cDNA. In the experiments described above, we instead used an EphA5 mutant in which the intracellular kinase domain of EphA5 is replaced by lacZ, which yields RGCs that produce an EphA5 protein that retains its ability to bind to ligands but is kinase-dead (Feldheim et al., 2004). Beta-galactosidase staining is evident in the optic tract of these *EphA5-lacZ* mutant mice at post-natal day 5 (our unpublished data; Cooper et al., 2009), suggesting that RGC localization of mutant EphA5 is similar to that of wild-type. The fact that the predictions of the RS model are valid in these mice suggests that ΣEphA represents both the summed expression level and the summed *kinase activity* of its component EphA receptors.

Competition/Relative Signaling as a mapping constraint

The RS model integrates competition as a constraint based on previous theoretical considerations of retino-collicular mapping. Experiments showing map compression, in which part of the SC is removed before development of retinotopy and all of the RGCs are compressed into the remaining SC and map expansion, in which part of the retina is removed and the remaining RGCs expand their map to cover the entire SC (Schmidt et al. 1978; Sharma 1972), demonstrated that the mapping process requires an element of competition among RGCs for a limiting factor present in the SC (Prestige et al. 1975).

Likewise, for compression and expansion of the map to occur, RGCs must read their molecular cues *relative* to other RGCs. Competition is evident in the mapping behavior of *Isl2-EphA3* homozgotes alone. In these mice, the TZs of all wild-type RGCs are pushed caudally from their normal mapping position by their Isl2+/EphA3+ neighbors, in spite of the fact that their ΣEphA profile is entirely normal (Brown et al., 2000).

Many models of retinocollicular mapping have posited that competition between RGCs for a limiting factor in the SC (Goodhill et al. 2005) balances the unidirectional force of EphA-ephrin-A forward signaling, but a molecular basis for competition in mapping has not been established. We present an extension of the RS model that describes the mapping *density* of a population of RGCs in the SC - the population relative signaling ratio (R_{prs}) – and that also reflects competition. Calculation of the R_{prs} involves an arithmetic that is very similar to that of the R_{lrs} but applies this arithmetic to a *population* of cells (RGCs) rather than to a pair of cells. The ability of the R_{prs} ratio to reconcile mapping density and population EphA expression levels suggests that changes in mapping density are a manifestation of competition.

A final indicator of opponent activities is the sudden mapping collapse that we consistently see across multiple compound genotypes heterozygous for the *Isl2- EphA3* allele. At the point at which mapping collapse occurs, adjacent Isl2+/EphA3+ and Isl2-/EphA3- RGCs are subject to two opponent effects: a disparity in ΣEphA that pushes these RGCs apart with respect to their termination in the SC, and a correlation in the pattern of their firing that brings their TZs together (Butts 2002). When the ratiometric difference in ΣEphA is too low for the mapping system to discriminate, the effect of correlated activity is suddenly revealed, causing collapse. Correlated electrical firing is

well-known for its ability to refine and consolidate retinocollicular TZs (McLaughlin et al. 2003b; Chandrasekaran et al. 2005; Mrsic-Flogel et al. 2005; Cang et al. 2008), although the molecules that underlie this activity remain a focus of study.

EphA reverse signaling during development

EphAs can act as ligands for ephrinA expressing cells and this ephrinA-EphA reverse signaling has been shown to inhibit the outgrowth of axon branches (Rashid et al. 2005; Lim et al. 2008). Co-expressed ephrinAs and EphAs localize to different membrane domains, allowing EphA forward and reverse signaling to be segregated (Marquardt et al. 2005). The ectopic expression of ephrinAs in cells projecting an axon to a target leads to abnormal mapping of olfactory sensory neurons (Cutforth et al. 2003) and motor neurons (Marquardt et al. 2005).

EphAs are expressed in a high-caudal-to-low-rostral gradient in the SC, and ephrinAs are expressed in a high-nasal-to-low-temporal gradient by RGCs (Rashid et al. 2005; Lim et al. 2008). A mouse knock-out of EphA7, one of the EphAs expressed as a gradient in the SC, leads to errors in mapping in the SC (Rashid et al. 2005). A mouse knock-out of P75, a presumptive co-receptor for ephrinAs acting as a receptor, also shows mapping errors in the SC (Lim et al. 2008).

These activities and mapping relationships have led to a proposed role of EphA reverse signaling in topographic mapping (Feldheim et al. 2010) as a repulsive countergradient system, similar to that of the EphA-ephrin-A forward signaling gradient but orientated in such a way that the maximal repulsion is situated at the rostral end of the

SC, effectively countering the force of the EphA-ephrin-A forward signal (Gierer 1988; Goodhill and Xu 2005). The RS model, as described here, does not take into account the predicted diminution of EphA reverse signaling that would be expected to occur with EphA4 and EphA5 loss of function, as both these EphAs are expressed in the SC (Walkenhorst et al. 2000; Feldheim et al. 2004). Thus, to the extent that our model is correct in its predictions, EphA reverse signaling does not play a role in retino-collicular mapping. However, other interpretations of the data generated here may be consistent with EphA reverse signaling playing a role in mapping. The key experiment of ectopically expressing an ephrinA in RGCs has yet to be carried out.

Comparison of the RS model with in silico considerations of retino-collicular mapping

Models of biological phenomena may be more informative than direct observation of experimental data alone. Computational models highlight parts of a complex process to make it more easily understood, but must, at the same time, also ignore or overly simplify other parts of that same process. A model is, by necessity, "a simplification and an idealization, and consequently a falsification" (Turing 1952). A complete model of retinotopic map formation requires greater detail than the RS model (Goodhill et al. 1999), and many computational models attempt to model the process in its entirety (Goodhill 2007). These models are usually too complex to be directly tested by tractable *in vivo* experiments and are instead tested *in silico*. In fact, these models are often tested by their ability to recreate the altered topography in Isl2-EphA3 knock-in animals reported in Brown et al. 2000 and Reber et al. 2004, and can also be tested using the data

we report here (Honda 2003; Koulakov et al. 2004; Willshaw 2006; Simpson et al. 2011). The RS model provides useful information that would not be apparent without computation, while at the same time makes concrete, prospective, testable predictions as to the configuration of the map in genetically manipulated animals that grounds abstraction in experimental data.

Further applications of the Relative Signaling model

The cellular mechanisms of map formation that we infer from the utility of the RS model, such as the aggregate signaling of EphA receptors, may also be crucial for the development of topography in other locations where EphA receptors are expressed as gradients. These include the olfactory bulb (Cutforth et al. 2003), the projections of motor neurons to muscles (Helmbacher et al. 2000; Eberhart et al. 2002; Kania et al. 2003), and the hippocampal-septal projection (Gao et al. 1996). Indeed, many aspects of neural development dynamics are similar to those of retinotopic mapping and may be governed by relative signaling rules similar to those we describe.

Chapter Two, in part, is a reprint of the material which has been submitted for publication. I was the primary researcher, Dr. Greg Lemke and Dr. Michael Reber directed and supervised the research which forms the basis for this chapter.

Materials and Methods

Animal Subjects

The *Isl2-EphA3* knock-in (Brown et al., 2000), *EphA4* knock-out (Dottori et al. 1998), and *EphA5* knock-out (Feldheim et al., 2004) mice have all been described previously. All procedures used in these experiments were reviewed and approved by the Institutional Animal Care and Use Committee at the Salk Institute for Biological Studies. Animals were cared for and used in accordance with guidelines of the *U.S. Public Health Service Policy on Humane Care and Use of Laboratory Animals* and the *NIH Guide for the Care and Use of Laboratory Animals* and following institutional Association for Assessment and Accreditation of Laboratory Animal Care-approved practices.

Anterograde labeling

RGC axons were anterogradely labeled by a focal injection of DiI (1,1'-dioctadecyl-3,3,3'3'-tetramethylindocarbocyanine perchlorate) into the retina, as described previously (Brown et al. 2000; Reber et al. 2004). DiI was dissolved in dimethylformamide, loaded into a pulled glass pipette, and pressure injected into the retina using a picospritzer. P7-8 mice were injected and the DiI was given 24 hours to migrate along RGC axons, after which time the mice were sacrificed and their SC dissected. The SC was visualized in a whole mount preparation using rhodamine optics on a Zeiss axioskop 2 upright scope using a 2.5X objective. The retina was fixed for 48-72 hours in 2% PFA and then dissected and visualized as a whole mount preparation.

References

Brown, A., P. A. Yates, P. Burrola, D. Ortuño, A. Vaidya, T. M. Jessell, S. L. Pfaff, D. D. O'Leary and G. Lemke (2000). "Topographic mapping from the retina to the midbrain is controlled by relative but not absolute levels of EphA receptor signaling." Cell **102**(1): 77-88.

Butts, D. A. (2002). "Retinal waves: implications for synaptic learning rules during development." The Neuroscientist : a review journal bringing neurobiology, neurology and psychiatry **8**(3): 243-53.

Cang, J., L. Wang, M. P. Stryker and D. A. Feldheim (2008). "Roles of Ephrin-As and Structured Activity in the Development of Functional Maps in the Superior Colliculus." Journal of Neuroscience **28**(43): 11015-11023.

Chandrasekaran, A. R., D. T. Plas, E. Gonzalez and M. C. Crair (2005). "Evidence for an instructive role of retinal activity in retinotopic map refinement in the superior colliculus of the mouse." J Neurosci **25**(29): 6929-38.

Cheng, H. J. and J. G. Flanagan (1994). "Identification and cloning of ELF-1, a developmentally expressed ligand for the Mek4 and Sek receptor tyrosine kinases." Cell **79**(1): 157-68.

Cheng, H. J., M. Nakamoto, A. D. Bergemann and J. G. Flanagan (1995). "Complementary gradients in expression and binding of ELF-1 and Mek4 in development of the topographic retinotectal projection map." Cell **82**(3): 371-81.

Chow, R. L. and R. A. Lang (2001). "Early eye development in vertebrates." Annu Rev Cell Dev Biol **17**: 255-96.

Cooper, M. A., D. P. Crockett, R. S. Nowakowski, N. W. Gale and R. Zhou (2009). "Distribution of EphA5 receptor protein in the developing and adult mouse nervous system." J Comp Neurol **514**(4): 310-28.

Cutforth, T., L. Moring, M. Mendelsohn, A. Nemes, N. M. Shah, M. M. Kim, J. Frisén and R. Axel (2003). "Axonal ephrin-As and odorant receptors: coordinate determination of the olfactory sensory map." Cell **114**(3): 311-22.

Davis, S., N. W. Gale, T. H. Aldrich, P. C. Maisonpierre, V. Lhotak, T. Pawson, M. Goldfarb and G. D. Yancopoulos (1994). "Ligands for EPH-related receptor tyrosine kinases that require membrane attachment or clustering for activity." Science **266**(5186): 816-9.

Díaz, E., Y. H. Yang, T. Ferreira, K. C. Loh, Y. Okazaki, Y. Hayashizaki, M. Tessier-Lavigne, T. P. Speed and J. Ngai (2003). "Analysis of gene expression in the developing mouse retina." Proc Natl Acad Sci USA **100**(9): 5491-6.

Dottori, M., L. Hartley, M. Galea, G. Paxinos, M. Polizzotto, T. Kilpatrick, P. F. Bartlett, M. Murphy, F. Köntgen and A. W. Boyd (1998). "EphA4 (Sek1) receptor tyrosine kinase is required for the development of the corticospinal tract." Proc Natl Acad Sci USA **95**(22): 13248-53.

Dräger, U. C. and D. H. Hubel (1976). "Topography of visual and somatosensory projections to mouse superior colliculus." Journal of Neurophysiology **39**(1): 91-101.

Drescher, U., C. Kremoser, C. Handwerker, J. Löschinger, M. Noda and F. Bonhoeffer (1995). "In vitro guidance of retinal ganglion cell axons by RAGS, a 25 kDa tectal protein related to ligands for Eph receptor tyrosine kinases." Cell **82**(3): 359-70.

Dressler, G. R., U. Deutsch, K. Chowdhury, H. O. Nornes and P. Gruss (1990). "Pax2, a new murine paired-box-containing gene and its expression in the developing excretory system." Development **109**(4): 787-95.

Eberhart, J., M. E. Swartz, S. A. Koblar, E. B. Pasquale and C. E. Krull (2002). "EphA4 constitutes a population-specific guidance cue for motor neurons." Dev Biol **247**(1): 89-101.

Feldheim, D. A., Y. I. Kim, A. D. Bergemann, J. Frisén, M. Barbacid and J. G. Flanagan (2000). "Genetic analysis of ephrin-A2 and ephrin-A5 shows their requirement in multiple aspects of retinocollicular mapping." Neuron **25**(3): 563-74.

Feldheim, D. A., M. Nakamoto, M. Osterfield, N. W. Gale, T. M. DeChiara, R. Rohatgi, G. D. Yancopoulos and J. G. Flanagan (2004). "Loss-of-function analysis of EphA receptors in retinotectal mapping." J Neurosci **24**(10): 2542-50.

Feldheim, D. A. and D. D. M. O'Leary (2010). "Visual map development: bidirectional signaling, bifunctional guidance molecules, and competition." Cold Spring Harb Perspect Biol **2**(11): a001768.

Frisén, J., P. A. Yates, T. Mclaughlin, G. C. Friedman, D. D. O'Leary and M. Barbacid (1998). "Ephrin-A5 (AL-1/RAGS) is essential for proper retinal axon guidance and topographic mapping in the mammalian visual system." Neuron **20**(2): 235-43.

Gale, N. W., S. J. Holland, D. M. Valenzuela, A. Flenniken, L. Pan, T. E. Ryan, M. Henkemeyer, K. Strebhardt, H. Hirai, D. G. Wilkinson, T. Pawson, S. Davis and G. D. Yancopoulos (1996). "Eph receptors and ligands comprise two major specificity subclasses and are reciprocally compartmentalized during embryogenesis." Neuron **17**(1): 9-19.

Gao, P. P., J. H. Zhang, M. Yokoyama, B. Racey, C. F. Dreyfus, I. B. Black and R. Zhou (1996). "Regulation of topographic projection in the brain: Elf-1 in the hippocamposeptal system." Proc Natl Acad Sci USA **93**(20): 11161-6.

Gierer, A. (1988). "Spatial organization and genetic information in brain development." Biol Cybern **59**(1): 13-21.

Goodhill, G. and J. Xu (2005). "The development of retinotectal maps: A review of models based on molecular gradients." Network: Computation in Neural Systems.

Goodhill, G. J. (2007). "Contributions of theoretical modeling to the understanding of neural map development." Neuron **56**(2): 301-11.

Goodhill, G. J. and L. J. Richards (1999). "Retinotectal maps: molecules, models and misplaced data." Trends Neurosci **22**(12): 529-34.

Helmbacher, F., S. Schneider-Maunoury, P. Topilko, L. Tiret and P. Charnay (2000). "Targeting of the EphA4 tyrosine kinase receptor affects dorsal/ventral pathfinding of limb motor axons." Development **127**(15): 3313-24.

Hindges, R., T. McLaughlin, N. Genoud, M. Henkemeyer and D. D. M. O'Leary (2002). "EphB forward signaling controls directional branch extension and arborization required for dorsal-ventral retinotopic mapping." Neuron **35**(3): 475-87.

Honda, H. (2003). "Competition between retinal ganglion axons for targets under the servomechanism model explains abnormal retinocollicular projection of Eph receptor-overexpressing or ephrin-lacking mice." J Neurosci **23**(32): 10368-77.

Jeon, C. J., E. Strettoi and R. H. Masland (1998). "The major cell populations of the mouse retina." J Neurosci **18**(21): 8936-46.

Jurney, W. M., G. Gallo, P. C. Letourneau and S. C. McLoon (2002). "Rac1-mediated endocytosis during ephrin-A2- and semaphorin 3A-induced growth cone collapse." J Neurosci **22**(14): 6019-28.

Kaas, J. H. (1997). "Topographic maps are fundamental to sensory processing." Brain Res Bull **44**(2): 107-12.

Kania, A. and T. M. Jessell (2003). "Topographic motor projections in the limb imposed by LIM homeodomain protein regulation of ephrin-A:EphA interactions." Neuron **38**(4): 581-96.

Koshiba-Takeuchi, K., J. K. Takeuchi, K. Matsumoto, T. Momose, K. Uno, V. Hoepker, K. Ogura, N. Takahashi, H. Nakamura, K. Yasuda and T. Ogura (2000). "Tbx5 and the retinotectum projection." Science **287**(5450): 134-7.

Koulakov, A. A. and D. N. Tsigankov (2004). "A stochastic model for retinocollicular map development." BMC neuroscience **5**: 30.

Law, M. I. and M. Constantine-Paton (1980). "Right and left eye bands in frogs with unilateral tectal ablations." Proc Natl Acad Sci USA **77**(4): 2314-8.

Lemke, G. (1997). "A coherent nomenclature for Eph receptors and their ligands." Mol Cell Neurosci **9**(5-6): 331-2.

Lemke, G. and M. Reber (2005). "Retinotectal mapping: new insights from molecular genetics." Annu Rev Cell Dev Biol **21**: 551-80.

Lim, Y.-S., T. McLaughlin, T.-C. Sung, A. Santiago, K.-F. Lee and D. D. M. O'Leary (2008). "p75(NTR) mediates ephrin-A reverse signaling required for axon repulsion and mapping." Neuron **59**(5): 746-58.

Luo, L. and J. Flanagan (2007). "Development of continuous and discrete neural maps." Neuron.

Marcus, R. C., G. A. Matthews, N. W. Gale, G. D. Yancopoulos and C. A. Mason (2000). "Axon guidance in the mouse optic chiasm: retinal neurite inhibition by ephrin "A"-expressing hypothalamic cells in vitro." Dev Biol **221**(1): 132-47.

Marquardt, T., R. Shirasaki, S. Ghosh, S. E. Andrews, N. Carter, T. Hunter and S. L. Pfaff (2005). "Coexpressed EphA receptors and ephrin-A ligands mediate opposing actions on growth cone navigation from distinct membrane domains." Cell **121**(1): 127-39.

McLaughlin, T., R. Hindges, P. A. Yates and D. D. M. O'Leary (2003a). "Bifunctional action of ephrin-B1 as a repellent and attractant to control bidirectional branch extension in dorsal-ventral retinotopic mapping." Development **130**(11): 2407-18.

McLaughlin, T. and D. D. M. O'Leary (2005). "Molecular gradients and development of retinotopic maps." Annu Rev Neurosci **28**: 327-55.

McLaughlin, T., C. L. Torborg, M. B. Feller and D. D. M. O'Leary (2003b). "Retinotopic map refinement requires spontaneous retinal waves during a brief critical period of development." Neuron **40**(6): 1147-60.

Monschau, B., C. Kremoser, K. Ohta, H. Tanaka, T. Kaneko, T. Yamada, C. Handwerker, M. R. Hornberger, J. Löschinger, E. B. Pasquale, D. A. Siever, M. F. Verderame, B. K. Müller, F. Bonhoeffer and U. Drescher (1997). "Shared and distinct functions of RAGS and ELF-1 in guiding retinal axons." EMBO J **16**(6): 1258-67.

Mrsic-Flogel, T. D., S. B. Hofer, C. Creutzfeldt, I. Cloëz-Tayarani, J.-P. Changeux, T. Bonhoeffer and M. Hübener (2005). "Altered map of visual space in the superior colliculus of mice lacking early retinal waves." J Neurosci **25**(29): 6921-8.

Mui, S. H., R. Hindges, D. D. M. O'Leary, G. Lemke and S. Bertuzzi (2002). "The homeodomain protein Vax2 patterns the dorsoventral and nasotemporal axes of the eye." Development **129**(3): 797-804.

O'Leary, D. D. and D. G. Wilkinson (1999a). "Eph receptors and ephrins in neural development." Curr Opin Neurobiol **9**(1): 65-73.

O'Leary, D. D., P. A. Yates and T. Mclaughlin (1999b). "Molecular development of sensory maps: representing sights and smells in the brain." Cell **96**(2): 255-69.

Pak, W., R. Hindges, Y.-S. Lim, S. L. Pfaff and D. D. M. O'Leary (2004). "Magnitude of binocular vision controlled by islet-2 repression of a genetic program that specifies laterality of retinal axon pathfinding." Cell **119**(4): 567-78.

Palmer, A. and R. Klein (2003). "Multiple roles of ephrins in morphogenesis, neuronal networking, and brain function." Genes Dev **17**(12): 1429-50.

Pasquale, E. B. (2005). "Eph receptor signalling casts a wide net on cell behaviour." Nat Rev Mol Cell Biol **6**(6): 462-75.

Prestige, M. C. and D. J. Willshaw (1975). "On a role for competition in the formation of patterned neural connexions." Proc R Soc Lond, B, Biol Sci **190**(1098): 77-98.

Rashid, T., A. L. Upton, A. Blentic, T. Ciossek, B. Knöll, I. D. Thompson and U. Drescher (2005). "Opposing gradients of ephrin-As and EphA7 in the superior colliculus are essential for topographic mapping in the mammalian visual system." Neuron **47**(1): 57-69.

Reber, M., P. Burrola and G. Lemke (2004). "A relative signalling model for the formation of a topographic neural map." Nature **431**(7010): 847-53.

Sanyanusin, P., L. A. Schimmenti, L. A. McNoe, T. A. Ward, M. E. Pierpont, M. J. Sullivan, W. B. Dobyns and M. R. Eccles (1995). "Mutation of the PAX2 gene in a family with optic nerve colobomas, renal anomalies and vesicoureteral reflux." Nat Genet **9**(4): 358-64.

Schmidt, J. T. and S. S. Easter (1978). "Independent biaxial reorganization of the retinotectal projection: a reassessment." Experimental brain research Experimentelle Hirnforschung Expérimentation cérébrale **31**(2): 155-62.

Schmitt, A. M., J. Shi, A. M. Wolf, C.-C. Lu, L. A. King and Y. Zou (2006). "Wnt-Ryk signalling mediates medial-lateral retinotectal topographic mapping." Nature **439**(7072): 31-7.

Schulte, D., T. Furukawa, M. A. Peters, C. A. Kozak and C. L. Cepko (1999). "Misexpression of the Emx-related homeobox genes cVax and mVax2 ventralizes the retina and perturbs the retinotectal map." Neuron **24**(3): 541-53.

Sharma, S. C. (1972). "Redistribution of visual projections in altered optic tecta of adult goldfish." Proc Natl Acad Sci USA **69**(9): 2637-9.

Shintani, T., A. Kato, J. Yuasa-Kawada, H. Sakuta, M. Takahashi, R. Suzuki, T. Ohkawara, H. Takahashi and M. Noda (2004). "Large-scale identification and characterization of genes with asymmetric expression patterns in the developing chick retina." J Neurobiol **59**(1): 34-47.

Simpson, H. D. and G. J. Goodhill (2011). "A simple model can unify a broad range of phenomena in retinotectal map development." Biol Cybern.

Sperry, R. W. (1963). "Chemoaffinity in the orderly growth of nerve fiber patterns and connections." Proc Natl Acad Sci USA **50**: 703-10.

Takahashi, H., H. Sakuta, T. Shintani and M. Noda (2009). "Functional mode of FoxD1/CBF2 for the establishment of temporal retinal specificity in the developing chick retina." Dev Biol.

Takahashi, H., T. Shintani, H. Sakuta and M. Noda (2003). "CBF1 controls the retinotectal topographical map along the anteroposterior axis through multiple mechanisms." Development **130**(21): 5203-15.

Triplett, J. W., M. T. Owens, J. Yamada, G. Lemke, J. Cang, M. P. Stryker and D. A. Feldheim (2009). "Retinal input instructs alignment of visual topographic maps." Cell **139**(1): 175-85.

Turing, A. (1952). "The Chemical Basis of Morphogenesis." Philosophical Transactions of the Royal Society of London. Series BBiological Sciences **237**(641): 37-72.

Wahl, S., H. Barth, T. Ciossek, K. Aktories and B. K. Mueller (2000). "Ephrin-A5 induces collapse of growth cones by activating Rho and Rho kinase." J Cell Biol **149**(2): 263-70.

Walkenhorst, J., D. Dütting, C. Handwerker, J. Huai, H. Tanaka and U. Drescher (2000). "The EphA4 receptor tyrosine kinase is necessary for the guidance of nasal retinal ganglion cell axons in vitro." Mol Cell Neurosci **16**(4): 365-75.

Walter, J., S. Henke-Fahle and F. Bonhoeffer (1987a). "Avoidance of posterior tectal membranes by temporal retinal axons." Development **101**(4): 909-13.

Walter, J., B. Kern-Veits, J. Huf, B. Stolze and F. Bonhoeffer (1987b). "Recognition of position-specific properties of tectal cell membranes by retinal axons in vitro." Development **101**(4): 685-96.

Willshaw, D. (2006). "Analysis of mouse EphA knockins and knockouts suggests that retinal axons programme target cells to form ordered retinotopic maps." Development **133**(14): 2705-17.

Wong, E. V., J. A. Kerner and D. G. Jay (2004). "Convergent and divergent signaling mechanisms of growth cone collapse by ephrinA5 and slit2." J Neurobiol **59**(1): 66-81.

Chapter Three – Correlated Activity and Retinotopic Mapping

Abstract

It has been hypothesized that neural activity instructs the development of retinotopic maps by creating patterns of activity that lead to rearrangements of synaptic connections between cells. During the time period when retinocollicular mapping occurs, the retina exhibits spontaneous neural activity. The activity is patterned such that adjacent RGCs in the retina fire synchronously and non-adjacent RGCs fire asynchronously. This pattern of activity may be instructive to the development of retinotopy. Mice lacking the β2 subunit of the nicotinic acetylcholine receptor do not have normally patterned activity in the retina and also have altered retinocollicular projections. To test whether patterned activity in the retina is instructive for the development of retinocollicular topography, we crossed mice that do not express the β2 subunit of the nicotinic acetylcholine receptor with the *Isl2-EphA3* knock-in mice described in Chapter two. If the collapse phenomenon described in *Isl2-EphA3* heterozygous mice is caused by an instructive, activity-based mechanism, then the combined *β2* knock-out, *Isl2-EphA3* heterozygous knock-in mouse should not show a collapse. The results of RGC labeling experiments done in compound mutant mice were ambiguous, making it difficult to determine whether activity is instructive for retinocollicular mapping.

Introduction

Instructive activity based mechanisms

Neurons undergo rapid and reversible changes in membrane potential in response to both extracellular and intracellular processes. This activity is required for the nervous system to make the rapid computations necessary for an organism to quickly respond to its environment. Electrical activity occurs during a time scale of milliseconds, which is several orders of magnitude faster than the cellular processes of axon guidance and cellular migration that occur during CNS development. Despite the difference in time scales, it is clear that activity can instruct the development of cellular location and connections in the nervous system (Harris 1981). For example, the work of David Hubel and Torsten Wiesel demonstrated that activity is instructive in the formation of ocular dominance columns in the visual cortex (Wiesel 1982).

Donald Hebb postulated that action by a pre-synaptic neuron could act to permanently increase the efficacy of synaptic transmission between the pre- and post-synaptic cell, and this activity-instructed change in synaptic efficacy could serve as the cellular basis of memory (Hebb 1966). It has been hypothesized that activity instructs the development of ocular dominance columns through an associative learning mechanism similar to that originally proposed by Donald Hebb (Stent 1973). Subsequent studies have demonstrated that electrical activity does indeed instruct synaptic efficacy (Caporale et al. 2008) as well as cellular morphology and gene expression (Flavell et al. 2008; Shen et al. 2010). Indeed, many of these processes are now accepted to be the molecular basis of learning and memory in adult animals (Kandel 2009).

While it is now generally accepted that activity can, and does, instruct the development and efficacy of synapses, gene expression, morphology of individual cells, and the architecture of some neural circuits, it remains to be demonstrated that activity instructs the development of retinotopic maps in mammals. The experiments described in this chapter aimed to determine whether activity is *instructive* to the development of the retinotopic map in the mouse SC.

RGC activity is necessary for retinotopic mapping

To test if activity, either patterned or unpatterned, is required for retinotopic mapping, one can simply inhibit all activity in RGCs and observe the effect on retinotopic maps. This can be done by exposing RGCs to Tetrodotoxin (TTX), a sodium channel blocker that inhibits all action potentials (Evans 1972). In non-mammalian vertebrates, reports of the effects of intraocular TTX injection during retino-tectal mapping are contradictory and differ among species (Cline 1991). These discrepancies may be due to differential and incomplete sensitivities to TTX among species, differing roles of activity in retinotopic mapping among species, or subtle differences among the experimental techniques used. In rodents, intraocular injections of TTX result in an increase in the number of cells that are mis-targeted in the SC (O'Leary et al. 1986). These experiments demonstrate that activity plays a role in retinotopic mapping, as TTX injections do change the map. These experiments, however, do not demonstrate what role activity plays in mapping.

Activity in the perinatal retina is patterned

The retina of teleosts and amphibians continues to grow throughout the life of the animal, requiring continuous refinement of retinotectal projections to maintain accurate retinotopic maps as new RGCs are born and project axons to the tectum (Gaze et al. 1974). While mapping occurrs, RGC activity is driven by visual stimuli (Demas et al. 2011). Altering the nature of the visual stimuli that the animals are subjected to alters the formation of their retinotopic maps (Yoon 1975; Schmidt et al. 1985; Udin 1985; Keating et al. 1986).

In contrast, retinotopic mapping in mammals occurs before eye opening (Simon et al. 1992a). RGCs show spontaneous activity not induced by light, beginning in utero (Galli et al. 1988) and continuing until eye opening (Wong 1999). Using multi-electrode arrays, it was observed that the spontaneous activity in the retina is spatially synchronized, meaning that cells located near each other in the retina are more likely to fire at the same moment than cells located far from each other (Meister et al. 1991; Wong et al. 1993). Calcium imaging, in which fluorescent indicators of cellular influx of calcium ions are used to monitor cellular activity, were used to image the activity of large portions of the retina in *ex vivo* preparations (Feller et al. 1997). Using this technique, it became clear that spontaneous activity in RGCs propagates across the retina, creating waves of activity beginning at various locations, propagating for a finite distance, and then dying out (Feller et al. 1997). After cells participate in a wave they are refractory to participation in subsequent waves (Feller et al. 1997).

In the mouse, the properties of retinal waves undergo three distinct stages defined by the pharmacological properties of the waves (Torborg et al. 2005). Stage I waves

occur in the embryonic retina and are blocked by gap junction blockers (Stacy et al. 2005). Stage II waves begin at postnatal day 0 (P0), which is when cholinergic synapses between RGCs and cells of the inner plexiform layer of the retina develop (Zheng et al. 2006). Stage II waves can be blocked by nicotinc acetycholine receptor (nAChR) antagonists (Feller et al. 1996). Stage III waves begin at postnatal day 10 and can be blocked by ionotropic glutamate receptor antagonists (Bansal et al. 2000). Retinocollicular mapping is concurrent with the presence of stage II waves; thus, I will refer to stage II waves simply as 'waves.'

During the time of stage II waves, starburst amacrine cells (SACs) are the only source of acetylcholine in the retina (Zhou 2001). SACs are spontaneously active without synaptic input (Zheng et al. 2006) and form active synapses with each other and with RGCs (Zhou 1998). Wave activity is initiated by the spontaneous activity of SACs, and propagates to adjacent SACs, which also depolarize neighboring RGCs (Zheng et al. 2006) (Butts et al. 1999). SACs downregulate expression of nAchRs around P10, causing stage II wave activity to end (Zheng et al. 2004).

Wave activity may contain spatial information instructive for topographic mapping

The spatiotemporal properties of wave activity, such as wave domain size, interwave interval, and wavefront velocity are statistically similar among retinas (Feller et al. 1997). The properties of wave activity contain spatial information about the distance between a pair of RGCs: adjacent RGCs are likely to fire at the same time because they are activated by a wave at the same time, whereas RGCs separated by a

short distance will be activated by the same wave, but with a time delay as the wave travels between RGCs (Butts et al. 2001). Similarly, wave activity also contains information about whether RGCs whose axons terminate in the same topographic location in the LGN are in the same or different eyes: RGCs located in the same eye will have highly correlated activity patterns whereas RGCs located in different eyes will not have correlated activity patterns (Butts et al. 2001). Thus, wave activity contains information that could be instructive for the development of topography in the SC and the LGN, as well as eye-specific segregation in the LGN (Butts 2002).

Correlated activity could be translated into cellular function through the coincidence detecting properties of the NMDA subclass of glutamate receptors. The NMDA receptor requires both extracellular glutamate and post-synaptic depolarization in order for it to open (Mayer et al. 1984). Once opened, the NMDA receptor allows both sodium and calcium ions to flux through it (MacDermott et al. 1986). The influx of calcium ions leads to a signaling cascade in the postsynaptic cell (Greer et al. 2008), which can lead to long-lasting changes in synaptic efficacy and changes in cellular morphology (Bliss et al. 1993).

RGCs release glutamate into the synapse formed between RGCs and their target cells in the SC, where NMDA receptors are expressed (Simon et al. 1992b). Consistent with NMDA receptors playing a role in retinotopic mapping, pharmacological inhibition of NMDA receptor activity alters retinotectal mapping in amphibians (Cline et al. 1989; Scherer et al. 1989) and teleosts (Schmidt 1990). In rodents, inhibition of NMDA activity prevents retraction (Simon et al. 1992b).

Together, these observations suggest a model of activity-instructed development that occurs in several steps (Eglen et al. 2003; Grubb et al. 2003; McLaughlin et al. 2003). The first step is the creation of an imprecise retinotopic map instructed by molecular cues. Wave activity in the retina creates correlated activity patterns between RGCs located adjacently in the retina, and anti-correlated activity patterns between cells located distantly in the retina. The imprecise map is refined by repeated cycles of wave activity that strengthen those connections where activity is correlated and weaken or eliminate those connections where activity is anti-correlated (Figure 3.1).

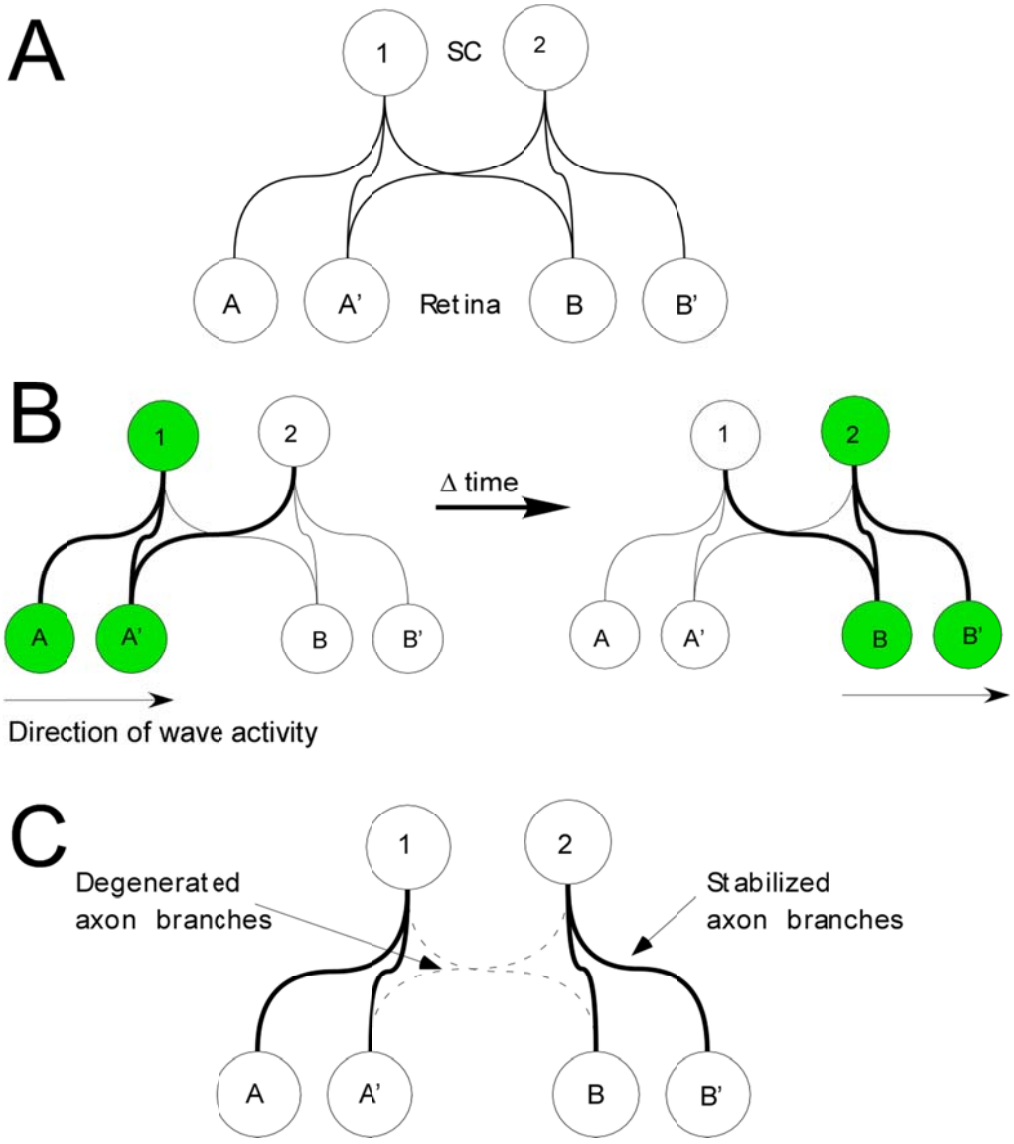

Figure 3.1 Hypothesis of how correlated activity leads to topography

A Schematic of RGCs and the SC before map refinement. The pair of RGCs labeled A and A' are adjacent in the retina and their appropriate topographic location in the SC is labeled as 1. The pair of RGCs labeled B and B' are adjacent to each other in the retina and their appropriate topographic location in the SC is labeled as 2. Pair A and pair B are located distantly in the retina. Before the refinement of projections, RGC A' has an ectopic connection to location 2 in the SC, and RGC B has an ectopic connection to location 1 in the SC.

B Waves of correlated activity travel through the RGCs, moving from left to right. The waves cause adjacent RGCs to fire simultaneously. Thus, RGCs A and A' synchronously fire (indicated by a green fill), and some time later RGCs B and B' synchronously fire. The simultaneous firing of 2 RGCs connected to 1 cell in the SC is enough to cause the SC cell to fire as well.

C Multiple iterations of wave activity through the retina will cause those connections that cause simultaneous activity in the RGC and SC to be strengthened (i.e. A and A' to 1, B and B' to 2). Those connections that do not cause simultaneous activity will degenerate (i.e. A' to 2 and B to 1). Thus, topographically appropriate connections will be strengthened and topographically inappropriate connections will degenerate and be lost.

Testing the instructive role of correlated activity

The hypothesis that activity, interpreted by individual cells, is instructive to the development of retinotopic maps is simple and elegant but must be tested. Activity is also *permissive* to the interpretation of guidance molecule gradients through changes in the intracellular concentration of cAMP (Song et al. 1997; Nicol et al. 2007). Thus, attempts to experimentally manipulate instructive activity may be confounded by inadvertently altering the permissive aspects of activity.

One tool that can be used to do just that is the nicotinic acetylcholine receptor, which is required for stage II wave activity (Feller 2002). NAChRs are ionotropic receptors composed of genetically distinct subunits (Dani et al. 2007). The subunits that compose an individual channel vary among cell types, and each unique composition has different pharmacological sensitivities (Dani et al. 2007). Of the nAchR subtypes expressed in the early retina (Moretti et al. 2004), it was observed that channels containing the $\alpha 3$ and $\beta 2$ subunits are required for correlated wave activity, but not spontaneous uncorrelated activity, in RGCs (Bansal et al. 2000). Thus, by altering the activity of this subset of nAchRs, one can theoretically dissociate the instructive from the permissive aspects of spontaneous activity.

Epibatadine is a nAChR partial agonist that binds to nAChRs with a higher affinity than nicotine or acetylcholine (Buisson et al. 2000). Application of epibatidine to retinal explants abolishes stage II retinal waves without silencing RGC action potentionals by decorrelating RGC firing patterns (Sun et al. 2008a). Epibatadine can be injected into the vitreous humor of the eye, where its actions are restricted to the cells of

the retina. Injections of epibatadine into the eye inhibit LGN eye-specific segregation (Penn et al. 1998; Pfeiffenberger et al. 2005) and refinement of topography in the retinocollicular projection (Chandrasekaran et al. 2005). Molecular genetic techniques also allow for the disruption of wave activity. As mentioned previously, the nAChR subtype involved in wave activity contains the α3 and β2 subunits (Bansal et al. 2000). Genetic knock-out of the α3 subunit leads to waves with altered spatiotemporal properties (Bansal et al. 2000). Genetic knock-out of the β2 subunit leads to the elimination of wave activity without ablating spontaneous uncorrelated activity (Bansal et al. 2000). The β2 knockout is a whole mouse knockout, meaning that β2 expression is ablated from all cells in the entire mouse, including *both* RGCs and target cells in the SC. Mapping phenomena seen in *β2* knock-out mice may therefore be caused by changes to cells in the SC, and not due to changes in correlated activity in RGCs. However, intra-ocular injections of epibatadine phenocopy the β2 knock-out, suggesting that the effects of β2 loss of function are due to an effect in the retina and not the SC. Thus the *β2* knock-out mouse is a good genetic tool for investigating the instructive role of waves in the development retinal output.

Several experiments have used the *β2* knock-out mouse to investigate the role of correlated activity in the retina in different aspects visual system development. For example, *β2* knock-out mice fail to segregate eye specific inputs to the LGN (Rossi et al. 2001; Grubb et al. 2003; Pfeiffenberger et al. 2005).

The *β2* knock-out mouse also has an altered retino-collicular map. As measured by anterograde labeling, *β2* knock-out mice have a less refined retinotopic map in the SC,

meaning that focal labeling in the retina labels a larger area in the SC in *β2* knock-out mice compared to WT mice (McLaughlin et al. 2003; Mrsic-Flogel et al. 2005). Labeling single RGCs has also demonstrated that the size of axonal arborizations in the LGN and SC are larger in *β2* knock-out mice as compared to WT mice (Dhande et al. 2011). Recordings from individual cells in the SC demonstrate that *β2* knock-out mice have an increase in the receptive field size for individual cells, consistent with a less refined map.

These experiments demonstrate that wave activity mediated by the nAChRs containing the β2 subunit plays a role in retinocollicular mapping. However, it remains an open question whether activity refines the retinocollicular map by decreasing the receptive field size in the SC, changing the topographic location of RGC axon branches and synapses, or both. Combining the *β2* knock-out mouse with the *Isl2-EphA3* knock-in described in Chapter two may allow these distinctions to be made.

Results

Hypothesized results

As described in Chapter 2, the *Isl2-EphA3* homozygous knock-in displays a fully duplicated map across the entire N-T axis of the retina, whereas the *Isl2-EphA3* heterozygous knock-in displays a partially duplicated map (Brown et al. 2000). In the *Isl2-EphA3*$^{ki/+}$ mouse, the retinocollicular map is duplicated for the nasal-most 75% of the retinal naso-temporal axis and displays only a single map in the temporal-most 25% of the retina (Brown et al. 2000). The ratio of EphA expressed by immediately adjacent pairs of Isl2-EphA3 expressing RGCs and WT cells predicts the occurrence and the

location of the collapse (Reber et al. 2004). The EphA-ephrinA interaction that instructs topography is overcome by another, unknown, mapping force when the ratio between adjacent cells falls below a threshold (Reber et al. 2004). Activity-instructed mechanisms are an excellent candidate to be the unknown force because the cells that collapse are adjacent in the retina, therefore their activity would be correlated, causing them to wire together. If this is indeed the case, then eliminating correlated activity should either eliminate or move the location of the collapse in those genotypes that are predicted to collapse by the RS signaling mechanisms described in Chapter 2.

To test this possibility, we created compound $\beta2^{-/-}$/ *Isl2-EphA3*$^{ki/+}$ mutants and observed their retinocollicular maps at postnatal day 7. The maps were observed at P7 because retinal waves that do not require nAchR transmission, potentially confounding our results, begin at P8 (Stafford et al. 2009). The $\beta2^{-/-}$ retinocollicular map is topographically similar to that of wildtype animals, but with larger TZs (Figure 3.2A). The *Isl2-EphA3*$^{ki/+}$ map has been described previously (Figure 3.2B). If correlated activity does not affect the establishment of topography, then one would expect the $\beta2^{-/-}$/ *Isl2-EphA3*$^{ki/+}$ map to be a linear combination of the $\beta2^{-/-}$ and *Isl2-EphA3*$^{ki/+}$ maps (Figure 3.2C). If correlated activity does not affect the establishment of topography then one would expect $\beta2^{-/-}$/ *Isl2-EphA3*$^{ki/+}$ map to not show a collapse in the temporal retina (Figure 3.2D).

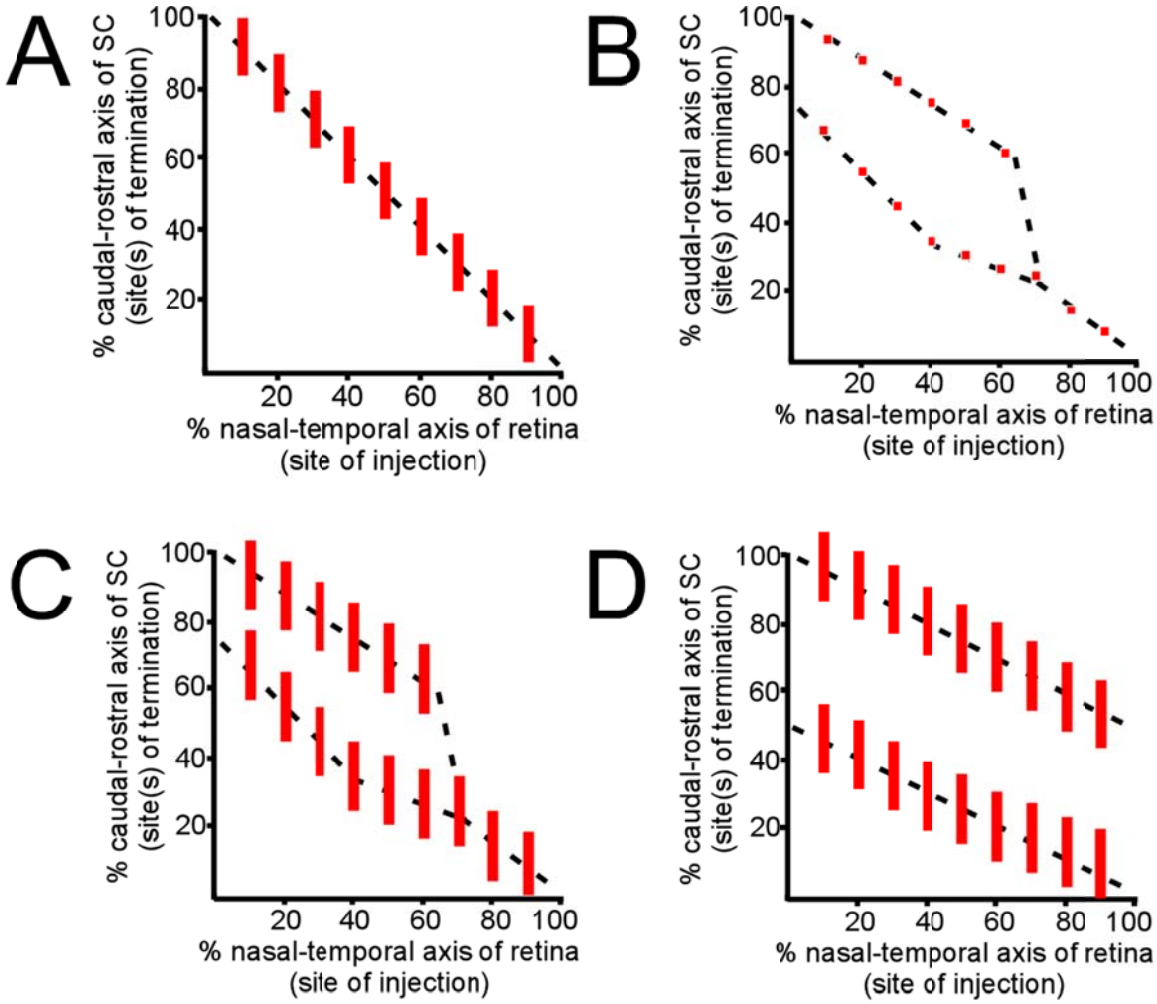

ıxis
k
ırs)

wo
ı

e
uld

If the

raphic

The distinguishing feature between the two hypothetical maps is whether one can observe a single or duplicated TZ after injection of tracer dye into the temporal retina. Thus, injections of fluorescent tracer dye were made into the temporal retina (>76% of the NT axis), to observe the retinocollicular projection of compound mutants (Figure 3.3A).

Retinocollicular map of compound *β2* knock-out; *Isl2-EphA3* knock-in mutant mice

Our injections in the temporal retina of $\beta2^{-/-}$ mice showed an enlarged TZ in the SC, consistent with previous reports (Figure 3.3B). We then crossed $\beta2^{-/-}$ mice with *Isl2-EphA3*$^{ki/ki}$ mice to create double heterozygous $\beta2^{+/-}$/ *Isl2-EphA3*$^{ki/+}$ mice. The $\beta2^{+/-}$/ *Isl2-EphA3*$^{ki/+}$ mice did not show any obvious behavioral phenotype. Injections in the temporal retina of $\beta2^{+/-}$/ *Isl2-EphA3*$^{ki/+}$ mice show a single TZ (Figures 3.3C and 3.3D). $\beta2^{+/-}$/ *Isl2-EphA3*$^{ki/+}$ mice were then crossed and the resulting $\beta2^{+/-}$/ *Isl2-EphA3*$^{ki/+}$, $\beta2^{+/-}$/ *Isl2-EphA3*$^{ki/ki}$, $\beta2^{-/-}$/ *Isl2-EphA3*$^{ki/+}$ and $\beta2^{-/-}$/ *Isl2-EphA3*$^{ki/ki}$ mice also did not display any obvious behavioral phenotype and were grossly indistinguishable from each other as pups or adults. Injections in the temporal retina of $\beta2^{+/-}$/ *Isl2-EphA3*$^{ki/ki}$ show two distinct TZs (Figures 3.3E and 3.3F).

Injections in the temporal retina of $\beta2^{-/-}$/ *Isl2-EphA3*$^{ki/+}$ animals often showed a single distinct TZ (Figure 3.4). However, many injections also showed a large, poorly defined and possibly duplicated TZ (Figure 3.5).

To determine if duplicated TZs could be distinguished in $\beta2^{-/-}$ mice, we performed DiI injections into the nasal retina, where the map is predicted to be duplicated. Injections in the nasal retina of $\beta2^{-/-}$/ *Isl2-EphA3*$^{ki/+}$ mice generally showed a large, poorly defined TZ. A single exception, showing what appears to be a duplicated TZ pattern is shown in Figure 3.6A. Injections in the nasal retina of $\beta2^{-/-}$/ *Isl2-EphA3*$^{ki/ki}$ mice were generally ambiguous (Figure 3.6B), but one mouse showed what appears to be a fully duplicated TZ (Figure 3.6C).

Retinocollicular map of $\beta2^{-/-}$/ *Isl2-EphA3*$^{ki/+}$/ *EphA4*$^{+/-}$ mice

To distinguish whether $\beta2^{-/-}$/ *Isl2-EphA3*$^{ki/+}$ mice display a single, enlarged TZ or two distinct TZs in the nasal retina, we combined the β2 and Isl2-EphA3 alleles with a mouse knock-out of the EphA4 allele (Dottori et al. 1998). The compound mutant *EphA4*$^{+/-}$/ *Isl2-EphA3*$^{ki/+}$ mice have a much larger separation between labeled TZs in the nasal retina (Reber et al. 2004) (Figure 3.6D). $\beta2^{-/-}$/ *Isl2-EphA3*$^{ki/+}$/ *EphA4*$^{+/-}$ mice were grossly normal without any apparent behavioral phenotype.

Temporal injections in $\beta2^{-/-}$/ *Isl2-EphA3*$^{ki/+}$ / *EphA4*$^{+/-}$ mice show an enlarged, ambiguous TZ similar to that observed in $\beta2^{-/-}$/ *Isl2-EphA3*$^{ki/+}$ mice (Figure 3.6E). Nasal injections in $\beta2^{-/-}$/ *EphA4*$^{+/-}$/ *Isl2-EphA3*$^{ki/+}$ mice also demonstrate a large, ambiguous TZ (Figure 3.6F).

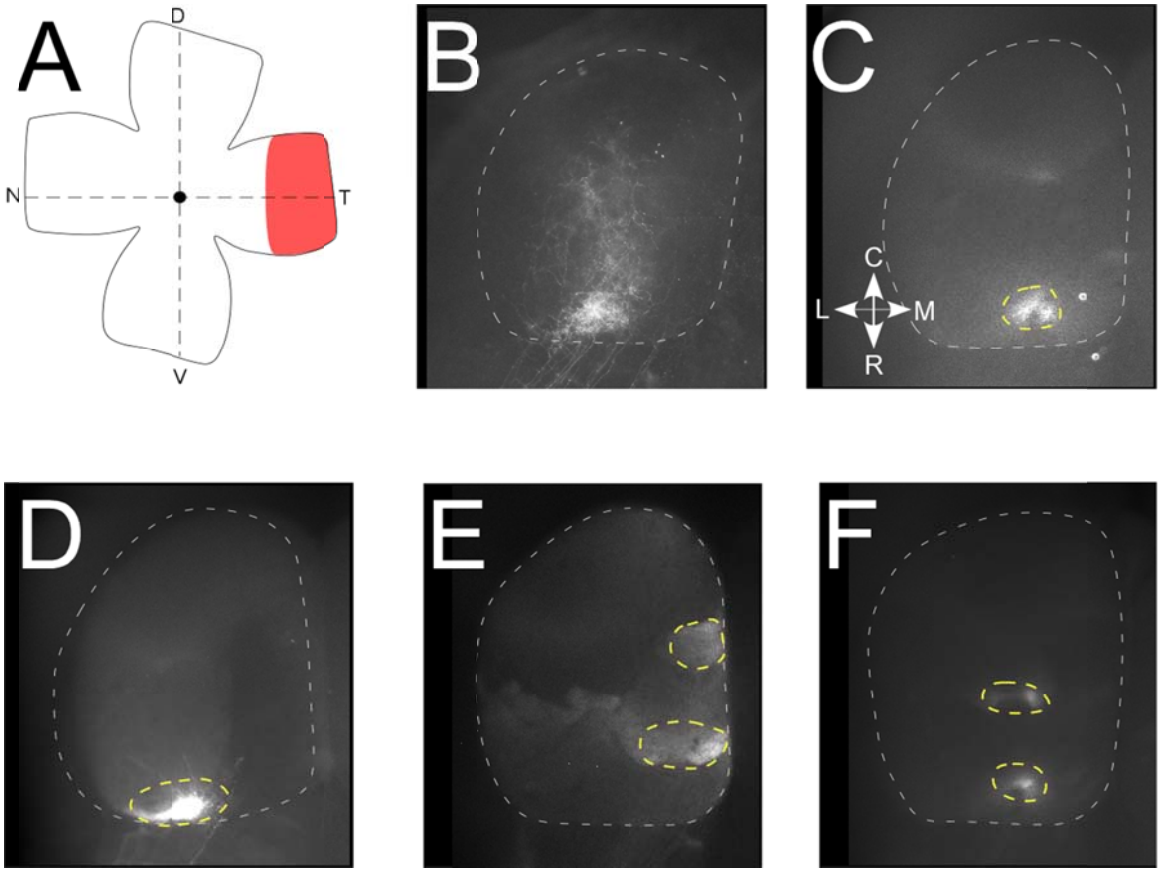

:ina

ı et al.

ΓZ.

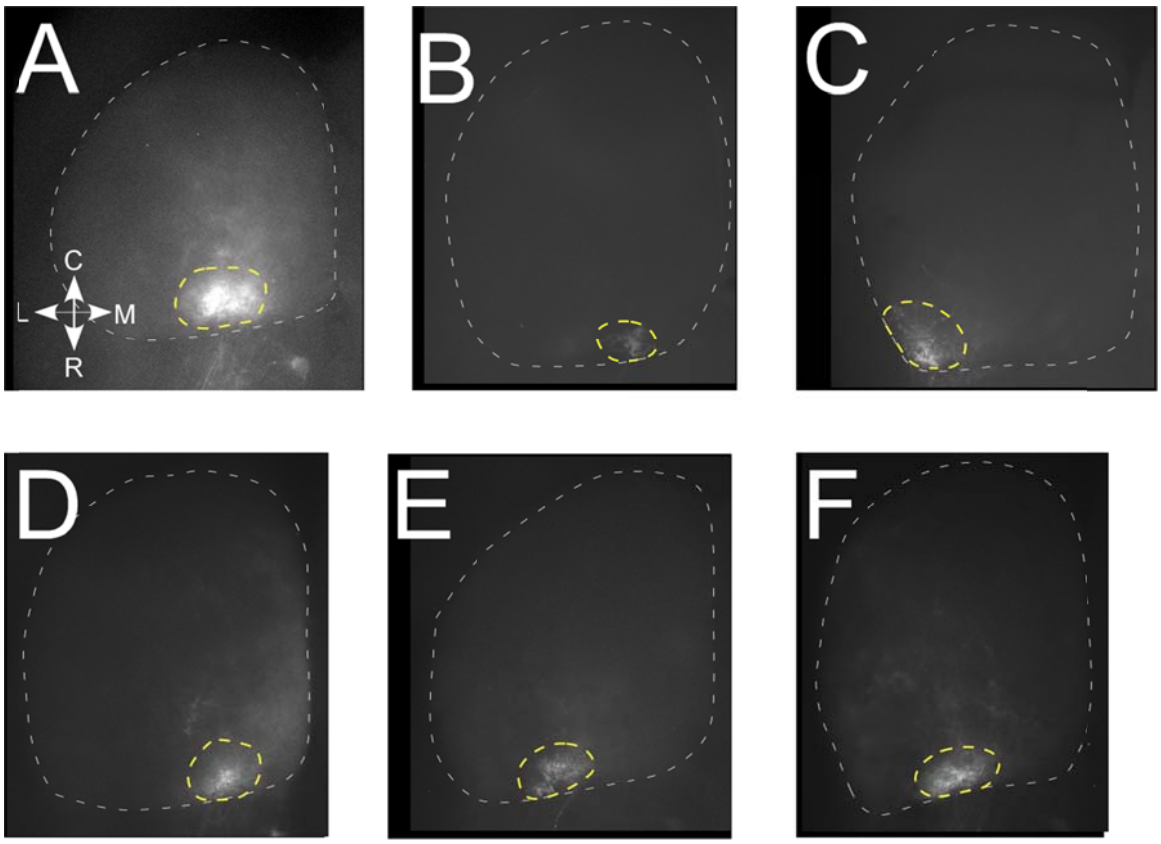

Figure 3.4 *β2*$^{-/-}$*/ Isl2-EphA3*$^{ki/+}$ retinocollicular maps with a single labeled a single TZ

A-F Injections in the temporal retina of *β2*$^{-/-}$*/ Isl2-EphA3*$^{ki/+}$ mice often appear to label only a single TZ.

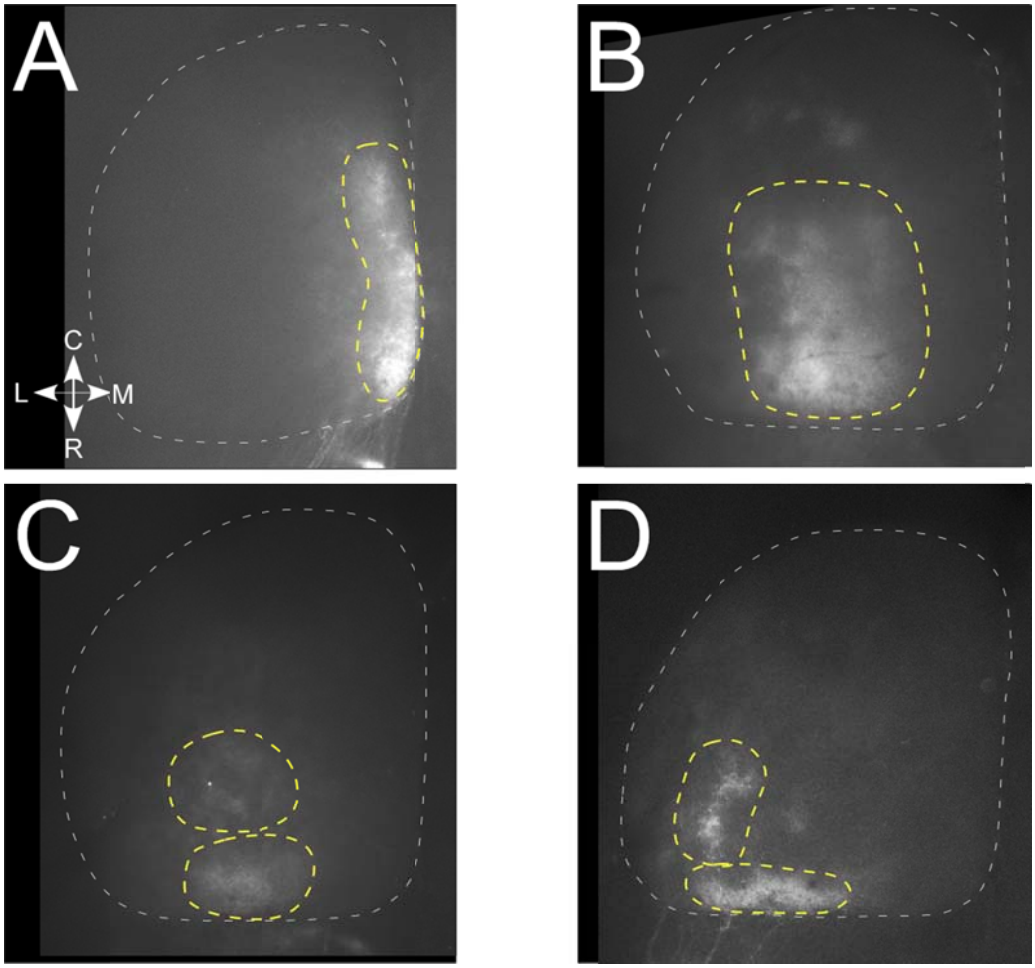

licated

arge,

nally

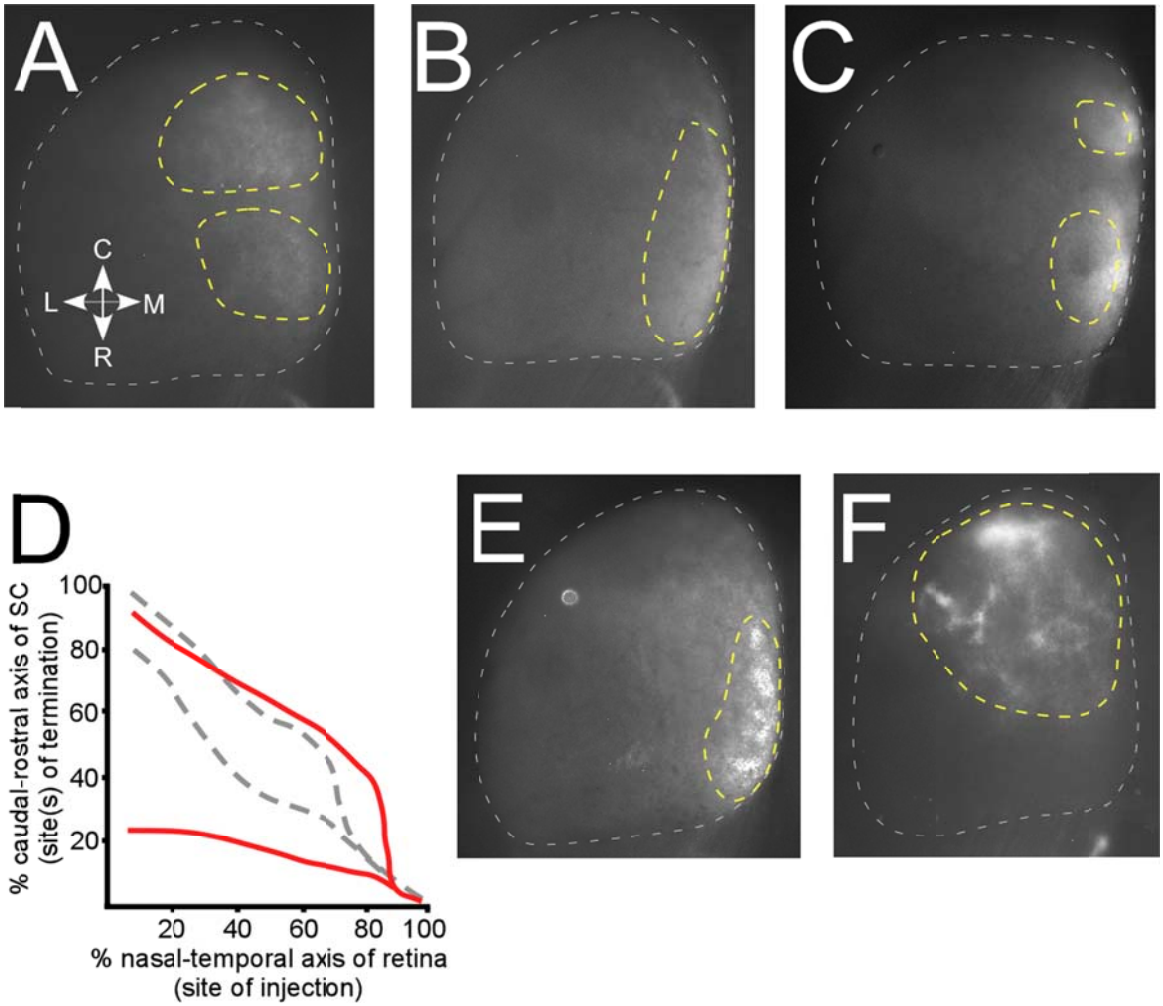
A
B
C
C
L
M
R
D
E
F
% caudal-rostral axis of SC
(site(s) of termination)
100
80
60
40
20
20
40
60
80
100
% nasal-temporal axis of retina
(site of injection)

wo

's.

Discussion

In general, the data suggest that in the *β2*$^{-/-}$*/ Isl2-EphA3*$^{ki/+}$ mice, there is a collapse in the temporal retina, which is consistent with correlated activity not playing a role in topography. However, these data are not of high enough resolution to be convincing. The TZs seen after temporal injections of *β2*$^{-/-}$*/ Isl2-EphA3*$^{ki/+}$ animals are not easily interpreted because of their variability. Many injections appear to label a single, enlarged TZ (Figure 3.4), while some appear to label duplicated TZs (Figure 3.5). These injections were all performed in locations where the *Isl2-EphA3*$^{ki/+}$ map shows a single TZ; thus, the appearance of an apparently duplicated TZ could be indicative of a shift in the location of the collapse point, consistent with correlated retinal activity playing a role in the collapse phenomenon.

We were not able to consistently resolve a duplicated TZ for a compound mutant with a homozygous loss of function for β2 (i.e. *β2*$^{-/-}$*/ Isl2-EphA3*$^{ki/+}$, *β2*$^{-/-}$*/ Isl2-EphA3*$^{ki/ki}$, *β2*$^{-/-}$*/ Isl2-EphA3*$^{ki/+}$*/ EphA4*$^{+/-}$). The majority of attempts to do so resulted in an enlarged, ambiguous area of labeling in the SC. Only a small minority of injections labeled what appeared to be two TZs. Thus, we cannot be confident whether an enlarged TZ is two overlapping TZs or one large TZ (Figure 3.7A).

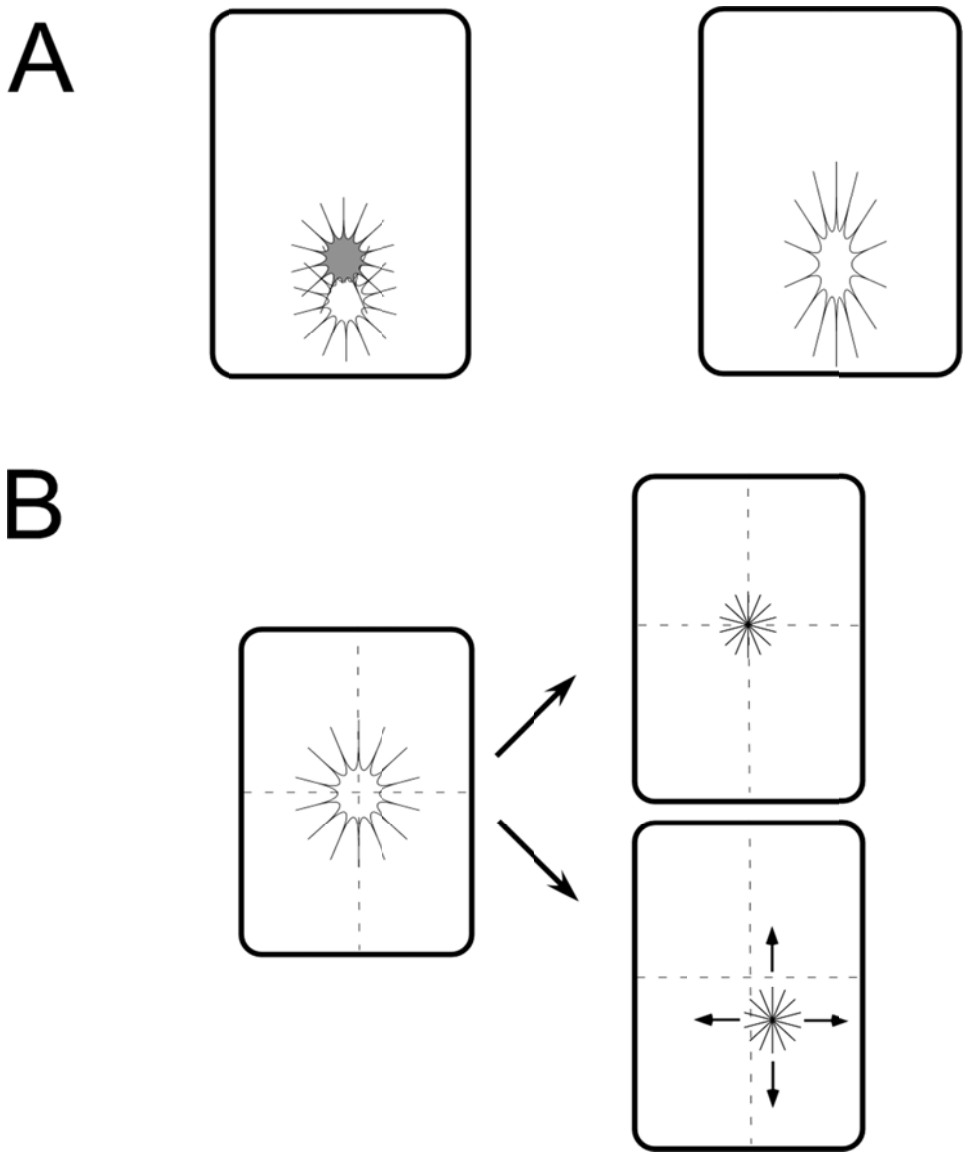

Figure 3.7 Interpretations of the data

A Schematic of two distinct, but largely overlapping TZs.

B Schematic of one, enlarged TZ.

C Correlated activity in the perinatal retina serves to refine the size of a TZ but does not affect its location in the SC.

D Correlated activity refines the size of a TZ, as well as defines its location in the SC.

The mapping phenomenon seen in $\beta2^{-/-}$ mice may not be caused by a loss of correlated activity

Since the inception of the experiments described in this chapter, a number of additional findings in the $\beta2^{-/-}$ mice have challenged the consensus that $\beta2^{-/-}$ lack correlated activity. It was observed that *ex vivo* retinas from peri-natal $\beta2^{-/-}$ mice do have waves if the recording conditions are altered to more closely match what are thought to be *in vivo* conditions (Sun et al. 2008b). Specifically, one group found that recordings performed at 37^{o}C showed correlated activity, whereas those done previously were performed at 30^{o}C (Feller et al. 1997). Perinatal pups do not regulate their temperature well and are dependent on external sources of heat. Thus, it is a matter of speculation as to whether the temperature inside the retina of a perinatal pup is 37^{o}C, the temperature of an adult animal, or several degrees cooler. These findings have led to an unresolved debate about if and how loss of the β2 subunit leads to meaningful changes in wave activity that are directly instructive for development of the visual system (Chalupa 2009; Feller 2009)

Ex vivo recordings of $\beta2^{-/-}$ mice at both 30^{o}C and 37^{o}C show that the spatio-temporal wave properties are different between $\beta2^{-/-}$ and WT retinae at any temperature (Stafford et al. 2009). In addition to the changes in correlated activity, there is also a change in the firing rate of individual RGCs (Stafford et al. 2009). Increased activity in individual RGCs could lead to changes in mapping independent of alterations in correlated activity. For example, increased RGC activity is known to increase the release

of BDNF in the SC (Cohen-Cory 1999), which could lead to the stabilization of ectopic RGC branches (Yates et al. 2001). This speculative phenomenon would occur regardless of whether activity is correlated.

Conclusion

The anatomical experiments described in this chapter do not provide data of sufficient resolution to distinguish whether there is a single or duplicated TZ in the temporal retina of $\beta 2^{-/-}$/ *Isl2-EphA3*$^{ki/+}$ mice.

The experimental paradigm described in the introduction may need to be revised to reflect a more nuanced understanding of the role that the β2 subunit plays in correlated activity. Ideally, to test the role of correlated activity in retinotopic mapping, one must know the spatiotemporal properties of activity that are meaningfully correlated between cells and disrupt only those properties of spontaneous activity while leaving those properties of activity that are not informative for retinotopic mapping unchanged.

The text of Chapter Three, in part, is a reprint of the material which is being prepared for publication. I was the primary researcher. Dr. Greg Lemke directed and supervised the research which forms the basis for this chapter.

Materials and Methods

Animal Subjects

The *Isl2-EphA3* knock-in (Brown et al., 2000), *EphA4* knock-out (Dottori et al. 1998),and *β2* knock-out (Xu et al. 1999) mice have all been described previously. All procedures used in these experiments were reviewed and approved by the Institutional Animal Care and Use Committee at the Salk Institute for Biological Studies. Animals were cared for and used in accordance with guidelines of the *U.S. Public Health Service Policy on Humane Care and Use of Laboratory Animals* and the *NIH Guide for the Care and Use of Laboratory Animals* and following institutional Association for Assessment and Accreditation of Laboratory Animal Care-approved practices.

Anterograde labeling

RGC axons were anterogradely labeled by a focal injection of DiI (1,1'-dioctadecyl-3,3,3'3'-tetramethylindocarbocyanine perchlorate) into the retina, as described previously (Brown et al. 2000; Reber et al. 2004). DiI was dissolved in dimethylformamide, loaded into a pulled glass pipette, and pressure injected into the retina using a picospritzer. P7-8 mice were injected and the DiI was given 24 hours to migrate along RGC axons, after which time the mice were sacrificed and their SC dissected. The SC was visualized in a whole mount preparation using rhodamine optics on a Zeiss axioskop 2 upright scope using a 2.5X objective. The retina was fixed for 48-72 hours in 2% PFA and then dissected and visualized as a whole mount preparation.

References

Bansal, A., J. H. Singer, B. J. Hwang, W. Xu, A. Beaudet and M. B. Feller (2000). "Mice lacking specific nicotinic acetylcholine receptor subunits exhibit dramatically altered spontaneous activity patterns and reveal a limited role for retinal waves in forming ON and OFF circuits in the inner retina." J Neurosci **20**(20): 7672-81.

Bliss, T. V. and G. L. Collingridge (1993). "A synaptic model of memory: long-term potentiation in the hippocampus." Nature **361**(6407): 31-9.

Brown, A., P. A. Yates, P. Burrola, D. Ortuño, A. Vaidya, T. M. Jessell, S. L. Pfaff, D. D. O'Leary and G. Lemke (2000). "Topographic mapping from the retina to the midbrain is controlled by relative but not absolute levels of EphA receptor signaling." Cell **102**(1): 77-88.

Buisson, B., Y. F. Vallejo, W. N. Green and D. Bertrand (2000). "The unusual nature of epibatidine responses at the alpha4beta2 nicotinic acetylcholine receptor." Neuropharmacology **39**(13): 2561-9.

Butts, D. A. (2002). "Retinal waves: implications for synaptic learning rules during development." The Neuroscientist : a review journal bringing neurobiology, neurology and psychiatry **8**(3): 243-53.

Butts, D. A., M. B. Feller, C. J. Shatz and D. S. Rokhsar (1999). "Retinal waves are governed by collective network properties." J Neurosci **19**(9): 3580-93.

Butts, D. A. and D. S. Rokhsar (2001). "The information content of spontaneous retinal waves." J Neurosci **21**(3): 961-73.

Caporale, N. and Y. Dan (2008). "Spike timing-dependent plasticity: a Hebbian learning rule." Annu Rev Neurosci **31**: 25-46.

Chalupa, L. M. (2009). "Retinal waves are unlikely to instruct the formation of eye-specific retinogeniculate projections." Neural Dev **4**: 25.

Chandrasekaran, A. R., D. T. Plas, E. Gonzalez and M. C. Crair (2005). "Evidence for an instructive role of retinal activity in retinotopic map refinement in the superior colliculus of the mouse." J Neurosci **25**(29): 6929-38.

Cline, H. T. (1991). "Activity-dependent plasticity in the visual systems of frogs and fish." Trends Neurosci **14**(3): 104-11.

Cline, H. T. and M. Constantine-Paton (1989). "NMDA receptor antagonists disrupt the retinotectal topographic map." Neuron **3**(4): 413-26.

Cohen-Cory, S. (1999). "BDNF modulates, but does not mediate, activity-dependent branching and remodeling of optic axon arbors in vivo." J Neurosci **19**(22): 9996-10003.

Dani, J. A. and D. Bertrand (2007). "Nicotinic acetylcholine receptors and nicotinic cholinergic mechanisms of the central nervous system." Annu. Rev. Pharmacol. Toxicol. **47**: 699-729.

Demas, J. A., H. Payne and H. T. Cline (2011). "Vision drives correlated activity without patterned spontaneous activity in developing Xenopus retina." Dev Neurobiol.

Dhande, O. S., E. W. Hua, E. Guh, J. Yeh, S. Bhatt, Y. Zhang, E. S. Ruthazer, M. B. Feller and M. C. Crair (2011). "Development of Single Retinofugal Axon Arbors in Normal and {beta}2 Knock-Out Mice." J Neurosci **31**(9): 3384-99.

Dottori, M., L. Hartley, M. Galea, G. Paxinos, M. Polizzotto, T. Kilpatrick, P. F. Bartlett, M. Murphy, F. Köntgen and A. W. Boyd (1998). "EphA4 (Sek1) receptor tyrosine kinase is required for the development of the corticospinal tract." Proc Natl Acad Sci USA **95**(22): 13248-53.

Eglen, S. J., J. Demas and R. O. L. Wong (2003). "Mapping by waves. Patterned spontaneous activity regulates retinotopic map refinement." Neuron **40**(6): 1053-5.

Evans, M. H. (1972). "Tetrodotoxin, saxitoxin, and related substances: their applications in neurobiology." Int Rev Neurobiol **15**: 83-166.

Feller, M. B. (2002). "The role of nAChR-mediated spontaneous retinal activity in visual system development." J Neurobiol **53**(4): 556-67.

Feller, M. B. (2009). "Retinal waves are likely to instruct the formation of eye-specific retinogeniculate projections." Neural Dev **4**: 24.

Feller, M. B., D. A. Butts, H. L. Aaron, D. S. Rokhsar and C. J. Shatz (1997). "Dynamic processes shape spatiotemporal properties of retinal waves." Neuron **19**(2): 293-306.

Feller, M. B., D. P. Wellis, D. Stellwagen, F. S. Werblin and C. J. Shatz (1996). "Requirement for cholinergic synaptic transmission in the propagation of spontaneous retinal waves." Science **272**(5265): 1182-7.

Flavell, S. W. and M. E. Greenberg (2008). "Signaling mechanisms linking neuronal activity to gene expression and plasticity of the nervous system." Annu Rev Neurosci **31**: 563-90.

Galli, L. and L. Maffei (1988). "Spontaneous impulse activity of rat retinal ganglion cells in prenatal life." Science **242**(4875): 90-1.

Gaze, R. M., M. J. Keating and S. H. Chung (1974). "The evolution of the retinotectal map during development in Xenopus." Proc R Soc Lond, B, Biol Sci **185**(80): 301-30.

Greer, P. L. and M. E. Greenberg (2008). "From synapse to nucleus: calcium-dependent gene transcription in the control of synapse development and function." Neuron **59**(6): 846-60.

Grubb, M. S., F. M. Rossi, J. P. Changeux and I. D. Thompson (2003). "Abnormal functional organization in the dorsal lateral geniculate nucleus of mice lacking the beta 2 subunit of the nicotinic acetylcholine receptor." Neuron **40**(6): 1161-72.

Harris, W. A. (1981). "Neural activity and development." Annu Rev Physiol **43**: 689-710.

Hebb, D. O. (1966). The organisation of behavior: a neuro-psychological theory, Wiley.

Kandel, E. R. (2009). "The biology of memory: a forty-year perspective." J Neurosci **29**(41): 12748-56.

Keating, M. J., S. Grant, E. A. Dawes and K. Nanchahal (1986). "Visual deprivation and the maturation of the retinotectal projection in Xenopus laevis." J Embryol Exp Morphol **91**: 101-15.

MacDermott, A. B., M. L. Mayer, G. L. Westbrook, S. J. Smith and J. L. Barker (1986). "NMDA-receptor activation increases cytoplasmic calcium concentration in cultured spinal cord neurones." Nature **321**(6069): 519-22.

Mayer, M. L., G. L. Westbrook and P. B. Guthrie (1984). "Voltage-dependent block by Mg2+ of NMDA responses in spinal cord neurones." Nature **309**(5965): 261-3.

McLaughlin, T., C. L. Torborg, M. B. Feller and D. D. M. O'Leary (2003). "Retinotopic map refinement requires spontaneous retinal waves during a brief critical period of development." Neuron **40**(6): 1147-60.

Meister, M., R. O. Wong, D. A. Baylor and C. J. Shatz (1991). "Synchronous bursts of action potentials in ganglion cells of the developing mammalian retina." Science **252**(5008): 939-43.

Moretti, M., S. Vailati, M. Zoli, G. Lippi, L. Riganti, R. Longhi, A. Viegi, F. Clementi and C. Gotti (2004). "Nicotinic acetylcholine receptor subtypes expression during rat retina development and their regulation by visual experience." Mol Pharmacol **66**(1): 85-96.

Mrsic-Flogel, T. D., S. B. Hofer, C. Creutzfeldt, I. Cloëz-Tayarani, J.-P. Changeux, T. Bonhoeffer and M. Hübener (2005). "Altered map of visual space in the superior colliculus of mice lacking early retinal waves." J Neurosci **25**(29): 6921-8.

Nicol, X., S. Voyatzis, A. Muzerelle, N. Narboux-Nême, T. C. Südhof, R. Miles and P. Gaspar (2007). "cAMP oscillations and retinal activity are permissive for ephrin signaling during the establishment of the retinotopic map." Nat Neurosci **10**(3): 340-7.

O'Leary, D. D., J. W. Fawcett and W. M. Cowan (1986). "Topographic targeting errors in the retinocollicular projection and their elimination by selective ganglion cell death." J Neurosci **6**(12): 3692-705.

Penn, A. A., P. A. Riquelme, M. B. Feller and C. J. Shatz (1998). "Competition in retinogeniculate patterning driven by spontaneous activity." Science **279**(5359): 2108-12.

Pfeiffenberger, C., T. Cutforth, G. Woods, J. Yamada, R. C. Rentería, D. R. Copenhagen, J. G. Flanagan and D. A. Feldheim (2005). "Ephrin-As and neural activity are

required for eye-specific patterning during retinogeniculate mapping." Nat Neurosci **8**(8): 1022-7.

Reber, M., P. Burrola and G. Lemke (2004). "A relative signalling model for the formation of a topographic neural map." Nature **431**(7010): 847-53.

Rossi, F. M., T. Pizzorusso, V. Porciatti, L. M. Marubio, L. Maffei and J. P. Changeux (2001). "Requirement of the nicotinic acetylcholine receptor beta 2 subunit for the anatomical and functional development of the visual system." Proc Natl Acad Sci USA **98**(11): 6453-8.

Scherer, W. J. and S. B. Udin (1989). "N-methyl-D-aspartate antagonists prevent interaction of binocular maps in Xenopus tectum." J Neurosci **9**(11): 3837-43.

Schmidt, J. T. (1990). "Long-term potentiation and activity-dependent retinotopic sharpening in the regenerating retinotectal projection of goldfish: common sensitive period and sensitivity to NMDA blockers." J Neurosci **10**(1): 233-46.

Schmidt, J. T. and L. E. Eisele (1985). "Stroboscopic illumination and dark rearing block the sharpening of the regenerated retinotectal map in goldfish." Neuroscience **14**(2): 535-46.

Shen, K. and P. Scheiffele (2010). "Genetics and cell biology of building specific synaptic connectivity." Annu Rev Neurosci **33**: 473-507.

Simon, D. K. and D. D. O'Leary (1992a). "Development of topographic order in the mammalian retinocollicular projection." J Neurosci **12**(4): 1212-32.

Simon, D. K., G. T. Prusky, D. D. O'Leary and M. Constantine-Paton (1992b). "N-methyl-D-aspartate receptor antagonists disrupt the formation of a mammalian neural map." Proc Natl Acad Sci USA **89**(22): 10593-7.

Song, H. J., G. L. Ming and M. M. Poo (1997). "cAMP-induced switching in turning direction of nerve growth cones." Nature **388**(6639): 275-9.

Stacy, R. C., J. Demas, R. W. Burgess, J. R. Sanes and R. O. L. Wong (2005). "Disruption and recovery of patterned retinal activity in the absence of acetylcholine." J Neurosci **25**(41): 9347-57.

Stafford, B. K., A. Sher, A. M. Litke and D. A. Feldheim (2009). "Spatial-temporal patterns of retinal waves underlying activity-dependent refinement of retinofugal projections." Neuron **64**(2): 200-12.

Stent, G. S. (1973). "A physiological mechanism for Hebb's postulate of learning." Proc Natl Acad Sci USA **70**(4): 997-1001.

Sun, C., C. M. Speer, G.-Y. Wang, B. Chapman and L. M. Chalupa (2008a). "Epibatidine application in vitro blocks retinal waves without silencing all retinal ganglion cell action potentials in developing retina of the mouse and ferret." Journal of Neurophysiology **100**(6): 3253-63.

Sun, C., D. K. Warland, J. M. Ballesteros, D. van der List and L. M. Chalupa (2008b). "Retinal waves in mice lacking the beta2 subunit of the nicotinic acetylcholine receptor." Proc Natl Acad Sci USA **105**(36): 13638-43.

Torborg, C. L. and M. B. Feller (2005). "Spontaneous patterned retinal activity and the refinement of retinal projections." Progress in Neurobiology **76**(4): 213-35.

Udin, S. B. (1985). "The role of visual experience in the formation of binocular projections in frogs." Cell Mol Neurobiol **5**(1-2): 85-102.

Wiesel, T. N. (1982). "Postnatal development of the visual cortex and the influence of environment." Nature **299**(5884): 583-91.

Wong, R. O. (1999). "Retinal waves and visual system development." Annu Rev Neurosci **22**: 29-47.

Wong, R. O., M. Meister and C. J. Shatz (1993). "Transient period of correlated bursting activity during development of the mammalian retina." Neuron **11**(5): 923-38.

Xu, W., A. Orr-Urtreger, F. Nigro, S. Gelber, C. B. Sutcliffe, D. Armstrong, J. W. Patrick, L. W. Role, A. L. Beaudet and M. De Biasi (1999). "Multiorgan autonomic dysfunction in mice lacking the beta2 and the beta4 subunits of neuronal nicotinic acetylcholine receptors." J Neurosci **19**(21): 9298-305.

Yates, P. A., A. L. Roskies, T. Mclaughlin and D. D. O'Leary (2001). "Topographic-specific axon branching controlled by ephrin-As is the critical event in retinotectal map development." J Neurosci **21**(21): 8548-63.

Yoon, M. G. (1975). "Effects of post-operative visual environments on reorganization of retinotectal projection in goldfish." J Physiol (Lond) **246**(3): 673-94.

Zheng, J., S. Lee and Z. J. Zhou (2006). "A transient network of intrinsically bursting starburst cells underlies the generation of retinal waves." Nat Neurosci **9**(3): 363-71.

Zheng, J.-J., S. Lee and Z. J. Zhou (2004). "A developmental switch in the excitability and function of the starburst network in the mammalian retina." Neuron **44**(5): 851-64.

Zhou, Z. J. (1998). "Direct participation of starburst amacrine cells in spontaneous rhythmic activities in the developing mammalian retina." J Neurosci **18**(11): 4155-65.

Zhou, Z. J. (2001). "The function of the cholinergic system in the developing mammalian retina." Prog Brain Res **131**: 599-613.

Chapter Four – The Degree of Encephalization of an Organism Determines its Mechanism of Retinotopic Mapping

Abstract

The mechanism of development of retinotopy in the SC/tectum of amniotes is contrasted to that of anamniotes. Anamniotes continuously map new RGCs to the tectum as RGCs are born throughout the life of the animal and can regenerate their retinotopic maps. In contrast, amniotes completely form their retinotopic maps during a critical period early in development and are not able to regenerate a topographic map if the retinal projection or target is damaged. The different dynamics of retinotopic mapping in amniotes and anamniotes may arise because of their differing contexts of map development. Amniotes generally have a higher degree of encephalization than anamniotes, and their high degree of encephalization may require rigid primary sensory maps to be developed early. An increase in encephalization allows for a greater behavioral repertoire but prevents regeneration and necessitates a greater time to develop. Humans have an extremely high level of encephalization, and the process human brain development may continue far into adulthood. The extended time frame of human brain development may have implications for the pathogenesis of behavioral disorders. The chapter ends with a summary of the dissertation and concluding remarks.

Introduction

The experiments of Chapters Two and Three describe the role of guidance molecules and patterned spontaneous activity in the formation of the retinotopic map in the Superior Colliculus (SC). These experiments utilize the power of mouse genetics to dissect the developmental processes of one region of the brain. The paradigms used to describe the development of retinotopy in the SC are applicable to the development of the rest of the brain. The physiology and morphology of the brain are restricted by the biophysical properties of its constituent cells. The retina and SC are composed of similar cells to the rest of the brain, and therefore, must develop their functional specifications under similar constraints. Most likely, a combination of genetic control of guidance molecule expression patterns and patterned activity provide information for the development of the simplest to most complex regions of the brain. In this chapter, I will speculate on how the process of retinotopic mapping, placed into the context of whole brain development, is informative as to the paradigms governing brain development and misdevelopment.

The context of retinotopic mapping determines its mechanism

Retinotopic mapping in mice occurs during the first two post-natal weeks (Simon et al. 1992). During this time, RGC axons overshoot their final TZ, grow extensive axon collaterals, then prune back those regions of the axon that are not in the topographically correct location (Simon et al. 1992; Yates et al. 2001). After the initial developmental

period is over, the retinocollicular map is essentially fixed, as no new RGCs are created. The development of the chick retino-tectal map follows the same dynamics (Yates et al. 2001), and this chronology of retinotopic mapping (Figure 4.1A) in the midbrain is likely to be found in all amniotes (vertebrates that develop with extra-embryonic membranes, including reptiles, birds, and mammals).

In contrast to amniotes, during mapping in anamniotes (vertebrates without extra-embryonic membranes, including amphibians and teleost fish)(Figure 4.1B) the growth cones of RGC axons project directly to their topographically appropriate location in the tectum (Sakaguchi et al. 1985; Stuermer 1988; Stuermer et al. 1989). The initial mapping is not as precise, and refinement occurs as the tectum grows and the percentage of the tectum taken up by individual RGC arbors decreases (Sakaguchi et al. 1985; Stuermer 1988; Stuermer et al. 1989). This process occurs continuously as additional RGCs are mapped into the tectum throughout the life of the animal (Gaze et al. 1974).

Another contrast between amniotes and anamniotes is that anamniotes are able to regenerate their retinotopic maps after resection of the optic nerve (Sperry 1944; Sperry 1948), whereas most amniotes cannot. In fact, it appears that mammals have developed several methods of actively blocking the regeneration of their CNS, such as the formation of glial scars after trauma (Goldberg et al. 2000; Brockes et al. 2008). The ability to regenerate is advantageous for the reproduction of anamniotes and has most likely been selected for during the course of evolution.

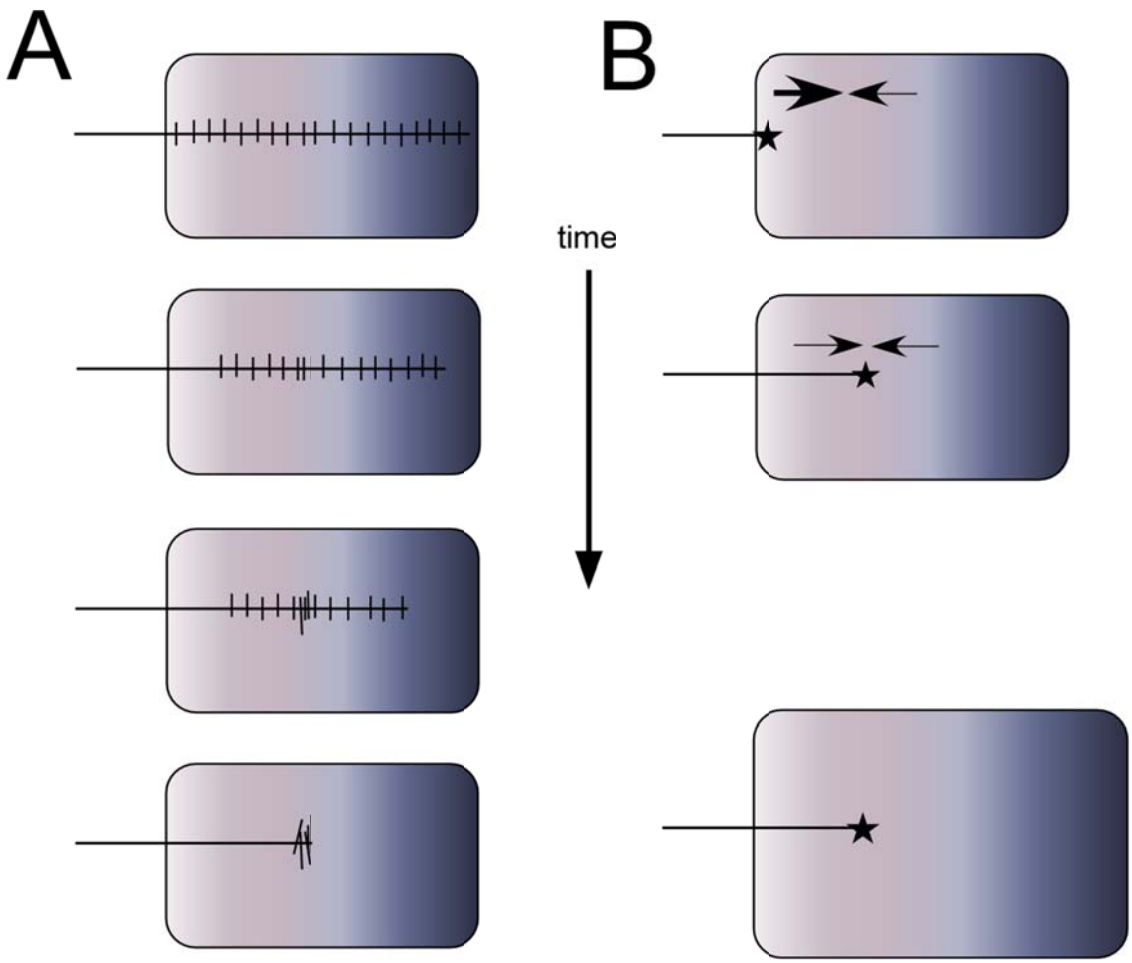

ns

alon.

nes
otes
size.

The difference between amniotic and anamniotic retinotectal mapping may arise because of the different degrees of complexity within the visual systems of amniotes and anamniotes. The amniotic mapping mechanism creates a fixed primary retinotopic map, which allows for the timely development of higher order visual maps based on a primary map. For example, area MT in extrastriate cortex contains a retinotopic map that is primarily sensitive to motion in the visual field and not to other visual stimuli (Albright 1984). The afferent input to area MT comes from V1 and the SC (Rodman et al. 1989; Rodman et al. 1990), and presumably, retinotopy must first develop in the afferent areas to MT before it is retinotopically organized. The telencephalon of anamniotes does contain some visually sensitive regions that may be analogous to the higher order regions of amniotic telencephalon (Liege et al. 1972; Gruberg et al. 1974). However, unlike those of amniotes, associational regions of anamniotes generally receive direct projections from the thalamus (Karamian et al. 1966).

Further integration and differentiation of visual stimuli leads to more specialized regions of the visual system within the telencephalon (Wandell et al. 2007). For example, regions of the temporal lobe of humans have been found to be especially sensitive to the visual presentation of faces (Kanwisher et al. 1997). The more hierarchical organization of the amniote visual system, compared to that of anamniotes, may necessitate that primary retinotopic maps be fully developed and static early during the development of the organism, allowing the emergence of higher order visual areas to make use of the topography found in lower order regions. If amniotes continuously changed their primary visual maps or had the ability to regenerate a new map the process of re-wiring their

higher order regions would take far too long and the animal may be unable to appropriately respond to its environment during the period of re-wiring.

In mammals, the divergence of afferent visual information (Goodale et al. 2004) indicates that the organization of the brain is not strictly hierarchical and the patterning of the cortex before the development of functional specification (O'Leary et al. 2007) indicate and its development is not strictly linear. Like any model, simplifications allow for insight. The hierarchical organization of the amniotic visual system allows for a greater number of associational areas composed of multiple rounds of binding and parsing of a single visual stimulus. These areas allow an organism to have a more complex and nuanced interaction with its environment and a greater behavioral repertoire (Jerison 1977; Jerison 1985).

Discussion

The time dependence of complex development

Higher order brain associational regions found with increased encephalization are generally thought to develop by repeating the process of aligning and associating topographic maps (Dehaene et al. 2007). Recursion allows for the development of extensive complexity using relatively simple instructions and is likely required for the development of many structures in the CNS. There are 2×10^{10} neurons in the human cortex (Williams et al. 1988; Pakkenberg et al. 1997) and 3×10^{9} base pairs in the entire human genome (Lander et al. 2001). Clearly, recursion is required for the development of so many cells and their connections from the relatively simple instructions of the genome.

Given that maintenance of genetic material is metabolically expensive, it is advantageous for an organism to store the instructions for its development in a recursive form.

However, the development of greater complexity through recursion comes at a cost: the development is path-dependent, which makes regeneration unfeasible, and requires a greater amount of time, which makes breeding less efficient because organisms must wait longer before reaching sexual maturity. This is most clearly demonstrated in the relationship between brain size (corrected for genome size) and the age to reach sexual maturity in mammals, which have the greatest degree of encephalization among vertebrates (Jerison 1985) and have a layered neocortex (Krubitzer et al. 2000) (Figure 4.2). Mammals with a larger brain size relative to genome size (x axis of Figure 4.2) generally take longer to reach sexual maturity (y axis of Figure 4.2). Thus, higher degrees encephalization may represent an evolutionary trade-off between better behavioral performance and increased time to reach sexual maturity.

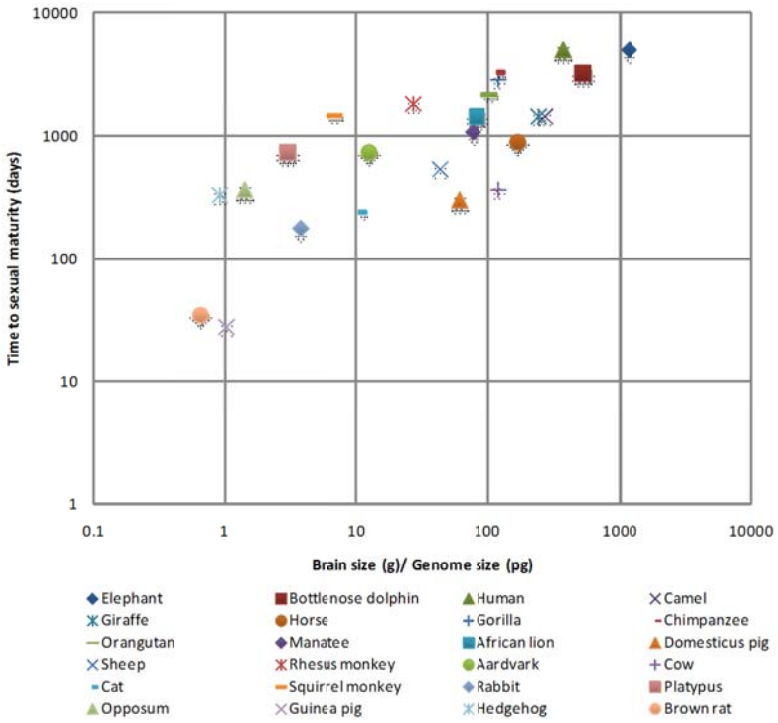

Figure 4.2 Correlations between brain size and time to sexual maturity in mammals

The brain size relative to genome size is shown on the x axis for several different mammals. The days to sexual maturity is shown on the y axis. The data follows a regression line with the equation $y = 140.8x^{0.4929}$ and an R^2 value of 0.6181. The data for this figure are shown in table 4.1.

Development of complexity and disease states

The sequential and recursive development of brain regions brings up the question of "what is a fully developed animal?" In humans, there is evidence that CNS development continues far past the age of sexual maturity. For example, maximum myelination of the brain does not occur until the 5th decade of life (Benes et al. 1994; Bartzokis et al. 2001; Walhovd et al. 2005; Walhovd et al. 2011). Maximum myelination is associated with increased maximum motor speed (Bartzokis et al. 2010). At the time of maximum myelination, other abilities such as spatial orientation and verbal memory have already declined from their peak earlier in life (Hedden et al. 2004). Thus, while any given aged individual may be declining on their performance of some cognitive tasks, they may be peaking in their performance of other tasks. These studies demonstrate that the distinction between 'mature' and 'developing' is not clear from the perspective of the individual organism, especially with regard to humans.

Similarly, when considering pathological brain states, it is difficult to distinguish those states that are a result of mis-development, and those that are caused by homeostatic perturbations to the adult nervous system. CNS diseases of a vascular or infectious etiology that arise in adults are clearly caused by perturbations independent of developmental processes. CNS disorders that occur later in life, when humans are generally considered to be 'mature' may have a neuro-developmental origin.

For example, schizophrenia generally presents in the third decade of life, suggesting that it is a disease of adulthood (Sham et al. 1994) and psychosis can be

induced later in life by insults to the CNS (Walker et al. 2008; Barkus et al. 2010; Gonzales et al. 2010). However, epidemiological evidence strongly links schizophrenia to genetics and perinatal events, which lead to an increased susceptibility to later insults (Bale et al. 2010; Kirkbride et al. 2011). Alternatively, these early events could set in motion a series of mis-developments that are sub-clinical in their presentation until later in life, when the development of social phenomenon is occurring (Jarskog et al. 2007; Thompson et al. 2010). Possibly, the discrete diagnosis of schizophrenia may be two disorders, one of a truly adult onset type, and one of a delayed neurodevelopmental type (Raine 2006).

In conclusion, many pathological brain states that have traditionally been thought to arise from damage may actually be the product of a recursive developmental process whose mis-development is not apparent until much later in the life of an individual. Those diseases that begin early in development may not be treatable once they have become clinically apparent, but early diagnosis and treatment may be a more efficacious approach to decrease their prevalence.

Conclusions

Chapter One is a description of the mouse visual system. It provides a description of the cellular and functional context of retinotopic development in the SC. It describes the functions of cells involved in mapping, and describes the functional circuits that must be developed.

Chapter Two describes how gradients of EphA receptor tyrosine kinases in the retina are translated into topography in the SC. The expression levels of EphAs in RGCs

are controlled by processing in the soma and dependent on position within the retina. EphAs are then transported down the axon to the SC, so that EphA levels in the axon reflect EphA amounts in the soma. Consequently, RGC axons in the SC have various levels of EphA expression, which creates graded sensitivities to the chemorepulsive effects of ephrinA-EphA interaction. Furthermore, we show that the activity of four distinct Epha genes, EphA3, EphA4, EphA5, and EphA6, are summed together during mapping. The graded activity of EphAs allows the RGCs to translate information about their position in the retina into expression levels and then back into position within the SC, creating a topographic map.

Chapter Three describes experiments aimed at showing the role of spontaneous, patterned activity in the development of the retinocollicular map. A key reagent in these experiments is a mouse knock-out, which was thought to lack spontaneous, patterned activity but was subsequently shown to contain *altered* spontaneous, patterned activity. This discrepancy confounded the interpretation of the experiments described. Furthermore, the data acquired were not of sufficiently high resolution to confidently assign a role to spontaneous activity. Nevertheless, the experiments suggested that patterned activity does not play a role in the development of topography but instead acts to restrict the size of receptive fields in the SC.

Chapter Four is a comparison between the mechanisms of development of retinotopy in the SC/tectum of amniotes and anamniotes. The different dynamics of retinotopic mapping in amniotes and anamniotes may arise because of the differing contexts of map development. Amniotes generally have a higher degree of encephalization than anamniotes, which may require rigid primary sensory maps. An

increase in encephalization allows for a greater behavioral repertoire, but comes at the costs of an inability to regenerate and a greater time to develop. Humans have an extremely high level of encephalization and the process human brain development may continue far into adulthood, with implications for the etiology of behavioral diseases.

In an undertaking as difficult as understanding the development of the brain, it is easy to lapse into vitalism. On the other hand, a fully developed model of the development and workings of the brain would be composed of so many pieces and connections that it would be incomprehensible. Instead, one must take a middle path, and make those simplifications that are useful. Each Chapter focuses on the development of the retinocollicular map from a different perspective, and each provides a different insight into the mechanisms of its development.

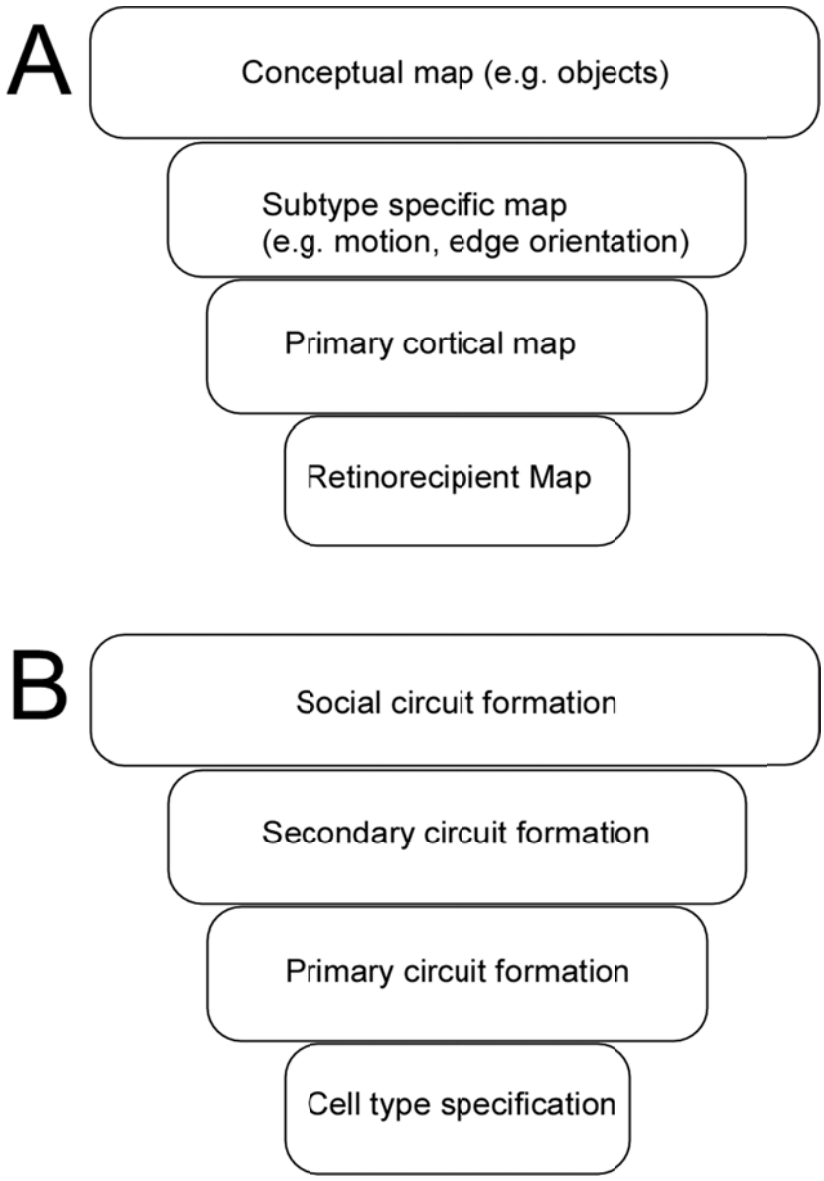

Figure 4.3 Parallel developmental paradigms of the visual system and social system

A The hierarchical development of the visual system begins with retinorecipient maps, such as the SC and LGN. These maps then necessarily inform the development of higher order maps in the cortex which are also retinotopic. These cortical visual maps are sensitive to subsets of the information available in a visual stimulus, such as edge orientation or motion. (object maps)

B Like the visual system, the development of the brain also has a hierarchical organization. It begins with early patterning of the embryo into specific cell types. These cells then form primary and secondary circuits with increasing levels of specificity and narrower receptive fields. Those functions that are most complex, such as social interactions, may occupy the highest level of the hierarchy.

Table 4.1 Brain weights, genome sizes, and age at sexual maturity of several mammals

Data of figure 4.2

Brain weights: (Kuhlenbeck 1967)
Genome size: (Gregory 2011)
Time to reproduction: (Macdonald 2009)

Common name	Binomial species name	brain weight (g)	Genome size (pg)	Age at sexual maturity (days
Elephant	*Loxodonta africana*	4783	4.11	5110
Bottlenose dolphin	*Tursiops truncatus*	1550	3.03	3285
Human	*Homo sapien*	1300	3.5	5110
Camel	*Camelus dromedarius*	762	2.86	1460
Giraffe	*Giraffa camelopardalis*	680	2.85	1460
Horse	*Equus ferus*	532	3.15	900
Gorilla	*Gorilla gorilla*	500	4.16	2920
Chimpanzee	*Pan troglodytes*	420	3.63	3285
Orangutan	*Pongo pygmaeus*	370	3.6	2190
Manatee	*Trichechus manatus*	360	4.67	1095
African lion	*Panthera leo*	240	2.95	1460
Domesticus pig	*Sus scrofa*	180	3	300
Sheep	*Ovis aries sheep*	140	3.3	540
Rhesus monkey	*Macaca mulatta*	96	3.59	1825
Aardvark	*Orycteropus afer*	72	5.86	730
Cow	*Bos taurus*	440	3.7	365
Cat	*Felis catus*	30	2.91	240
Squirrel monkey	*Saimiri sciureus*	22	3.3	1460
Rabbit	*Oryctolagus cuniculus*	12	3.26	180
Platypus	*Ornithorhynchus anatinus*	9	3.06	730
Opposum	*Didelphis aurita*	6	4.3	365
Guinea pig	*Cavia porcellus*	4	3.92	28
Hedgehog	*Erinaceus europaeus*	3.35	3.66	330
Brown rat	*Rattus norvegicus*	2	3.05	35

References

Albright, T. D. (1984). "Direction and orientation selectivity of neurons in visual area MT of the macaque." Journal of Neurophysiology **52**(6): 1106-30.

Bale, T. L., T. Z. Baram, A. S. Brown, J. M. Goldstein, T. R. Insel, M. M. McCarthy, C. B. Nemeroff, T. M. Reyes, R. B. Simerly, E. S. Susser and E. J. Nestler (2010). "Early life programming and neurodevelopmental disorders." Biol Psychiatry **68**(4): 314-9.

Barkus, E. and R. M. Murray (2010). "Substance use in adolescence and psychosis: clarifying the relationship." Annu. Rev. Clin. Psychol. **6**: 365-89.

Bartzokis, G., M. Beckson, P. H. Lu, K. H. Nuechterlein, N. Edwards and J. Mintz (2001). "Age-related changes in frontal and temporal lobe volumes in men: a magnetic resonance imaging study." Arch Gen Psychiatry **58**(5): 461-5.

Bartzokis, G., P. H. Lu, K. Tingus, M. F. Mendez, A. Richard, D. G. Peters, B. Oluwadara, K. A. Barrall, J. P. Finn, P. Villablanca, P. M. Thompson and J. Mintz (2010). "Lifespan trajectory of myelin integrity and maximum motor speed." Neurobiol Aging **31**(9): 1554-62.

Benes, F. M., M. Turtle, Y. Khan and P. Farol (1994). "Myelination of a key relay zone in the hippocampal formation occurs in the human brain during childhood, adolescence, and adulthood." Arch Gen Psychiatry **51**(6): 477-84.

Brockes, J. P. and A. Kumar (2008). "Comparative aspects of animal regeneration." Annu Rev Cell Dev Biol **24**: 525-49.

Dehaene, S. and L. Cohen (2007). "Cultural recycling of cortical maps." Neuron **56**(2): 384-98.

Gaze, R. M., M. J. Keating and S. H. Chung (1974). "The evolution of the retinotectal map during development in Xenopus." Proc R Soc Lond, B, Biol Sci **185**(80): 301-30.

Goldberg, J. L. and B. A. Barres (2000). "The relationship between neuronal survival and regeneration." Annu Rev Neurosci **23**: 579-612.

Gonzales, R., L. Mooney and R. A. Rawson (2010). "The methamphetamine problem in the United States." Annu. Rev. Public. Health. **31**: 385-98.

Goodale, M. A. and D. A. Westwood (2004). "An evolving view of duplex vision: separate but interacting cortical pathways for perception and action." Curr Opin Neurobiol **14**(2): 203-11.

Gregory, T. (2011). "Animal Genome Size Database." 2011, from www.genomesize.com.

Gruberg, E. R. and V. R. Ambros (1974). "A forebrain visual projection in the frog (Rana pipiens)." Exp Neurol **44**(2): 187-97.

Hedden, T. and J. D. E. Gabrieli (2004). "Insights into the ageing mind: a view from cognitive neuroscience." Nat Rev Neurosci **5**(2): 87-96.

Jarskog, L. F., S. Miyamoto and J. A. Lieberman (2007). "Schizophrenia: new pathological insights and therapies." Annu. Rev. Med. **58**: 49-61.

Jerison, H. J. (1977). "The theory of encephalization." Ann N Y Acad Sci **299**: 146-60.

Jerison, H. J. (1985). "Animal intelligence as encephalization." Philos Trans R Soc Lond, B, Biol Sci **308**(1135): 21-35.

Kanwisher, N., J. McDermott and M. M. Chun (1997). "The fusiform face area: a module in human extrastriate cortex specialized for face perception." J Neurosci **17**(11): 4302-11.

Karamian, A. I., N. P. Vesselkin, M. G. Belekhova and T. M. Zagorulko (1966). "Electrophysiological characteristics of tectal and thalamo-cortical divisions of the visual system in lower vertebrates." J Comp Neurol **127**(4): 559-76.

Kirkbride, J. B. and P. B. Jones (2011). "The prevention of schizophrenia--what can we learn from eco-epidemiology?" Schizophrenia Bulletin **37**(2): 262-71.

Krubitzer, L. and K. J. Huffman (2000). "Arealization of the neocortex in mammals: genetic and epigenetic contributions to the phenotype." Brain Behav Evol **55**(6): 322-35.

Kuhlenbeck, H. (1967). The central nervous system of vertebrates; a general survey of its comparative anatomy with an introduction to the pertinent fundamental biologic and logical concepts. New York,, Academic Press.

Lander, E. S., L. M. Linton, B. Birren, C. Nusbaum, M. C. Zody, J. Baldwin, K. Devon, K. Dewar, M. Doyle, W. FitzHugh, R. Funke, D. Gage, K. Harris, A. Heaford, J. Howland, L. Kann, J. Lehoczky, R. LeVine, P. McEwan, K. McKernan, J. Meldrim, J. P. Mesirov, C. Miranda, W. Morris, J. Naylor, C. Raymond, M. Rosetti, R. Santos, A. Sheridan, C. Sougnez, N. Stange-Thomann, N. Stojanovic, A. Subramanian, D. Wyman, J. Rogers, J. Sulston, R. Ainscough, S. Beck, D. Bentley, J. Burton, C. Clee, N. Carter, A. Coulson, R. Deadman, P. Deloukas, A. Dunham, I. Dunham, R. Durbin, L. French, D. Grafham, S. Gregory, T. Hubbard, S. Humphray, A. Hunt, M. Jones, C. Lloyd, A. McMurray, L. Matthews, S. Mercer, S. Milne, J. C. Mullikin, A. Mungall, R. Plumb, M. Ross, R. Shownkeen, S. Sims, R. H. Waterston, R. K. Wilson, L. W. Hillier, J. D. McPherson, M. A. Marra, E. R. Mardis, L. A. Fulton, A. T. Chinwalla, K. H. Pepin, W. R. Gish, S. L. Chissoe, M. C. Wendl, K. D. Delehaunty, T. L. Miner, A. Delehaunty, J. B. Kramer, L. L. Cook, R. S. Fulton, D. L. Johnson, P. J. Minx, S. W. Clifton, T. Hawkins, E. Branscomb, P. Predki, P. Richardson, S. Wenning, T. Slezak, N. Doggett, J. F. Cheng, A. Olsen, S. Lucas, C. Elkin, E. Uberbacher, M. Frazier, R. A. Gibbs, D. M. Muzny, S. E. Scherer, J. B. Bouck, E. J. Sodergren, K. C. Worley, C. M. Rives, J. H. Gorrell, M. L. Metzker, S. L. Naylor, R. S. Kucherlapati, D. L. Nelson, G. M. Weinstock, Y. Sakaki, A. Fujiyama, M. Hattori, T. Yada, A. Toyoda, T. Itoh, C. Kawagoe, H. Watanabe, Y. Totoki, T. Taylor, J. Weissenbach, R. Heilig, W. Saurin, F. Artiguenave, P. Brottier, T. Bruls, E. Pelletier, C. Robert, P. Wincker, D. R. Smith, L. Doucette-Stamm, M. Rubenfield, K. Weinstock, H. M. Lee, J. Dubois, A. Rosenthal, M. Platzer, G. Nyakatura, S. Taudien, A. Rump, H. Yang, J. Yu, J. Wang, G. Huang, J. Gu, L. Hood, L. Rowen, A. Madan, S. Qin, R. W. Davis, N. A. Federspiel, A. P. Abola, M. J. Proctor, R. M. Myers, J. Schmutz, M. Dickson, J. Grimwood, D. R. Cox, M. V. Olson, R. Kaul, C. Raymond, N. Shimizu, K. Kawasaki, S. Minoshima, G. A. Evans, M. Athanasiou, R. Schultz, B. A. Roe, F. Chen, H. Pan, J. Ramser, H. Lehrach, R. Reinhardt, W. R. McCombie, M. de la Bastide, N. Dedhia, H. Blöcker, K. Hornischer, G. Nordsiek, R. Agarwala, L. Aravind, J. A. Bailey, A. Bateman, S. Batzoglou, E. Birney, P. Bork, D. G. Brown, C. B. Burge, L. Cerutti, H. C. Chen, D. Church, M. Clamp, R. R. Copley, T. Doerks, S. R. Eddy, E. E. Eichler, T. S. Furey, J. Galagan, J. G. Gilbert, C. Harmon, Y. Hayashizaki, D. Haussler, H. Hermjakob, K. Hokamp, W. Jang, L. S. Johnson, T. A. Jones, S. Kasif, A. Kaspryzk, S. Kennedy, W. J. Kent, P. Kitts, E. V. Koonin, I. Korf, D. Kulp, D. Lancet, T. M. Lowe, A. McLysaght, T. Mikkelsen, J. V. Moran, N.

Mulder, V. J. Pollara, C. P. Ponting, G. Schuler, J. Schultz, G. Slater, A. F. Smit, E. Stupka, J. Szustakowski, D. Thierry-Mieg, J. Thierry-Mieg, L. Wagner, J. Wallis, R. Wheeler, A. Williams, Y. I. Wolf, K. H. Wolfe, S. P. Yang, R. F. Yeh, F. Collins, M. S. Guyer, J. Peterson, A. Felsenfeld, K. A. Wetterstrand, A. Patrinos, M. J. Morgan, P. de Jong, J. J. Catanese, K. Osoegawa, H. Shizuya, S. Choi, Y. J. Chen, J. Szustakowki and I. H. G. S. Consortium (2001). "Initial sequencing and analysis of the human genome." Nature **409**(6822): 860-921.

Liege, B. and G. Galand (1972). "Single-unit visual responses in the frog's brain." Vision Res **12**(4): 609-22.

Macdonald, D. (2009). The encyclopedia of mammals. Oxford ; New York, Oxford University Press.

O'Leary, D. D. M., S.-J. Chou and S. Sahara (2007). "Area patterning of the mammalian cortex." Neuron **56**(2): 252-69.

Pakkenberg, B. and H. J. Gundersen (1997). "Neocortical neuron number in humans: effect of sex and age." J Comp Neurol **384**(2): 312-20.

Raine, A. (2006). "Schizotypal personality: neurodevelopmental and psychosocial trajectories." Annu. Rev. Clin. Psychol. **2**: 291-326.

Rodman, H. R., C. G. Gross and T. D. Albright (1989). "Afferent basis of visual response properties in area MT of the macaque. I. Effects of striate cortex removal." J Neurosci **9**(6): 2033-50.

Rodman, H. R., C. G. Gross and T. D. Albright (1990). "Afferent basis of visual response properties in area MT of the macaque. II. Effects of superior colliculus removal." J Neurosci **10**(4): 1154-64.

Sakaguchi, D. S. and R. K. Murphey (1985). "Map formation in the developing Xenopus retinotectal system: an examination of ganglion cell terminal arborizations." J Neurosci **5**(12): 3228-45.

Sham, P. C., C. J. MacLean and K. S. Kendler (1994). "A typological model of schizophrenia based on age at onset, sex and familial morbidity." Acta Psychiatr Scand **89**(2): 135-41.

Simon, D. K. and D. D. O'Leary (1992). "Development of topographic order in the mammalian retinocollicular projection." J Neurosci **12**(4): 1212-32.

Sperry, R. (1944). "Optic nerve regeneration with return of vision in anurans." Journal of Neurophysiology **7**(1): 57.

Sperry, R. W. (1948). "Patterning of central synapses in regeneration of the optic nerve in teleosts." Physiological zoology **21**(4): 351-61.

Stuermer, C. A. (1988). "Retinotopic organization of the developing retinotectal projection in the zebrafish embryo." J Neurosci **8**(12): 4513-30.

Stuermer, C. A. and P. A. Raymond (1989). "Developing retinotectal projection in larval goldfish." J Comp Neurol **281**(4): 630-40.

Thompson, B. L. and P. Levitt (2010). "The clinical-basic interface in defining pathogenesis in disorders of neurodevelopmental origin." Neuron **67**(5): 702-12.

Walhovd, K. B., A. M. Fjell, I. Reinvang, A. Lundervold, A. M. Dale, D. E. Eilertsen, B. T. Quinn, D. Salat, N. Makris and B. Fischl (2005). "Effects of age on volumes of cortex, white matter and subcortical structures." Neurobiol Aging **26**(9): 1261-70; discussion 1275-8.

Walhovd, K. B., L. T. Westlye, I. Amlien, T. Espeseth, I. Reinvang, N. Raz, I. Agartz, D. H. Salat, D. N. Greve, B. Fischl, A. M. Dale and A. M. Fjell (2011). "Consistent neuroanatomical age-related volume differences across multiple samples." Neurobiol Aging **32**(5): 916-32.

Walker, E., V. Mittal and K. Tessner (2008). "Stress and the hypothalamic pituitary adrenal axis in the developmental course of schizophrenia." Annu. Rev. Clin. Psychol. **4**: 189-216.

Wandell, B. A., S. O. Dumoulin and A. A. Brewer (2007). "Visual field maps in human cortex." Neuron **56**(2): 366-83.

Williams, R. W. and K. Herrup (1988). "The control of neuron number." Annu Rev Neurosci **11**: 423-53.

Yates, P. A., A. L. Roskies, T. Mclaughlin and D. D. O'Leary (2001). "Topographic-specific axon branching controlled by ephrin-As is the critical event in retinotectal map development." J Neurosci **21**(21): 8548-63.